

NASA Technical Paper 1508

Theoretical and Experimental
Investigation of Ground-Induced
Effects for a Low-Aspect-Ratio
Highly Swept Arrow-Wing Configuration

Paul L. Coe, Jr., and James L. Thomas

SEPTEMBER 1979

PERSONAL COPY



Theoretical and Experimental
Investigation of Ground-Induced
Effects for a Low-Aspect-Ratio
Highly Swept Arrow-Wing Configuration

Paul L. Coe, Jr., and James L. Thomas
Langley Research Center
Hampton, Virginia



**Scientific and Technical
Information Branch**

SUMMARY

An investigation has been conducted in the Langley V/STOL tunnel to determine the influence of ground proximity on the aerodynamic characteristics of a low-aspect-ratio highly swept arrow-wing configuration. The tests were conducted using a moving-belt ground plane to simulate ground heights varying from 0.1 to 1.0 wing span.

The experimental results showed that as the height above the ground decreases, the configuration experiences substantial increases in lift and reductions in induced drag. Although a significant percentage of these ground-induced performance improvements are lost due to trim requirements, the net performance improvement remains quite favorable. The tests also showed that decreasing ground height results in a marked increase in the tail downwash factor ($1 - \frac{\partial C}{\partial \alpha}$) and therefore results in a substantial increase in the horizontal-tail contribution to longitudinal stability.

Comparison of the experimental results with results predicted by a planar vortex-lattice theoretical model shows that the theoretical model provides a good estimate of the ground-induced effect on lift, drag, and longitudinal stability for the wing-body combination. However, the theoretical model, which is restricted to a planar fuselage and planar wake representation, does not adequately predict either the zero-lift pitching moment or the horizontal-tail downwash characteristics.

INTRODUCTION

The National Aeronautics and Space Administration is currently investigating the aerodynamic characteristics of advanced aircraft concepts capable of cruising efficiently at supersonic speeds. In order to achieve the desired high levels of supersonic cruise efficiency, these conceptual designs typically incorporate a low-aspect-ratio highly swept arrow wing. (See, for example, ref. 1.) The desire for long-range capability and/or high payload capacity necessitates a relatively high wing loading which, when coupled with the relatively low lift-curve slope, requires that low-speed flight (for example, take-off and landing) utilize angles of attack on the order of 8° to 12° . Although these angles of attack would not be considered excessive for conventional designs intended for subsonic cruise conditions, past experience (ref. 2) has shown that even in this moderate angle-of-attack range, low-aspect-ratio highly swept wings may exhibit a markedly three-dimensional viscous flow field with pronounced leading-edge separation. Previous low-speed studies of the particular conceptual design tested herein (see, for example, refs. 2 and 3) have shown that deflecting leading-edge flaps may reduce the problem of leading-edge separation and thereby provide substantial improvements in low-speed performance, stability, and control.

The present study was undertaken to complement the previous low-speed study of reference 2 by experimentally determining the influence of ground proximity (simulating the initial take-off and final-approach conditions) on the aerodynamic characteristics of the configuration. The study was also intended to determine the degree of correlation between the experimental results and results predicted by the planar vortex-lattice theory of reference 4.

Tests were conducted in the Langley V/STOL tunnel using the moving-belt ground plane to simulate ground heights varying from 0.1 to 1.0 wing span. The tests were conducted over an angle-of-attack range of -2° to 12° at a Reynolds number (based on the reference mean aerodynamic chord) of about 2.0×10^6 .

SYMBOLS

The longitudinal data are referred to the stability system of axes as illustrated in figure 1. The moment reference center for the tests was located at 59.16 percent of the reference mean aerodynamic chord. (See fig. 2.) The reference wing area and chord are based on the wing planform which results from extending the inboard (74° swept) leading edge and the outboard (41.457° swept) trailing edge to the model center line.

The dimensional quantities herein are given in both the International System of Units (SI) and the U.S. Customary Units. Measurements were made in U.S. Customary Units.

b wing span, m (ft)

b_t span of horizontal tail, m (ft)

C_D drag coefficient, $\frac{\text{Drag}}{qS_{\text{ref}}}$

$C_{D,i}$ induced drag coefficient

C_L lift coefficient, $\frac{\text{Lift}}{qS_{\text{ref}}}$

C_m pitching-moment coefficient, $\frac{\text{Pitching moment}}{qS_{\text{ref}} c}$

$C_{m,o}$ pitching-moment coefficient at $C_L = 0$

$C_{m,t}$ contribution of horizontal tail to pitching-moment coefficient

$(C_{m\alpha})_t$ contribution of horizontal tail to $C_{m\alpha}$

C_T	thrust coefficient, $\frac{\text{Thrust}}{qS_{\text{ref}}}$
c	local wing chord at span station y , m (ft)
\bar{c}	reference wing mean aerodynamic chord, m (ft)
\bar{c}_t	mean aerodynamic chord of horizontal tail, m (ft)
h	height of moment reference center above ground plane, m (ft)
h_n	neutral point, expressed as percentage of \bar{c}
h_t	horizontal-tail height at $0.25\bar{c}_t$ above ground plane, m (ft)
i_t	horizontal-tail incidence, positive when leading edge is up, deg
l_t	horizontal-tail length (distance from moment reference center to $0.25\bar{c}_t$), m (ft)
q	free-stream dynamic pressure, Pa (lbf/ft ²)
q_t	dynamic pressure at horizontal-tail location, Pa (lbf/ft ²)
S_{ref}	reference wing area, m ² (ft ²)
S_t	horizontal-tail area, m ² (ft ²)
T/W	ratio of engine thrust to aircraft weight
V_d	vertical descent rate, m/sec (ft/sec)
$V_{d,\infty}$	vertical descent rate for $h/b = \infty$, m/sec (ft/sec)
x, y, z	body axis coordinates
α	angle of attack, deg
γ	flight-path angle, positive for flight path inclined above horizon, deg
δ_f	trailing-edge flap deflection, expressed as $\delta_{t_1}/\delta_{t_3}/\delta_{t_5}$, deg
δ_{le}	leading-edge flap deflection, measured perpendicular to hinge line, positive when leading edge is down, deg (see fig. 2)
$\delta_{t_1}, \delta_{t_3}, \delta_{t_5}$	deflection of trailing-edge flap segments t_1 , t_3 , and t_5 measured perpendicular to respective hinge lines, positive when trailing edge is down, deg (see fig. 2)

ϵ downwash at horizontal tail, deg
 ρ density, kg/m³ (slugs/ft³)
 θ inclination of X-axis relative to horizon, positive when above horizon, deg

Derivatives:

$$\begin{aligned}
 C_{L\alpha} &= \partial C_L / \partial \alpha \\
 (C_{L\alpha})_t &= \partial C_{L,t} / \partial \alpha_t \\
 C_{m\alpha} &= \partial C_m / \partial \alpha \\
 C_{m_{it}} &= \partial C_m / \partial \alpha_{it}
 \end{aligned}$$

Model component designations:

H horizontal tail
 L_1, L_2, L_3, L_4 wing leading-edge flap segments (see fig. 2)
 t_1, t_3, t_5, t_6 wing trailing-edge flap segments (see fig. 2)
 V center-line vertical tail
 WB wing-body combination (includes outboard vertical fins and flow-through nacelles)

MODEL

The dimensional characteristics of the model used in the present study are listed in table 1 and shown in figure 2. The model was constructed to conform with the cruise geometry as defined in reference 5. The model also incorporated leading- and trailing-edge flaps as defined in reference 2 and shown in figure 2. Inasmuch as the model is also intended to explore propulsion-induced effects in subsequent studies, the model nacelles included engine simulators consisting of tip-driven fans. (For the present study these fans were unpowered and were allowed to windmill freely.) A photograph of the model mounted for tests in the Langley V/STOL tunnel is presented in figure 3.

TESTS AND CORRECTIONS

Static force tests were conducted in the Langley V/STOL tunnel using the moving-belt ground plane (see ref. 6) to ensure an accurate simulation of configuration in proximity to the ground. The ground heights simulated ranged from 0.1 to 1.0 wing span, and the angle-of-attack range was from -2° to 12° (depending on model clearance limitations). The principal configuration variables included wing trailing-edge flap deflection and horizontal-tail incidence.

The tests were conducted at a dynamic pressure of 335.16 Pa ($7 \text{ lbf}/\text{ft}^2$) which resulted in a Reynolds number (based on the reference mean aerodynamic chord) of about 2.0×10^6 . The data presented have been corrected for jet-boundary effects (induced by the tunnel ceiling and sidewalls) by using the theory outlined in reference 7. Sting interference effects have been determined by the methods outlined in reference 8. Transition strips were placed on the wing, nacelles, and horizontal and vertical tails in accordance with the method of reference 9. The drag data have been adjusted to account for the presence of the windmilling engine-simulator fans.

PRESENTATION OF RESULTS

A brief discussion of the mechanism of ground-induced effects is presented in appendix A. A data supplement containing a run schedule and a tabular listing of data obtained from the present series of tests is provided in appendix B. Also included in the data supplement are selected plots and tabular data, taken from reference 2, which correspond to the appropriate out-of-ground-effect ($h/b = \infty$) condition. The results and discussion are presented in accordance with the following outline:

Figure

Ground-induced effects of the wing-body:

Effect on performance	4 to 9
Effect on longitudinal stability	10 and 11

Ground-induced effects of the wing-body with horizontal and vertical tail:

Effect on longitudinal stability	12 to 16
Effect on landing-approach maneuver	17 to 19

RESULTS AND DISCUSSION

Ground-Induced Effects for the Wing-Body

Effect on performance.— Figure 4 shows the longitudinal aerodynamic characteristics of the wing-body combination as a function of the simulated nondimensional height of the configuration above the ground (h/b). Data corresponding to the out-of-ground-effect condition ($h/b = \infty$, obtained from ref. 2) are also shown to establish reference values. The plotted results are based on an interpolation of the measured data such that variations of α and h/b can be eliminated. Data are presented for trailing-edge flap deflections of 0° , 10° , 20° , and 30° . In general, the data show an increase in C_L with decreasing h/b . The data also show that, with decreasing h/b , C_D decreases for low angles of attack but increases for moderate and high angles of attack.

As discussed in appendix A, the observed increase in C_L (with decreasing h/b) is due to a ground-induced upwash which results in an effective increase in lift at a given angle of attack. In order to more clearly illustrate this increase in lift and lift-curve slope, the data of figure 4(c) have been replotted to show the variation of C_L with α . These plots, which are presented in

figure 5, have been summarized in figure 6 to show the lift coefficient evaluated at $\alpha = 0^\circ$ and the lift-curve slope as a function of h/b . Also presented in figure 6 are results obtained with a theoretical model consisting of a planar vortex-lattice representation of the configuration, and including a plane of symmetry to simulate the ground plane. (See ref. 4 for a description of the vortex-lattice computer program.) As can be seen, excellent agreement exists between theory and experiment for values of h/b from ∞ to 0.3. For values of h/b less than 0.3, the theoretical results predict substantially larger increases in $C_L|_{\alpha=0}$ and $C_{L\alpha}$ than do the experimental results; however, the overall trends are seen to be in agreement.

As mentioned previously, the data of figure 4 show that with decreasing h/b , C_D decreases for low angles of attack but increases for moderate and high angles of attack. In order to more clearly show this influence of ground proximity on drag, the drag polars (obtained by cross plotting the data of fig. 4) are presented in figure 7. As would be expected, based on the discussion contained in appendix A, reducing h/b results in substantial reductions in induced drag. Figure 8 shows the theoretical induced-drag polars obtained with the previously discussed vortex-lattice model at several values of h/b . Consideration of the data of figures 7 and 8 shows that, for a given value of h/b , the theoretical model predicts substantially lower levels of induced drag than observed experimentally. This result is expected and is due to the fact that the theoretical model assumes 100-percent leading-edge suction, whereas the experimentally determined leading-edge suction is on the order of 70 percent. (See ref. 2.)

Although the absolute level of induced drag predicted by the simple vortex-lattice theory is found to be inappropriate, it should be noted (see fig. 9) that the theoretically predicted incremental reductions in C_D follow the same trend as the corresponding experimentally determined values.

Effect on longitudinal stability.- The data presented in figure 4 indicate that the wing-body configuration generally experiences a small positive increment in pitching moment with decreasing h/b . To more accurately portray this influence of ground height on the longitudinal stability characteristics of the wing-body combination, the data of figure 4 have been replotted to show the parametric dependence of C_m versus C_L on h/b . (See fig. 10.) Analysis of the data of figure 10 (summarized in fig. 11) shows that for the wing-body combination the pitching moment at zero lift $C_{m,0}$ is essentially independent of ground height. Analysis of these data also indicates that decreasing h/b has a slight stabilizing effect on static longitudinal stability, as illustrated by the small rearward shift in neutral point h_n . This stabilizing effect is associated with the distribution of the ground-induced upwash, as discussed in appendix A. Figure 11 also presents the variation of $C_{m,0}$ and h_n with h/b as predicted with the vortex-lattice theoretical model. As can be seen, for the range of h/b studied, the difference between the theoretical and experimentally determined neutral point is about $0.02c$, while the corresponding difference in $C_{m,0}$ is more pronounced. It should be noted that the particular vortex-lattice model upon which the theoretical calculations are based employed a flat fuselage representation which is thought to be responsible for the discrepancy between the theoretical and experimental values of $C_{m,0}$.

Ground-Induced Effects for the Wing-Body With
Horizontal and Vertical Tails

Effect on longitudinal stability.— Figure 12 presents the ground effects data for the complete configuration with a trailing-edge flap deflection δ_f of $20^\circ/20^\circ/20^\circ$. Data are presented for a range of horizontal-tail incidence angles of -20° to 10° . Examination of these data shows that the lift and drag trends are similar to those previously discussed for the tail-off condition, but that the pitching-moment characteristics are markedly altered by the addition of the horizontal tail. In order to eliminate angle-of-attack dependence, and thereby provide a better understanding of the influences of ground proximity on horizontal-tail effectiveness, the pitching-moment data of figures 12 and 4(c) have been replotted and are presented in figure 13. As can be seen from the data of figure 13, the incremental pitching moment produced by tail incidence is approximately independent of h/b for the range of ground heights tested. It should be noted, however, that the increment in pitching moment due to tail incidence is a nonlinear function of tail incidence. This is a result which is not presently understood.

The standard expressions for the horizontal-tail contribution to pitching moment, longitudinal control effectiveness, and longitudinal stability are as follows:

$$C_{m,t} = \frac{-l_t}{c} \frac{q_t}{q} \frac{s_t}{s_{ref}} (C_{L\alpha})_t (\alpha - \epsilon + i_t) \quad (1)$$

$$C_{m_{it}} = \frac{-l_t}{c} \frac{q_t}{q} \frac{s_t}{s_{ref}} (C_{L\alpha})_t \quad (2)$$

$$(C_{m\alpha})_t = \frac{-l_t}{c} \frac{q_t}{q} \frac{s_t}{s_{ref}} (C_{L\alpha})_t \left(1 - \frac{\partial \epsilon}{\partial \alpha} \right) \quad (3)$$

Noting that for the conditions under consideration $C_{m_{it}}$ has been observed to be approximately independent of h/b , it may be concluded (based on eq. (2)) that the lift-curve slope of the horizontal tail $(C_{L\alpha})_t$ is not significantly influenced by ground proximity for the range of ground heights considered herein. This result may have been anticipated by considering the horizontal-tail ground-height parameter h_t/b_t in place of the wing ground-height parameter h/b . Because of ground clearance constraints, minimum h_t/b_t was limited to values on the order of 0.4.

Although it has been shown that the lift-curve slope of the horizontal tail is essentially unaffected, equation (3) indicates that ground proximity may

still exhibit an influence on longitudinal stability if the downwash characteristics are altered. Figure 14 shows the variation of the calculated horizontal-tail downwash parameter ($1 - \partial\epsilon/\partial\alpha$) as a function of h/b . These results, obtained from standard analysis of the tail-on and tail-off data presented in figure 13, show that the downwash factor increases markedly as h/b decreases. Although an increase in the tail downwash parameter would be expected to result from the ground-induced upwash (as discussed in appendix A), it would not be expected to exceed a value of 1. Inasmuch as the calculated values of ($1 - \partial\epsilon/\partial\alpha$) rely on the linearity of C_m versus α_t , and since this quantity has been previously shown to be nonlinear, these values of the downwash parameter should only be considered as qualitative. Also presented in figure 14 is the theoretical downwash parameter computed using the vortex-lattice model. As can be seen, the theoretical values are significantly below those computed from the experimental data. The reason for this discrepancy is thought to lie partly in the assumption of a planar wake (inherent to the particular vortex-lattice program) and partly in the previously discussed nonlinear tail effectiveness.

As implied by equation (3), increases in the downwash parameter ($1 - \partial\epsilon/\partial\alpha$) result in increases in the horizontal-tail contribution to longitudinal stability and, consequently, increases in the stability of the complete configuration. Figure 15 (based on the data of fig. 12(b)) shows the variation of C_m with respect to C_L for values of h/b from ∞ to 0.20. Figure 16 summarizes these results in the form of the variation of $C_{m,0}$ and h_n with respect to h/b . Also presented for comparison in figure 16 are corresponding results for the wing-body combination previously presented in figure 11. Examination of the data of figures 15 and 16 indicates that the horizontal tail provides a positive increment in $C_{m,0}$ and that this increment remains approximately constant for values of h/b from ∞ to 0.25. The data of figures 15 and 16 also illustrate the anticipated result of an increase in longitudinal stability produced by ground-induced effects. For example (assuming a center of gravity at 59.16 percent \bar{c}), in the initial approach condition, the configuration is about 3 percent unstable (that is, $\partial C_m/\partial C_L = 0.03$ at $h/b = \infty$); however, as the descent progresses to the point where $h/b = 0.2$, the configuration is about 3.5 percent stable (that is, $\partial C_m/\partial C_L = -0.035$).

Effect on landing-approach maneuver.— In order to assess the significance of the ground-induced effects on the landing-approach condition, the trimmed drag polars have been determined for a 20° trailing-edge flap setting and are shown in figure 17. Comparison of the trimmed drag polars to corresponding untrimmed polars (see fig. 7(c)) shows that a substantial percentage of the performance improvement provided by ground-induced effects is lost; however, the resultant improvement in trimmed performance does remain significant.

Analysis of the trimmed drag polars (see fig. 18) shows that an assumed approach lift coefficient of 0.6 with a thrust-to-weight ratio T/W of 0.148 results in an initial ($h/b = \infty$) glide slope γ of -2.7° with $\alpha = 10.3^\circ$ and $\theta = 7.6^\circ$. Furthermore, an assumed quasi-steady-state approach, carried out holding attitude θ and thrust setting constant, results in a reduced glide-path angle as h/b decreases. Although the particular maneuver is not truly self-flaring (control deflections are required to maintain the trim condition), it does indicate that a simple constant-attitude approach maneuver may result in desired reductions in vertical descent rate. To illustrate this

point, figure 19 shows the nondimensional vertical descent rate as a function of h/b . The computations, performed for the conditions determined by the analysis of figure 18, show marked reductions in vertical descent rate with decreasing h/b .

It should, of course, be recognized that the foregoing discussion of the landing-approach maneuver, based on a simplistic quasi-steady-state assumption, represents the upper bounds for favorable ground effects. It should also be recognized that results for specific configurations should be determined by using the equations of motion throughout the landing maneuver.

SUMMARY OF RESULTS

The results of theoretical and experimental studies to determine the ground-induced effects for a low-aspect-ratio highly swept arrow-wing configuration may be summarized as follows:

Decreasing h/b resulted in substantial increases in lift and substantial reductions in induced drag. Although a significant percentage of the ground-induced performance improvement was lost due to trim requirements, the effect remained quite favorable.

The wing-body combination exhibited only a slight increase in longitudinal stability with decreasing h/b . However, as h/b decreased, there occurred a marked increase in the tail downwash factor $(1 - \partial\epsilon/\partial\alpha)$, which resulted in substantial increase in the horizontal-tail contribution to longitudinal stability.

The use of a planar vortex-lattice theoretical model, which included a ground-plane image system, provided a good estimate of the ground-induced effect on lift, drag, and longitudinal stability of the wing-body combination. However, the theoretical model, which was restricted to a planar fuselage and wake representation, did not adequately predict either the zero-lift pitching moment or the horizontal-tail downwash characteristics.

Langley Research Center
National Aeronautics and Space Administration
Hampton, VA 23665
July 20, 1979

TABLE 1.- DIMENSIONAL CHARACTERISTICS OF MODEL

Wing:

Reference area, m^2 (ft^2)	1.875 (20.187)
Gross area, m^2 (ft^2)	2.067 (22.25)
Span, m (ft)	1.89 (6.20)
Root chord, m (ft)	2.515 (8.252)
Tip chord, m (ft)	0.242 (0.794)
Reference mean aerodynamic chord, m (ft)	1.320 (4.331)
Distance of leading edge of c aft of wing apex, m (ft)	1.063 (3.487)
Gross mean aerodynamic chord, m (ft)	1.557 (5.109)
Leading-edge sweep, deg -	
At body station 0.574 m (1.883 ft)	74.0
At body station 2.141 m (7.024 ft)	70.5
At body station 2.827 m (9.277 ft)	60.0

Vertical tail:

Area, m^2 (ft^2)	0.0327 (0.352)
Span, m (ft)	0.171 (0.562)
Root chord, m (ft)	0.0732 (0.240)
Leading-edge sweep, deg	59.0

Vertical fin (two):

Area, m^2 (ft^2)	0.084 (0.906)
Span, m (ft)	0.147 (0.484)
Root chord, m (ft)	0.499 (1.637)
Tip chord, m (ft)	0.071 (0.233)
Leading-edge sweep, deg	73.4

Horizontal tail:

Area, m^2 (ft^2)	0.150 (1.613)
Span, m (ft)	0.457 (1.499)
Root chord, m (ft)	0.540 (1.772)
Tip chord, m (ft)	0.116 (0.380)
Mean aerodynamic chord, m (ft)	0.372 (1.221)
Horizontal-tail length, m (ft)	1.467 (4.811)
Leading-edge sweep, deg	43.0
Dihedral, deg	-15.0

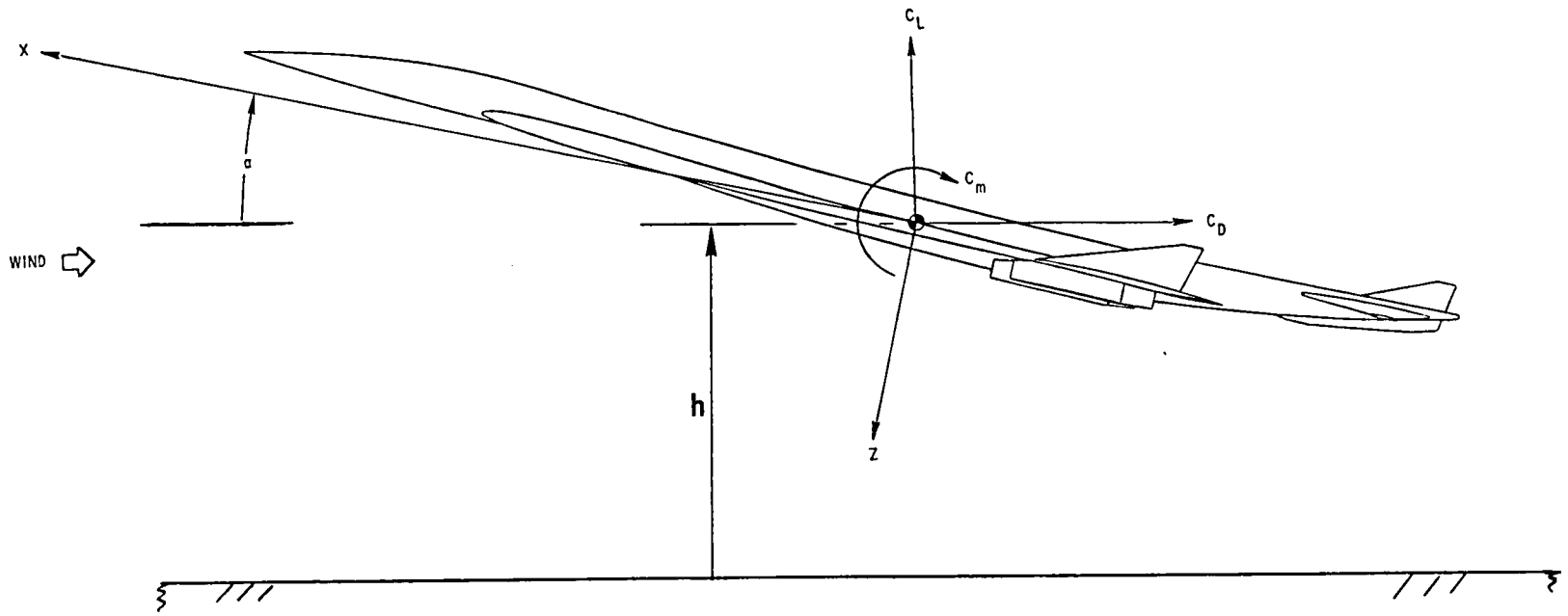


Figure 1.- System of axes.

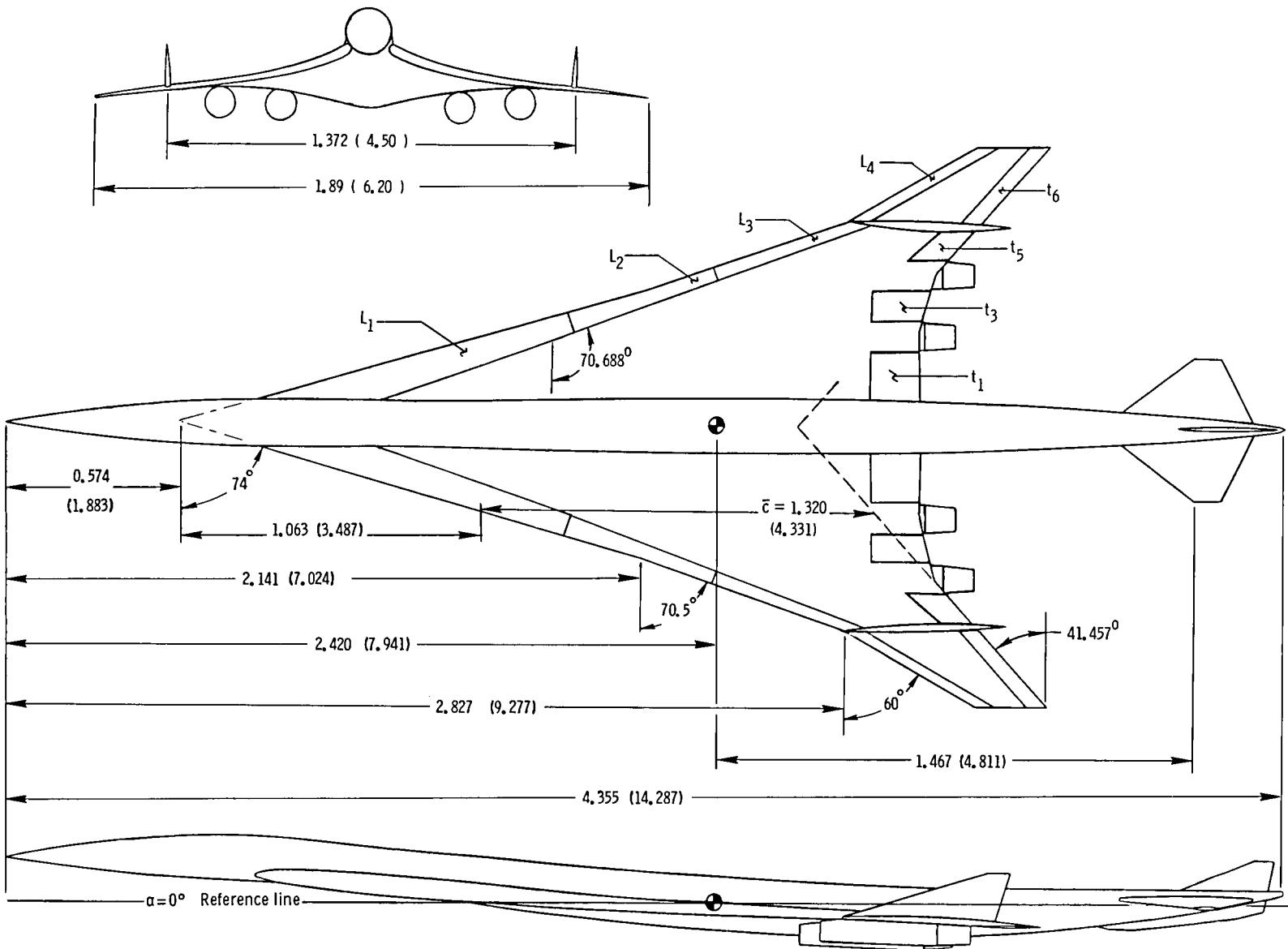
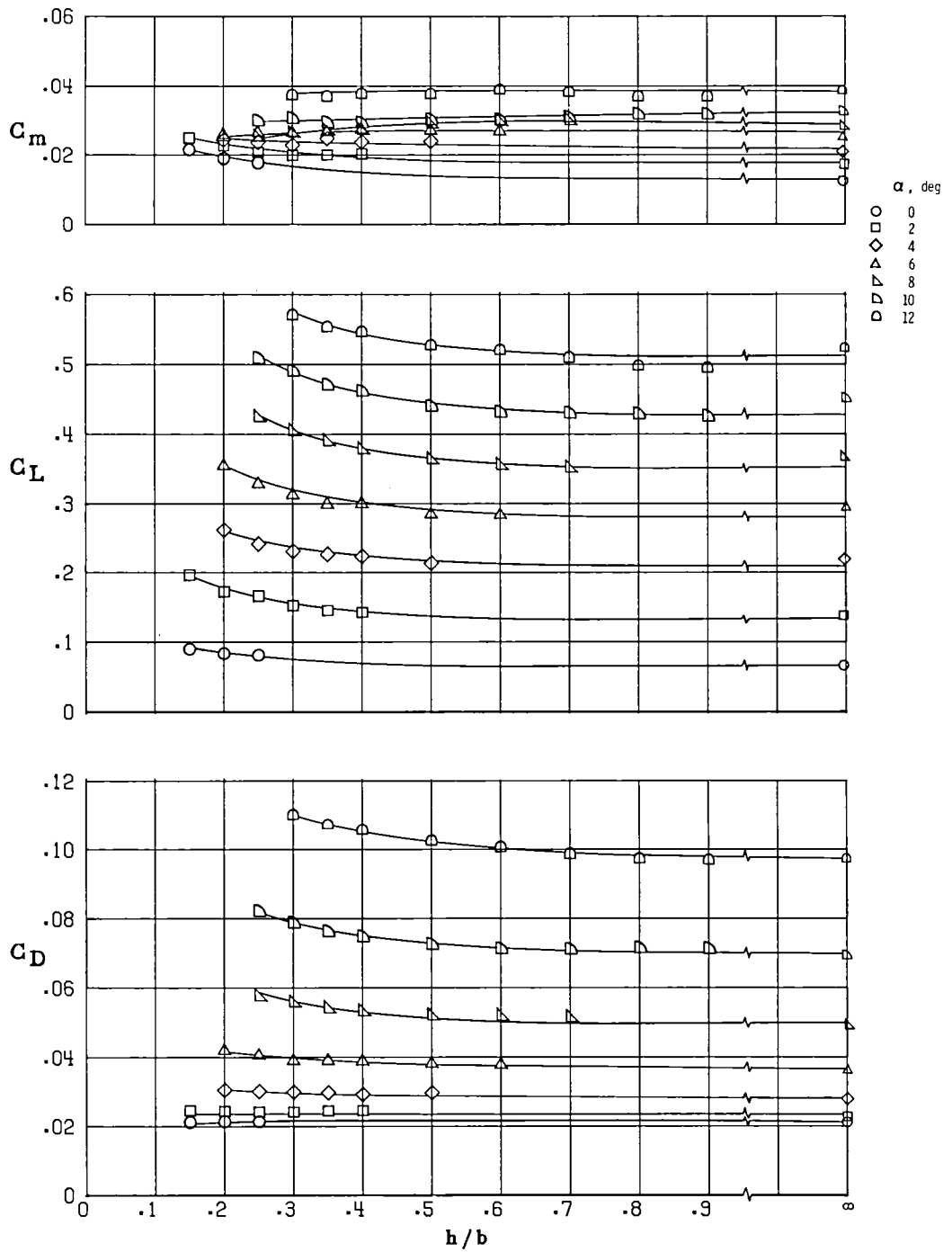


Figure 2.- Dimensional characteristics of model. Dimensions are given in meters and parenthetically in feet.



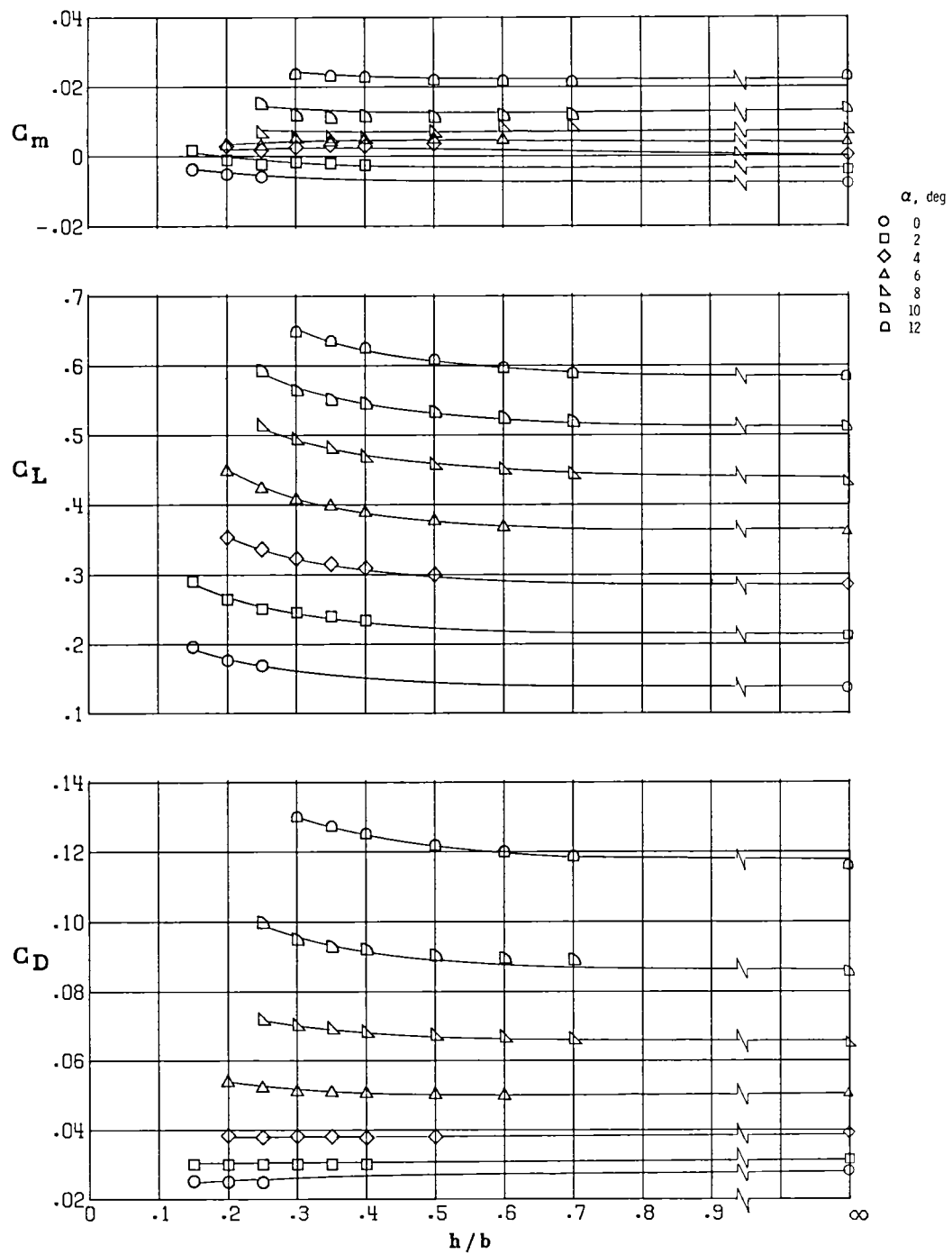
L-79-267

Figure 3.- Photograph of model mounted for ground-effects tests in Langley V/STOL tunnel.



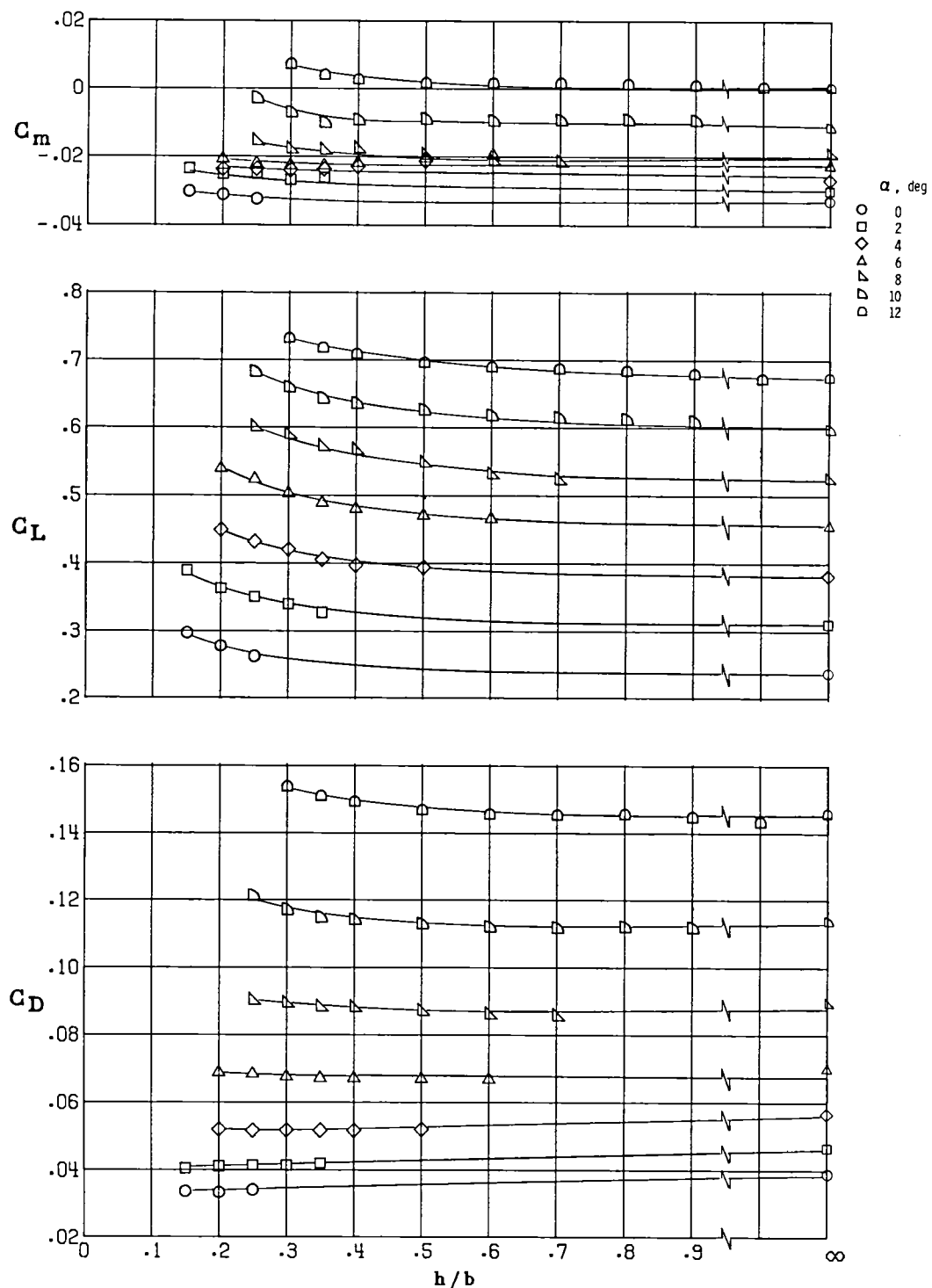
(a) $\delta_f = 0^\circ/0^\circ/0^\circ$.

Figure 4.- Longitudinal aerodynamic characteristics of the wing-body combination. $\delta_{le} = 30^\circ$.



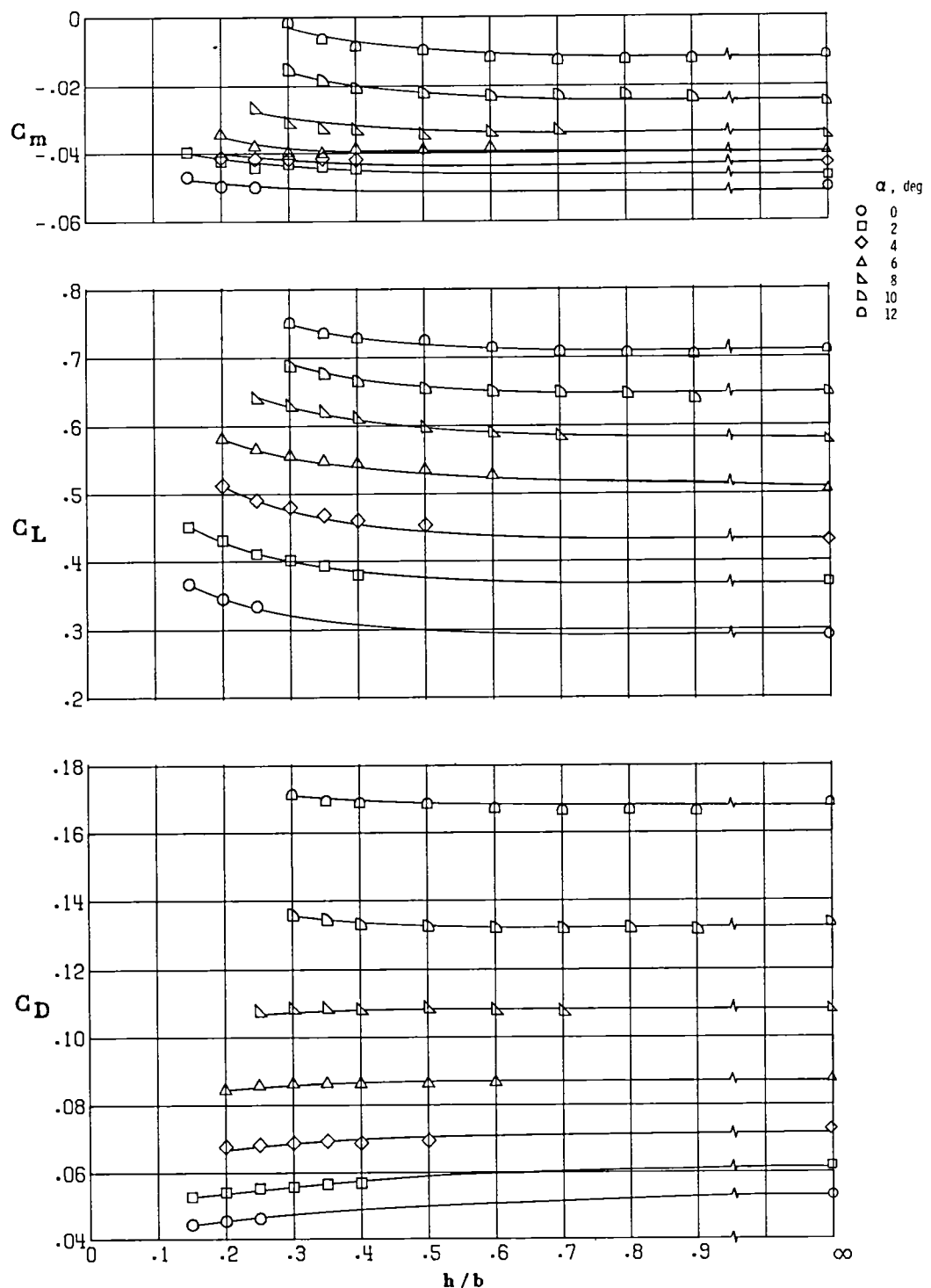
(b) $\delta_f = 10^\circ/10^\circ/10^\circ$.

Figure 4.- Continued.



(c) $\delta_F = 20^\circ/20^\circ/20^\circ$.

Figure 4.- Continued.



(d) $\delta_f = 30^\circ/30^\circ/20^\circ$.

Figure 4.- Concluded.

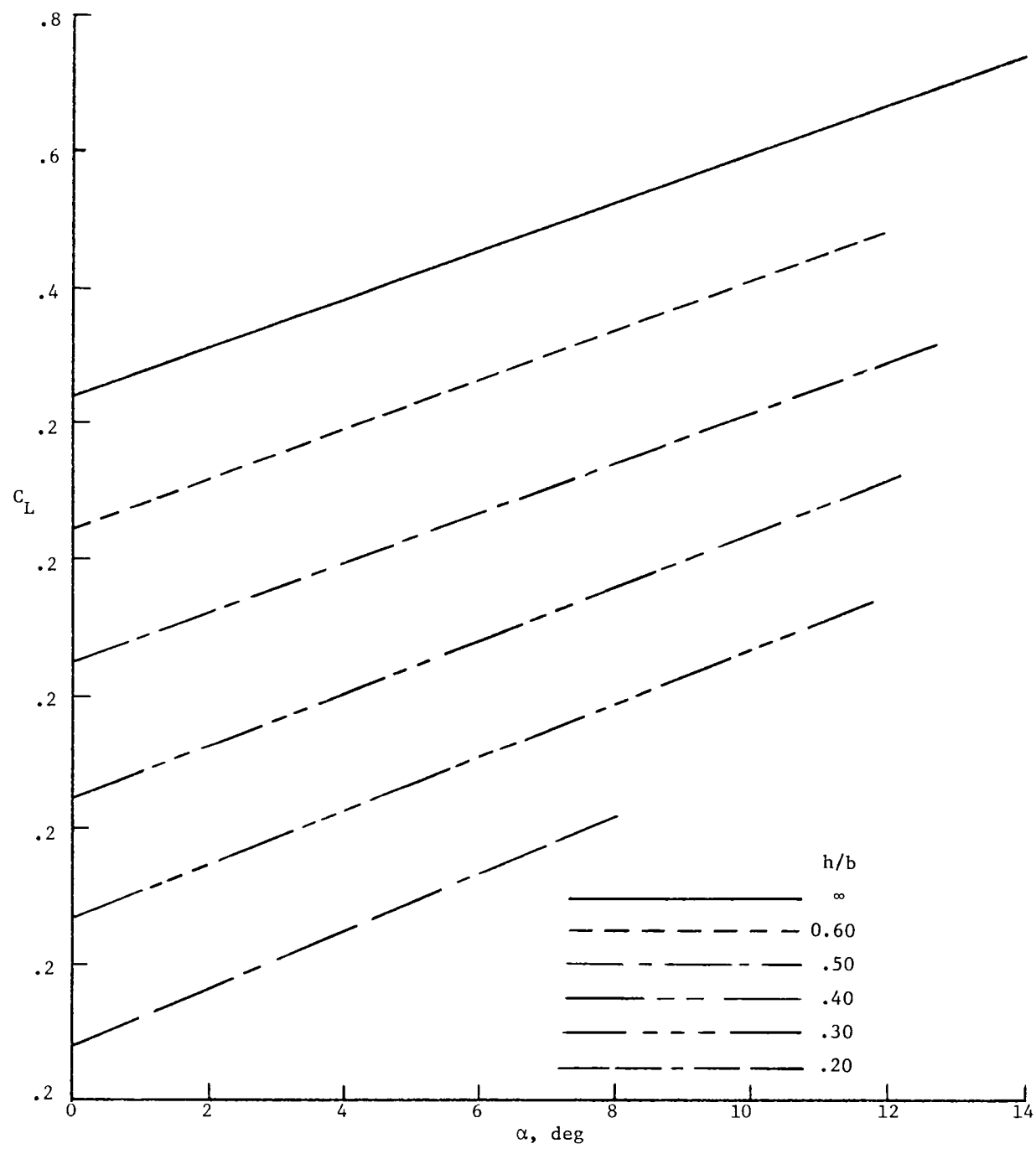


Figure 5.- Variation of C_L with α . WB; $\delta_f = 20^\circ/20^\circ/20^\circ$; $\delta_{le} = 30^\circ$.

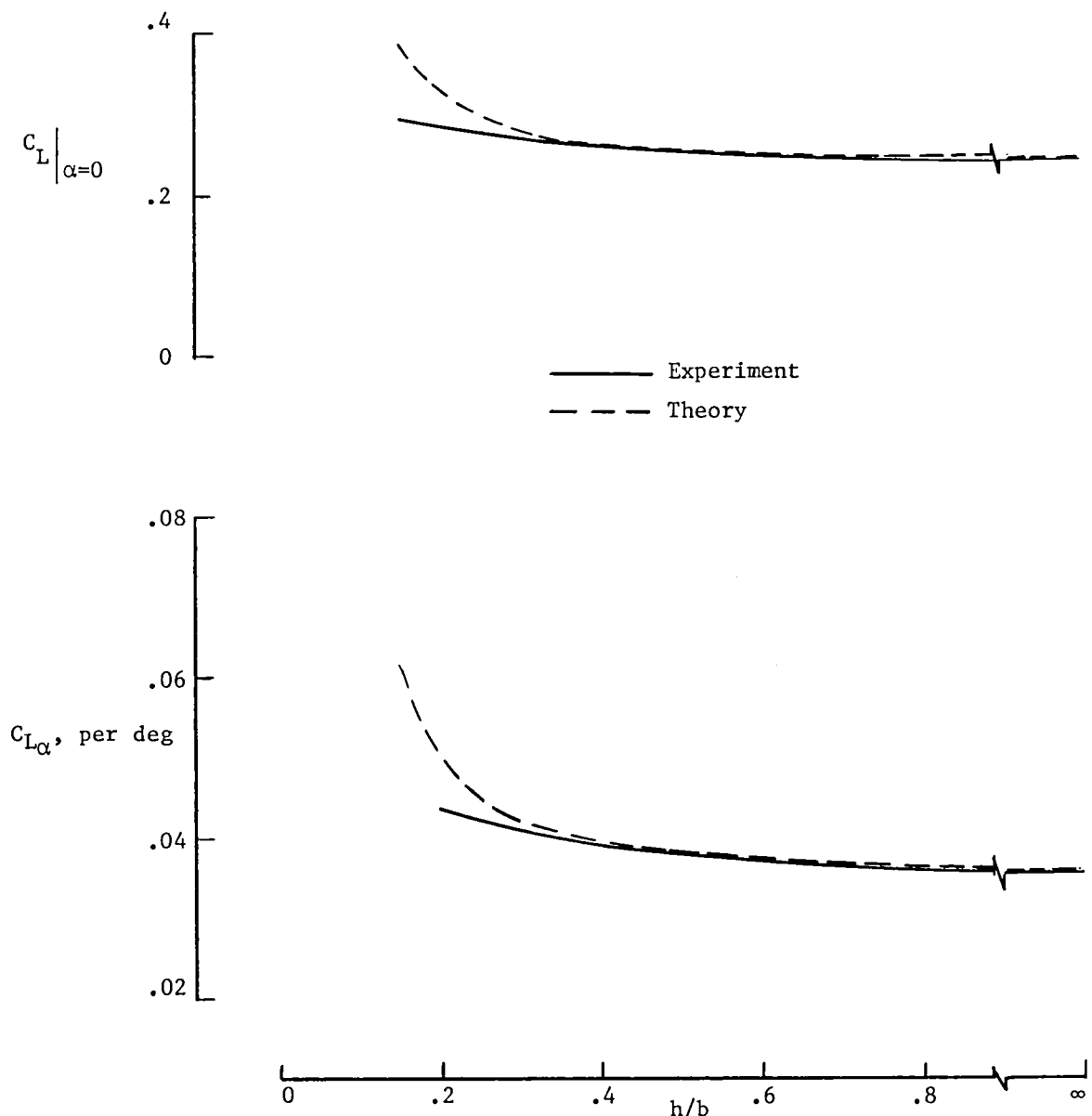
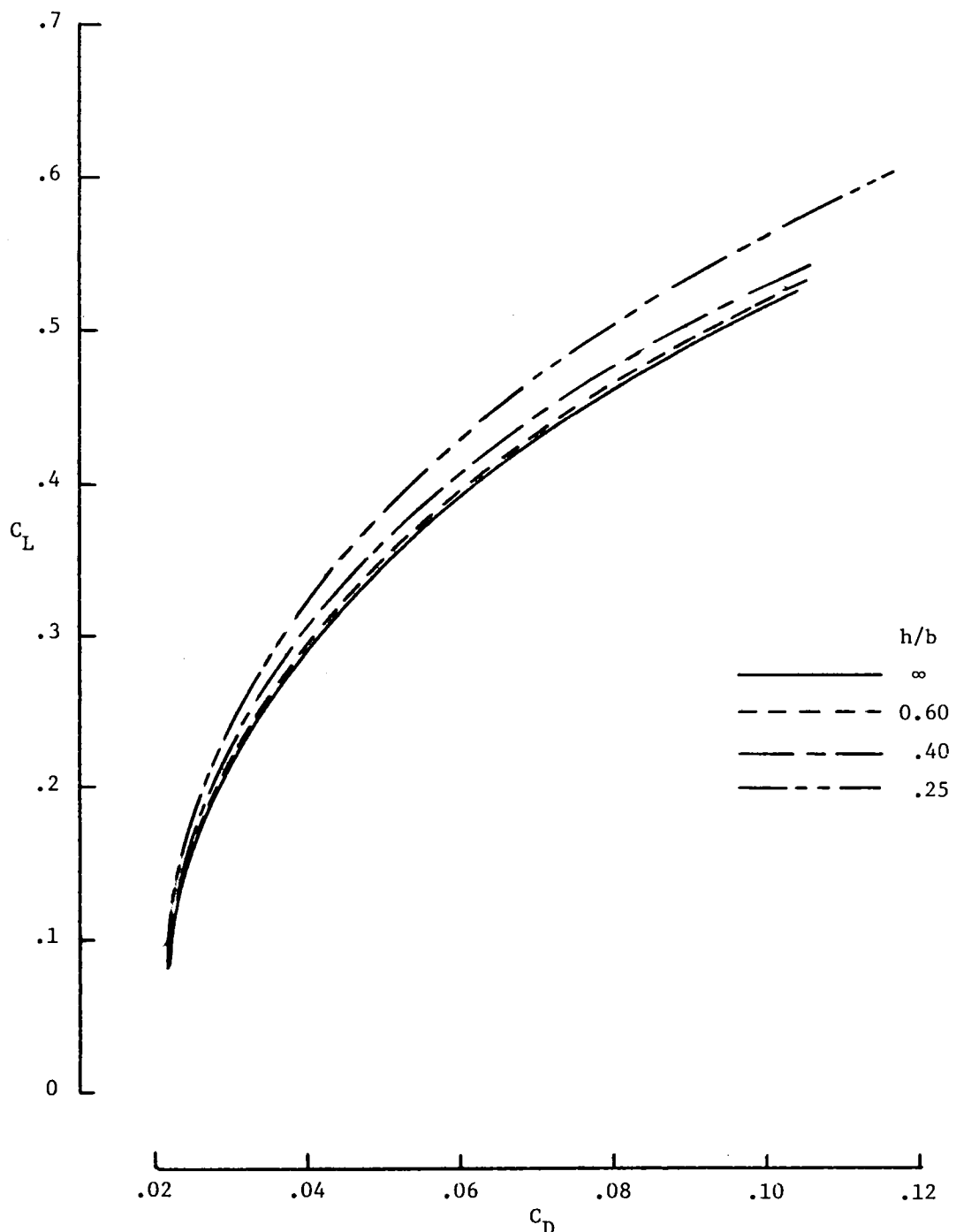
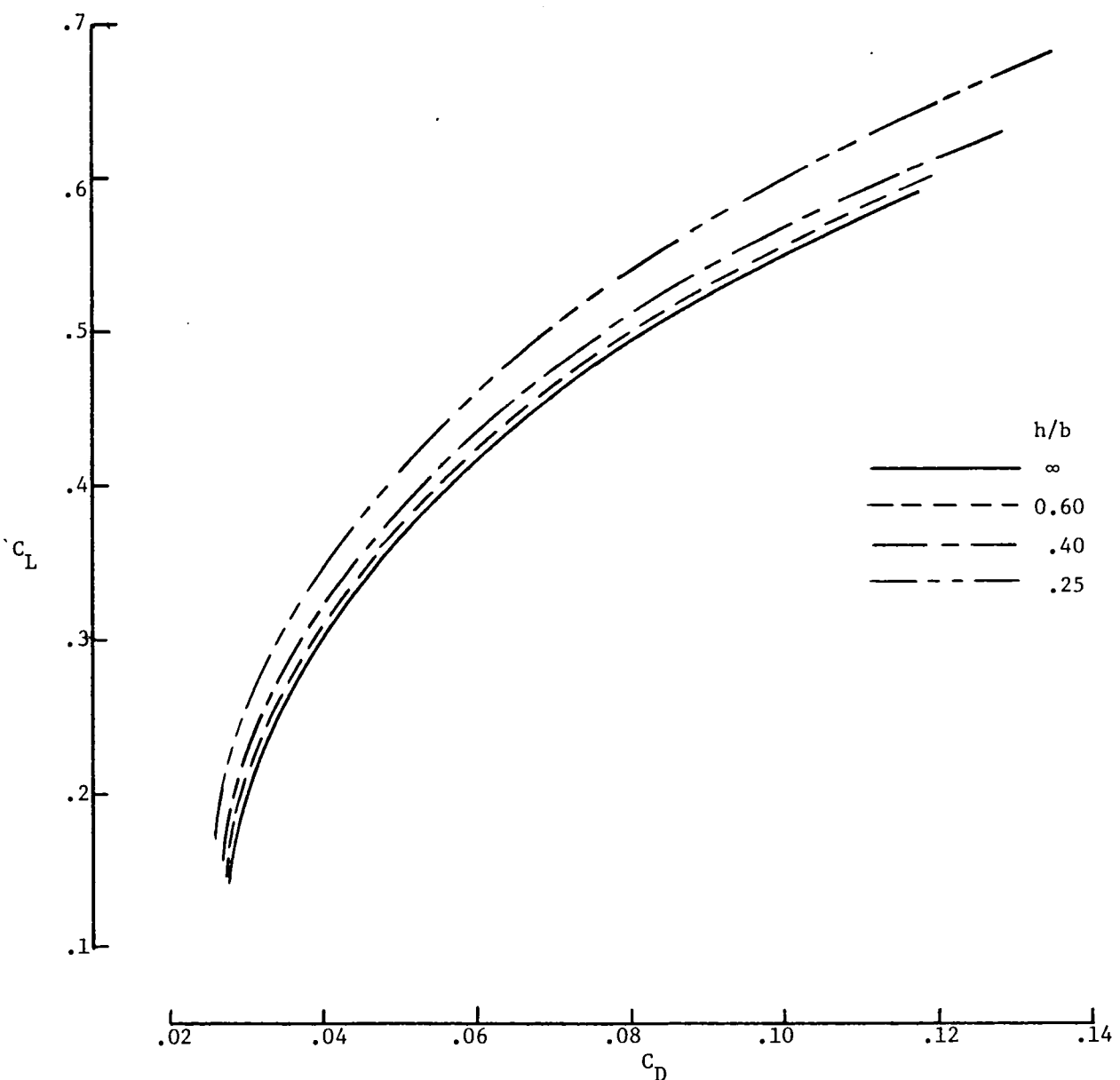


Figure 6.- Variation of $C_L|_{\alpha=0}$ and C_{L_α} with respect to h/b . WB;
 $\delta_f = 20^\circ/20^\circ/20^\circ$; $\delta_{le} = 30^\circ$.



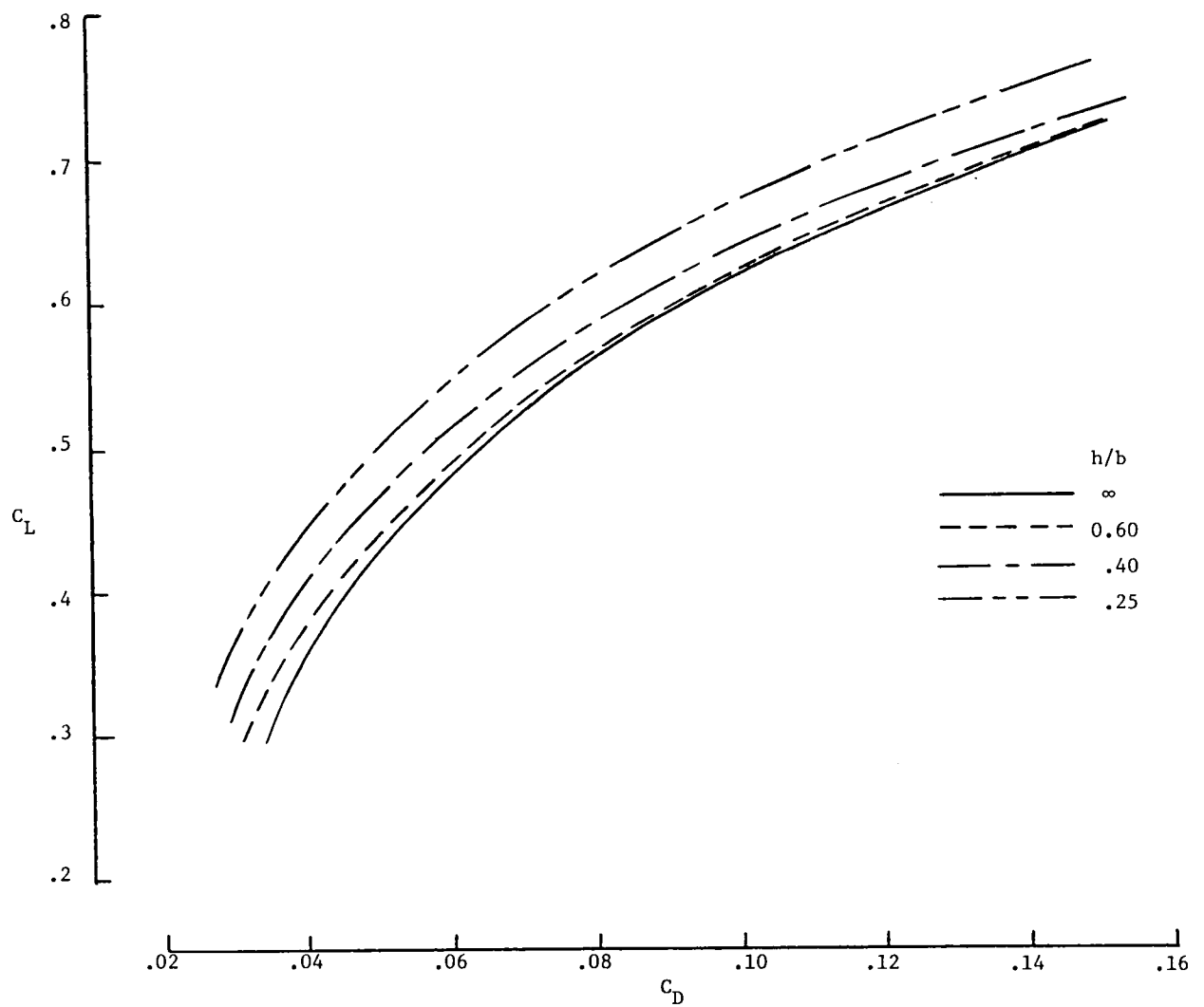
(a) $\delta_f = 0^\circ/0^\circ/0^\circ$.

Figure 7.- Experimentally determined variation of C_L with C_D . WB;
 $\delta_{le} = 30^\circ$.



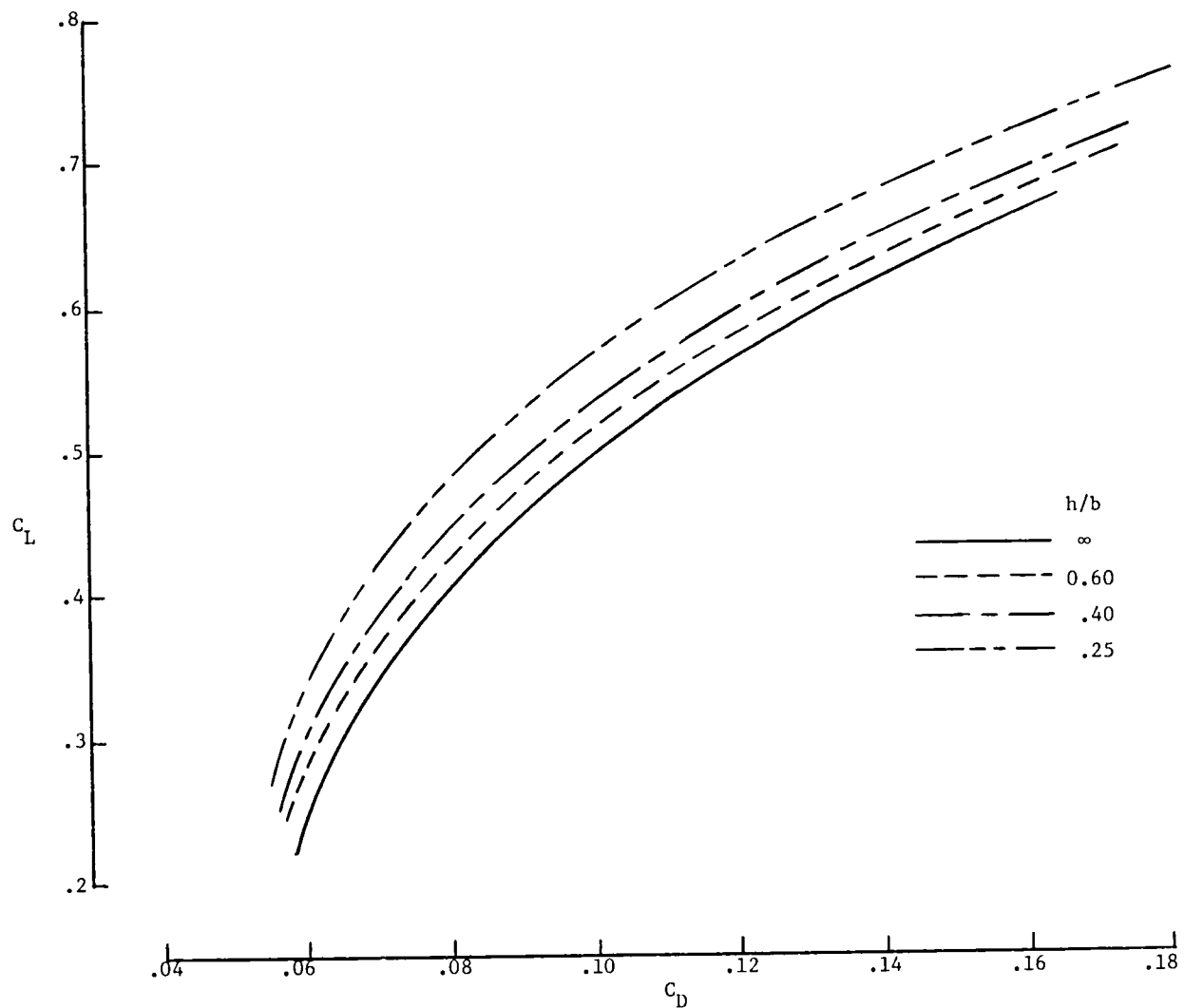
(b) $\delta_f = 10^\circ/10^\circ/10^\circ$.

Figure 7.- Continued.



(c) $\delta_f = 20^\circ/20^\circ/20^\circ$.

Figure 7.- Continued.



(d) $\delta_f = 30^\circ/30^\circ/20^\circ$.

Figure 7.- Concluded.

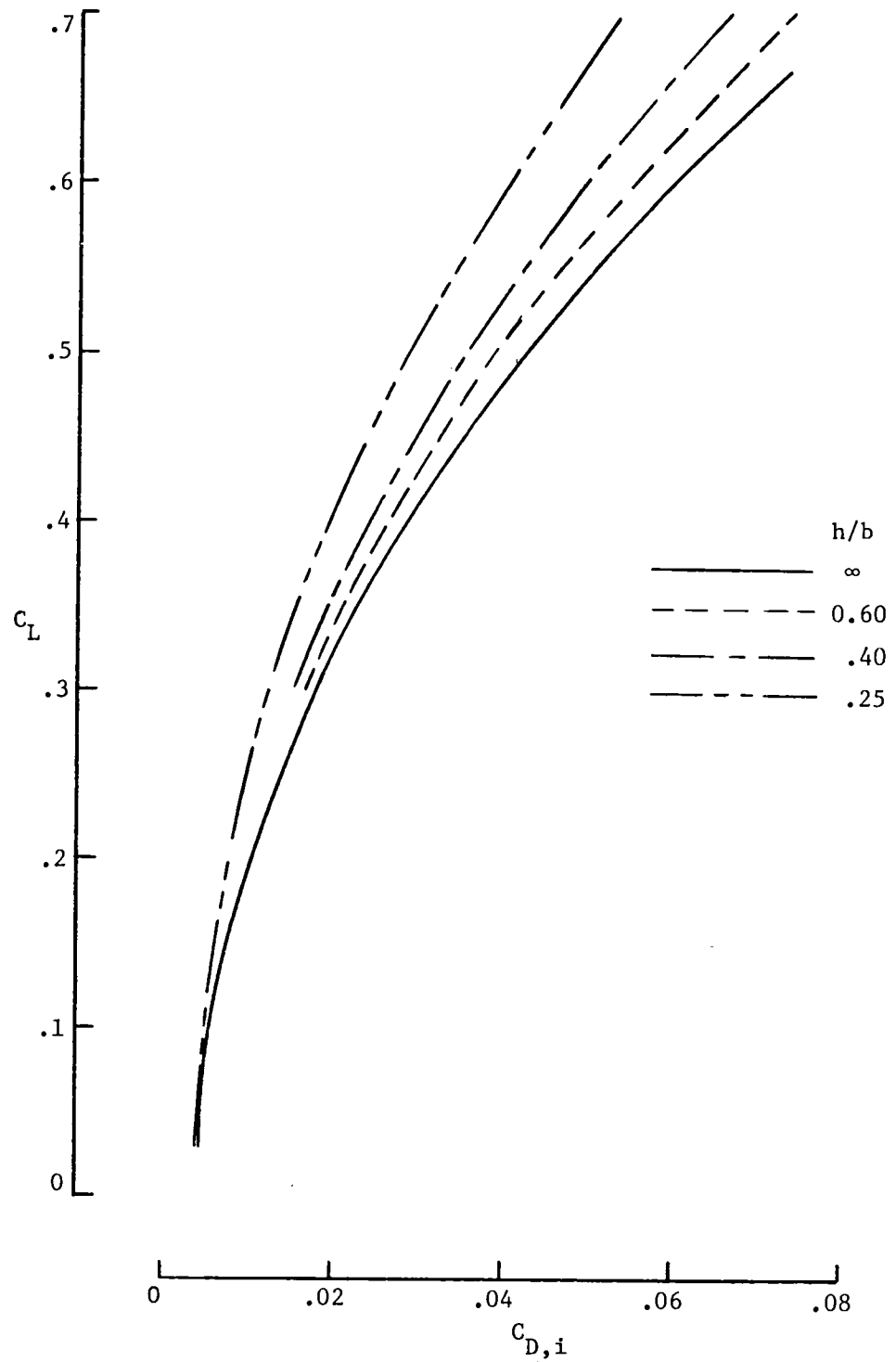


Figure 8.- Variation of C_L with $C_{D,i}$ determined for theoretical model.
WB; $\delta_f = 20^\circ/20^\circ/20^\circ$; $\delta_{le} = 30^\circ$.

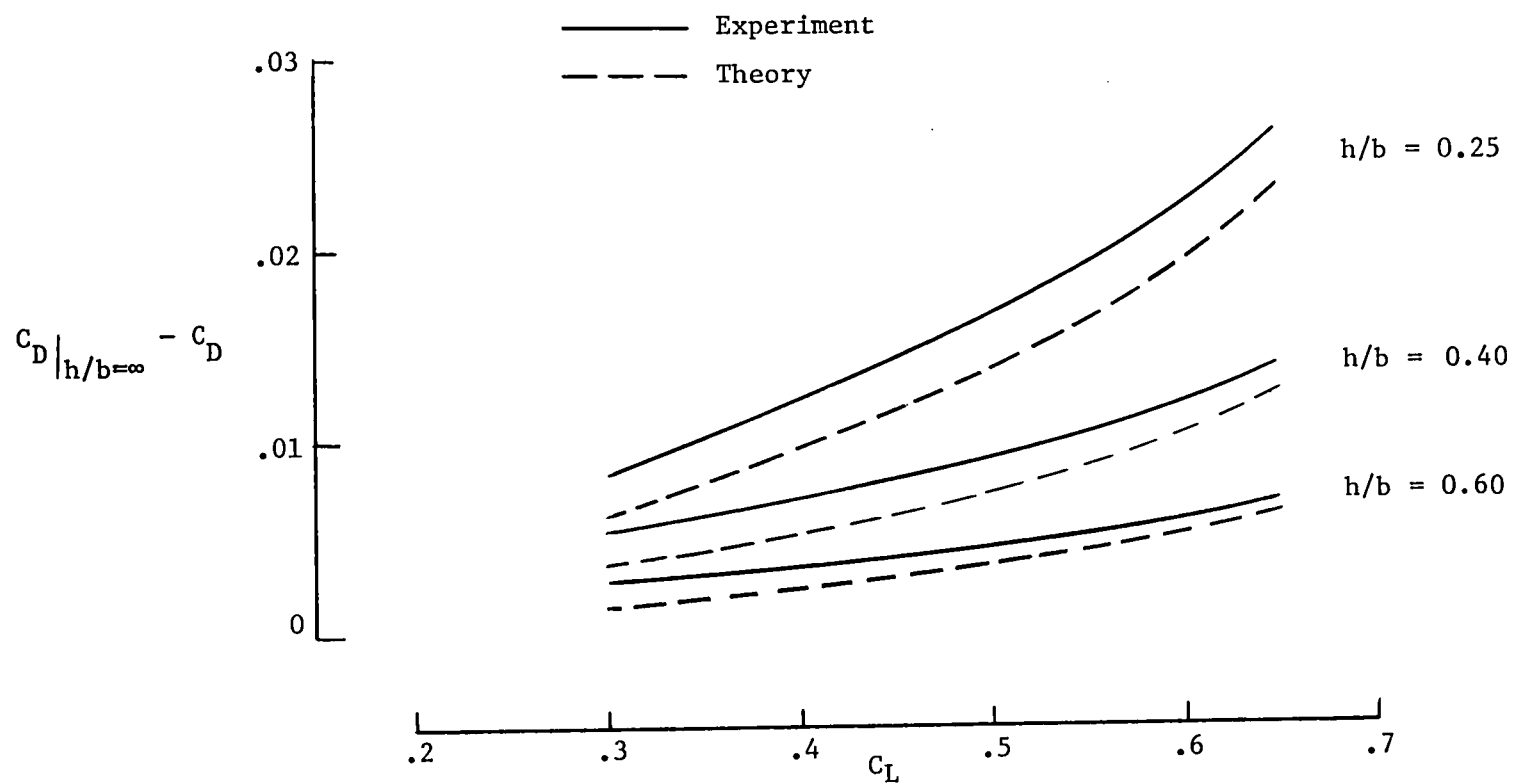


Figure 9.- Ground-induced drag reduction versus C_L . WB; $\delta_f = 20^\circ/20^\circ/20^\circ$; $\delta_{le} = 30^\circ$.

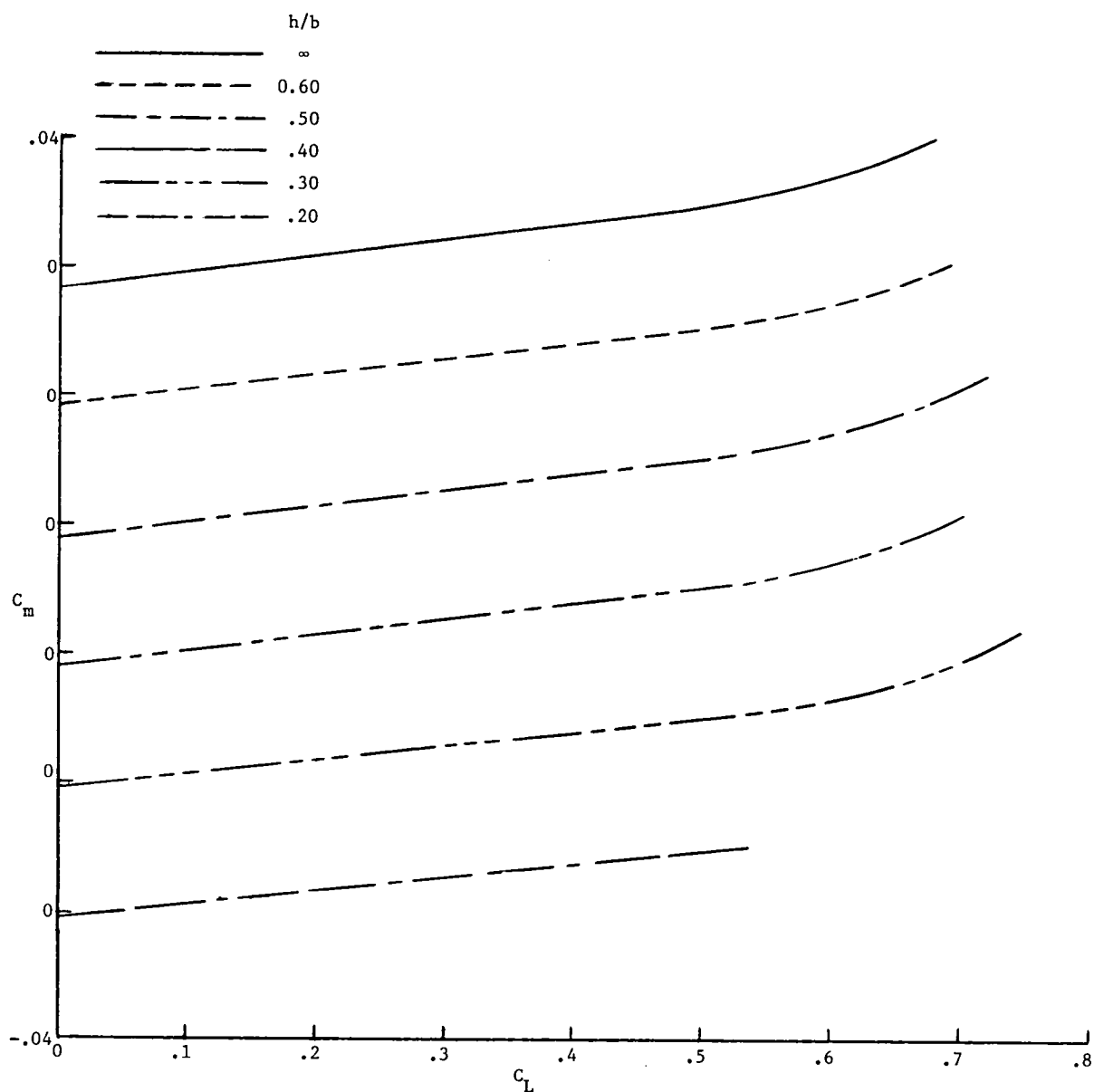


Figure 10.- Variation of C_m with C_L . WB; $\delta_f = 20^\circ/20^\circ/20^\circ$; $\delta_{le} = 30^\circ$.

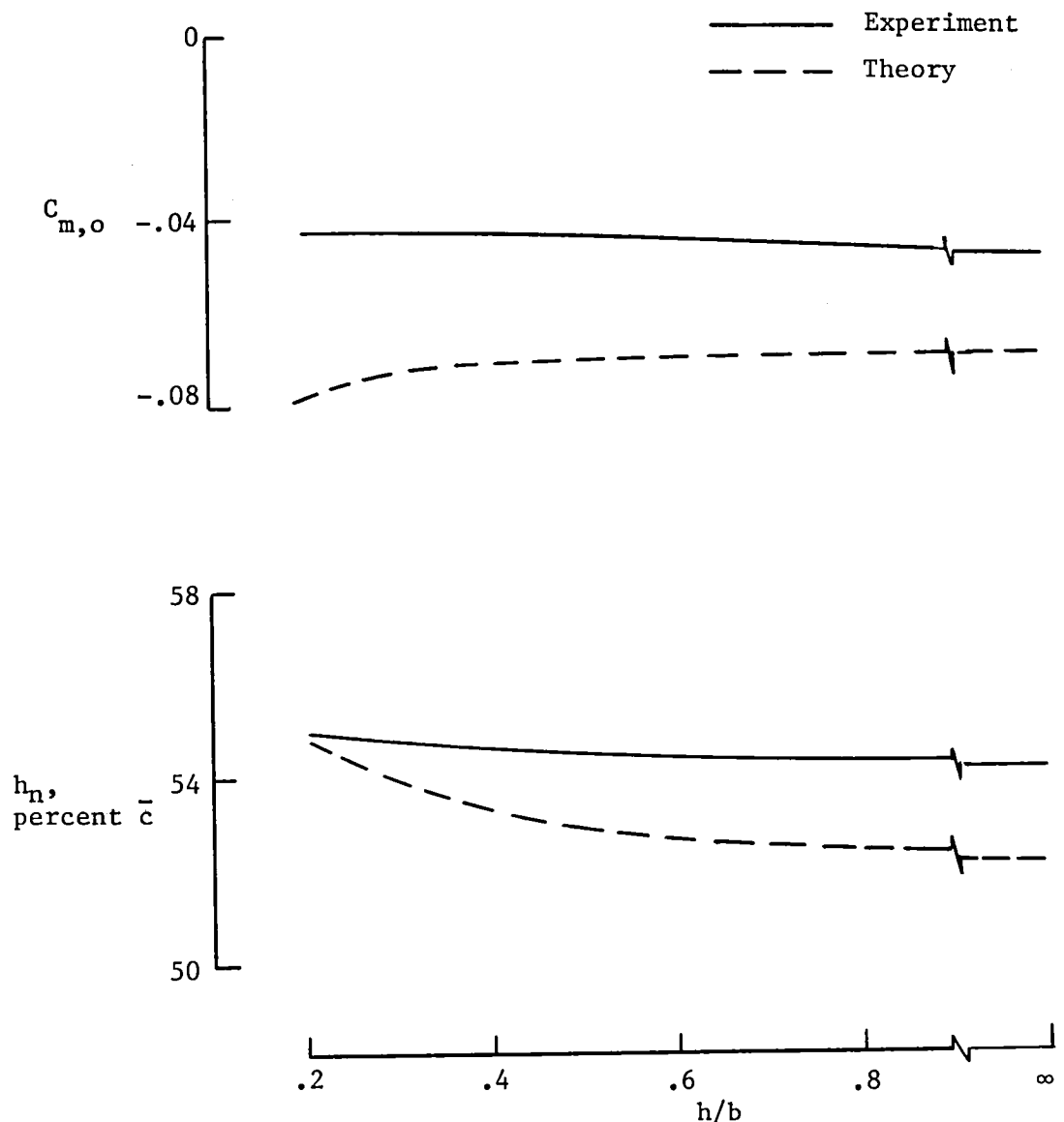
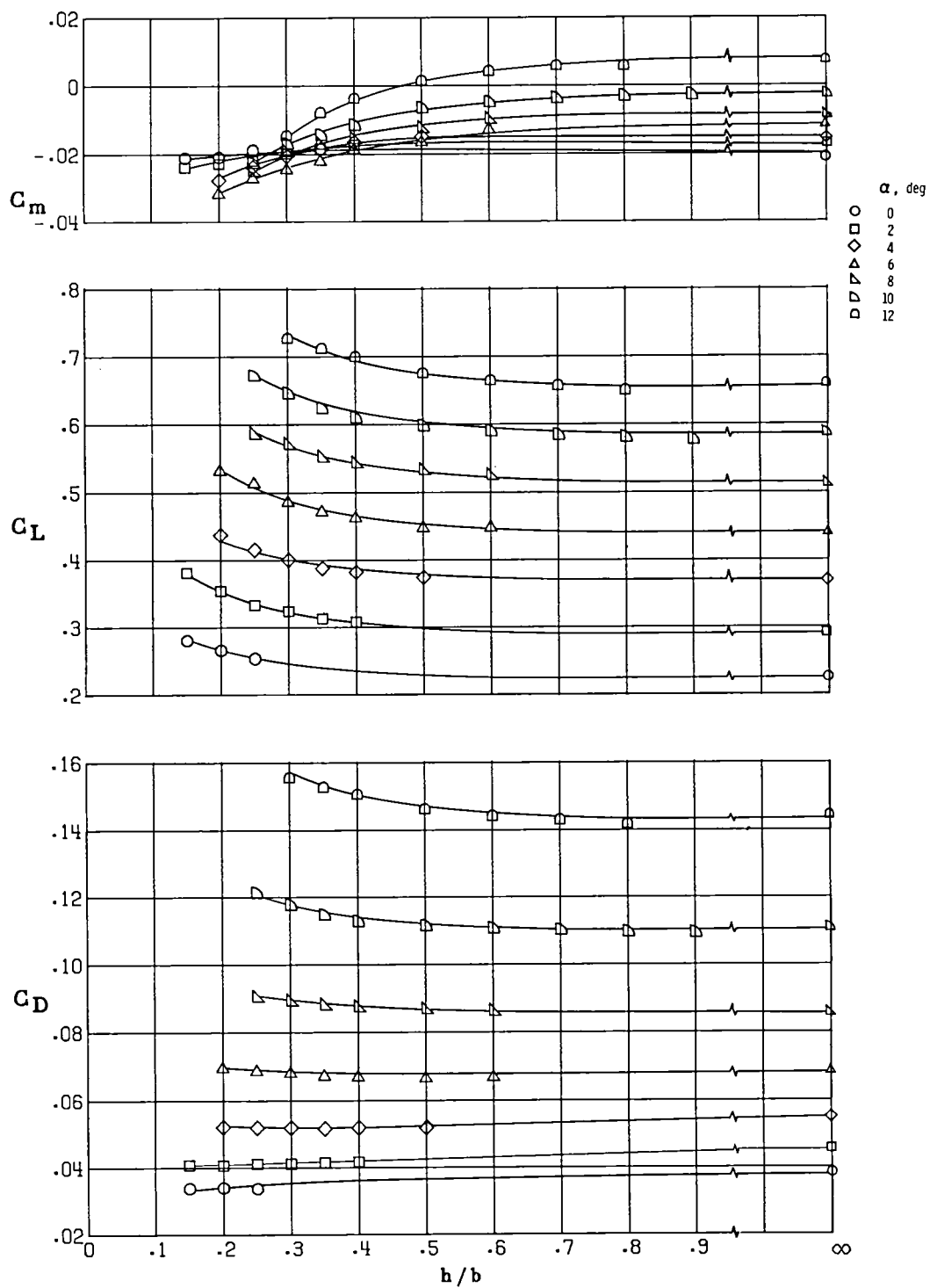
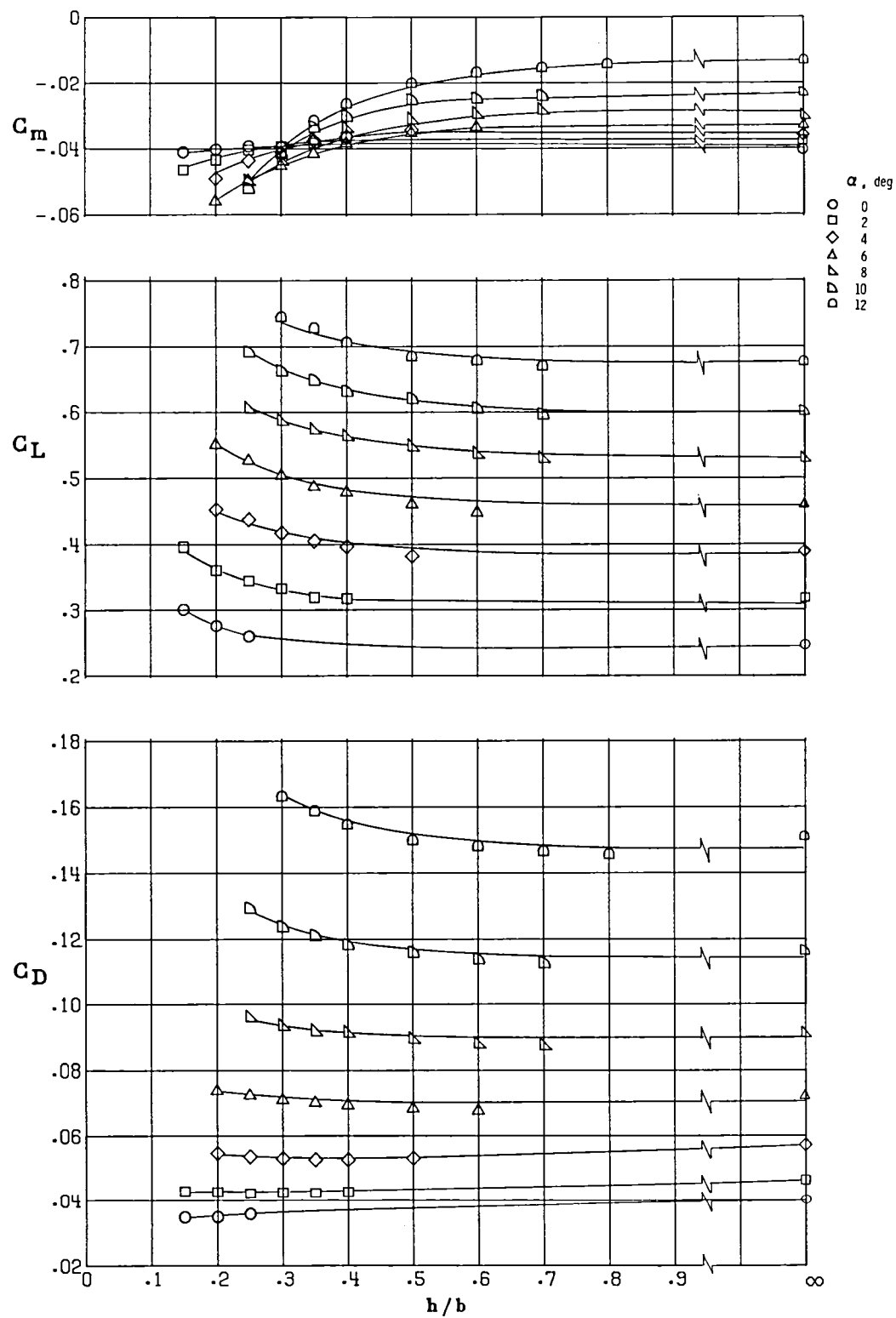


Figure 11.- Variation of $C_{m,o}$ and h_n with h/b . WB; $\delta_f = 20^\circ/20^\circ/20^\circ$; $\delta_{le} = 30^\circ$.



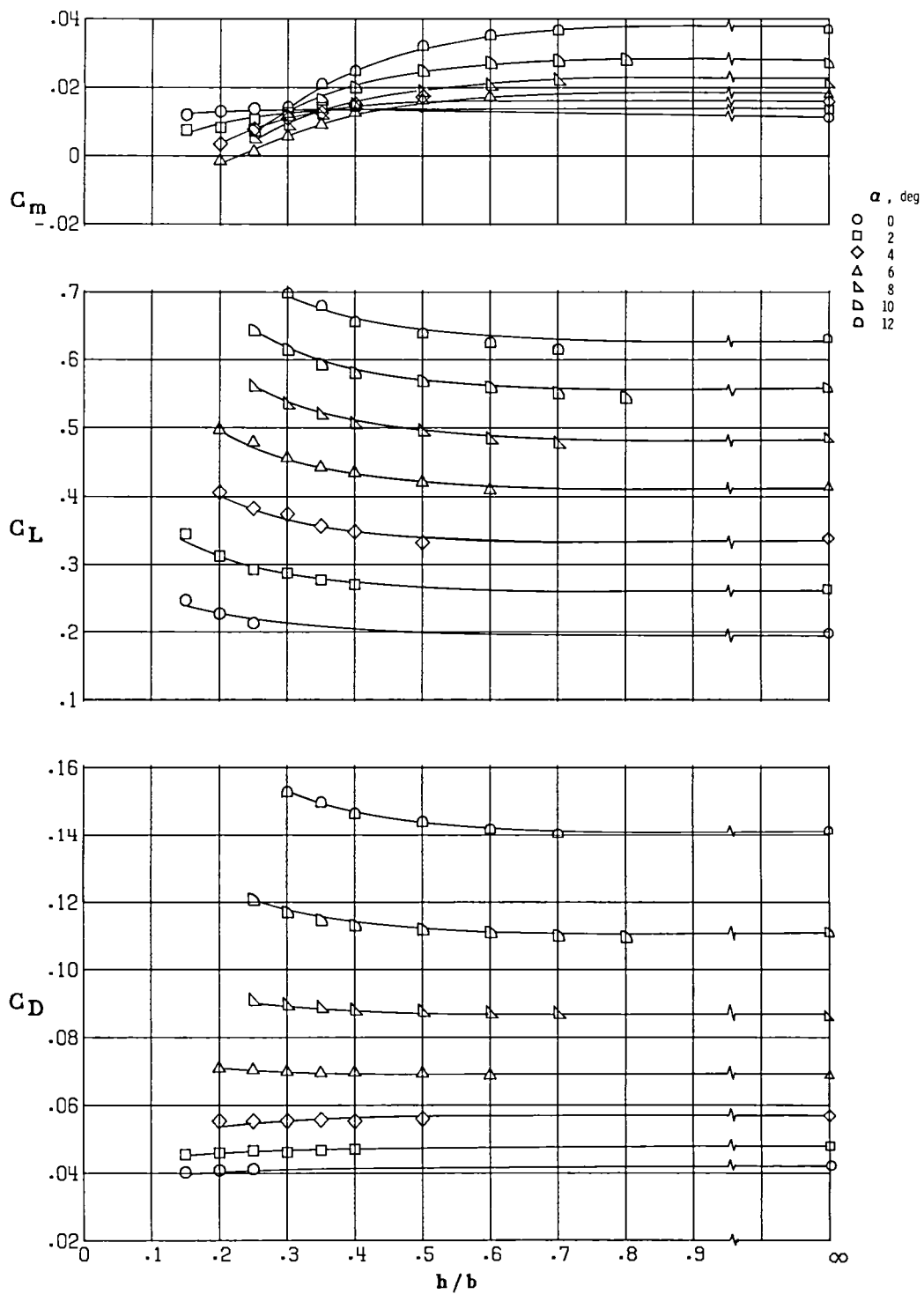
(a) $i_t = 0^\circ$.

Figure 12.- Longitudinal aerodynamic characteristics for the complete configuration. $\delta_f = 20^\circ/20^\circ/20^\circ$; $\delta_{le} = 30^\circ$.



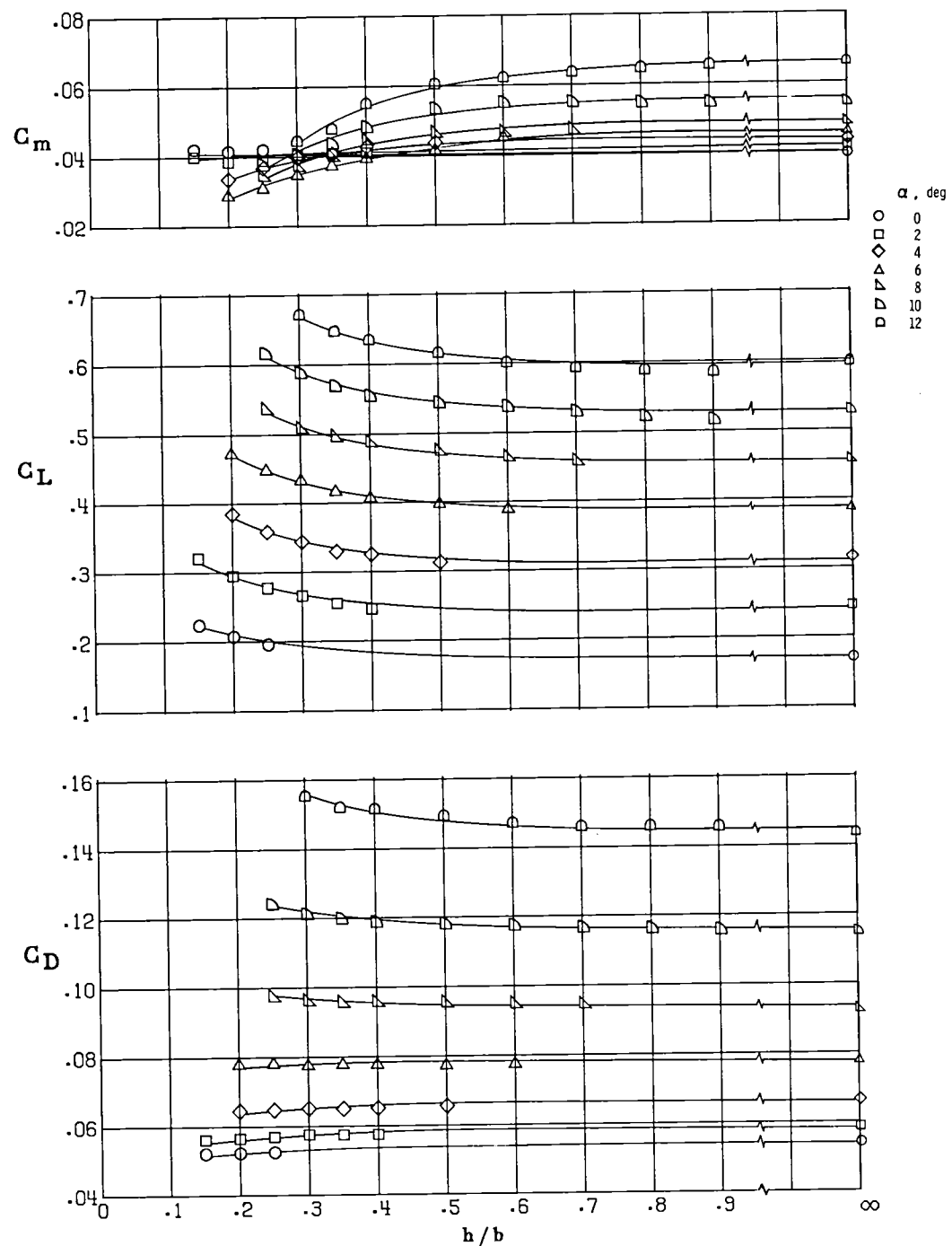
(b) $i_t = 10^\circ$.

Figure 12.- Continued.



(c) $i_t = -10^\circ$.

Figure 12.- Continued.



(d) $i_t = -20^\circ$.

Figure 12.- Concluded.

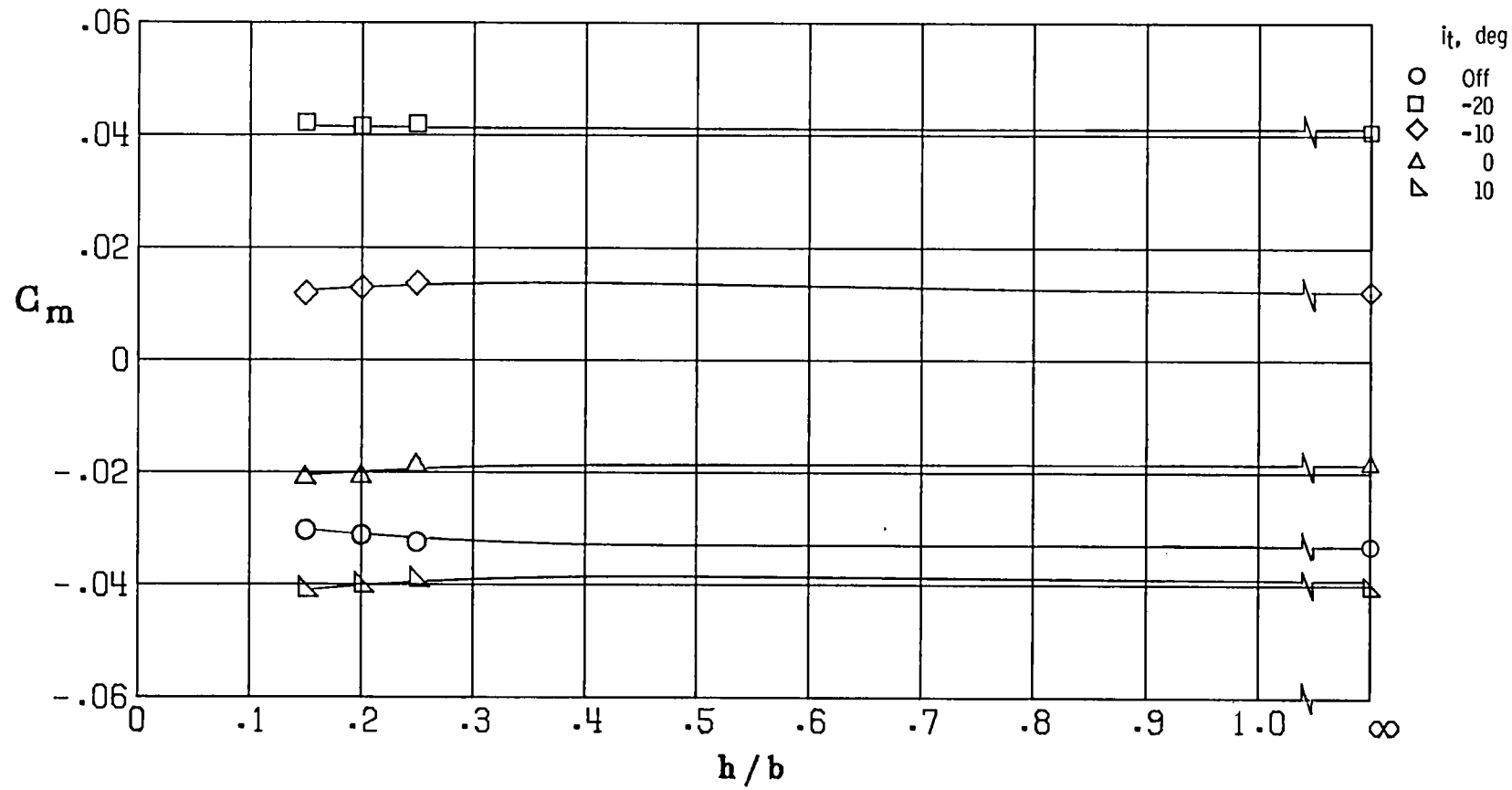
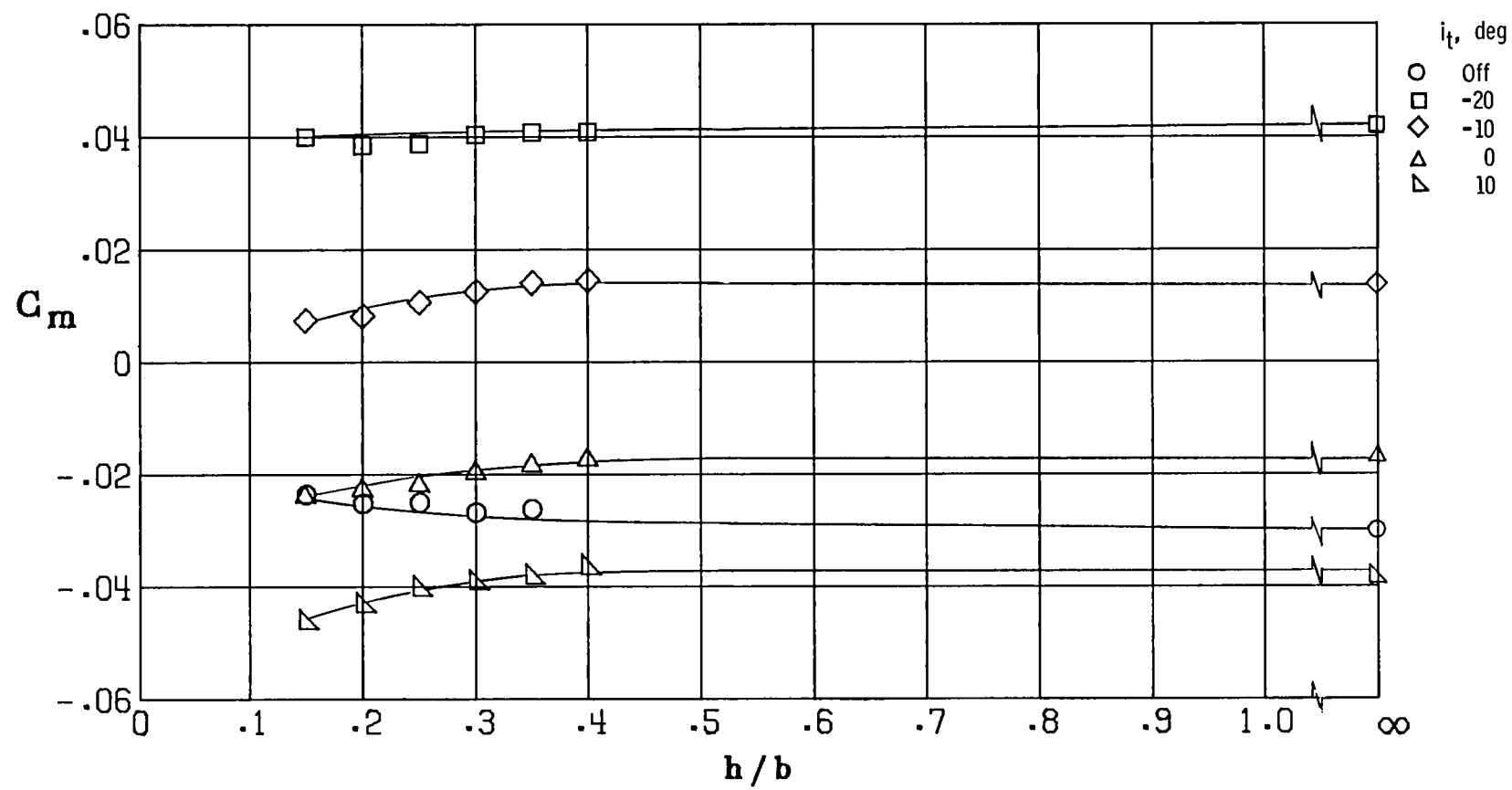
(a) $\alpha = 0^\circ$.

Figure 13.- Horizontal-tail effectiveness. $\delta_f = 20^\circ/20^\circ/20^\circ$; $\delta_{le} = 30^\circ$.



(b) $\alpha = 2^\circ$.

Figure 13.- Continued.

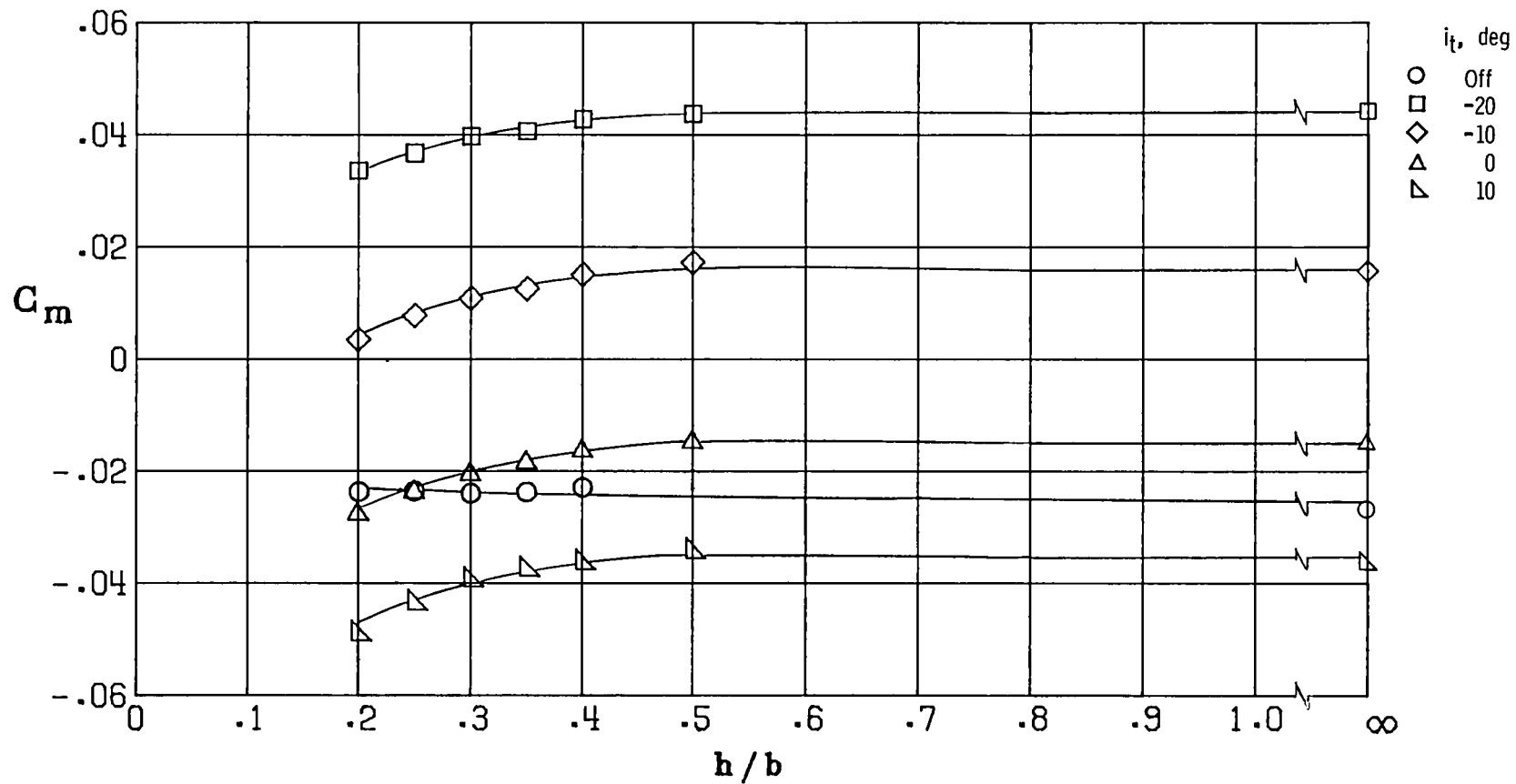
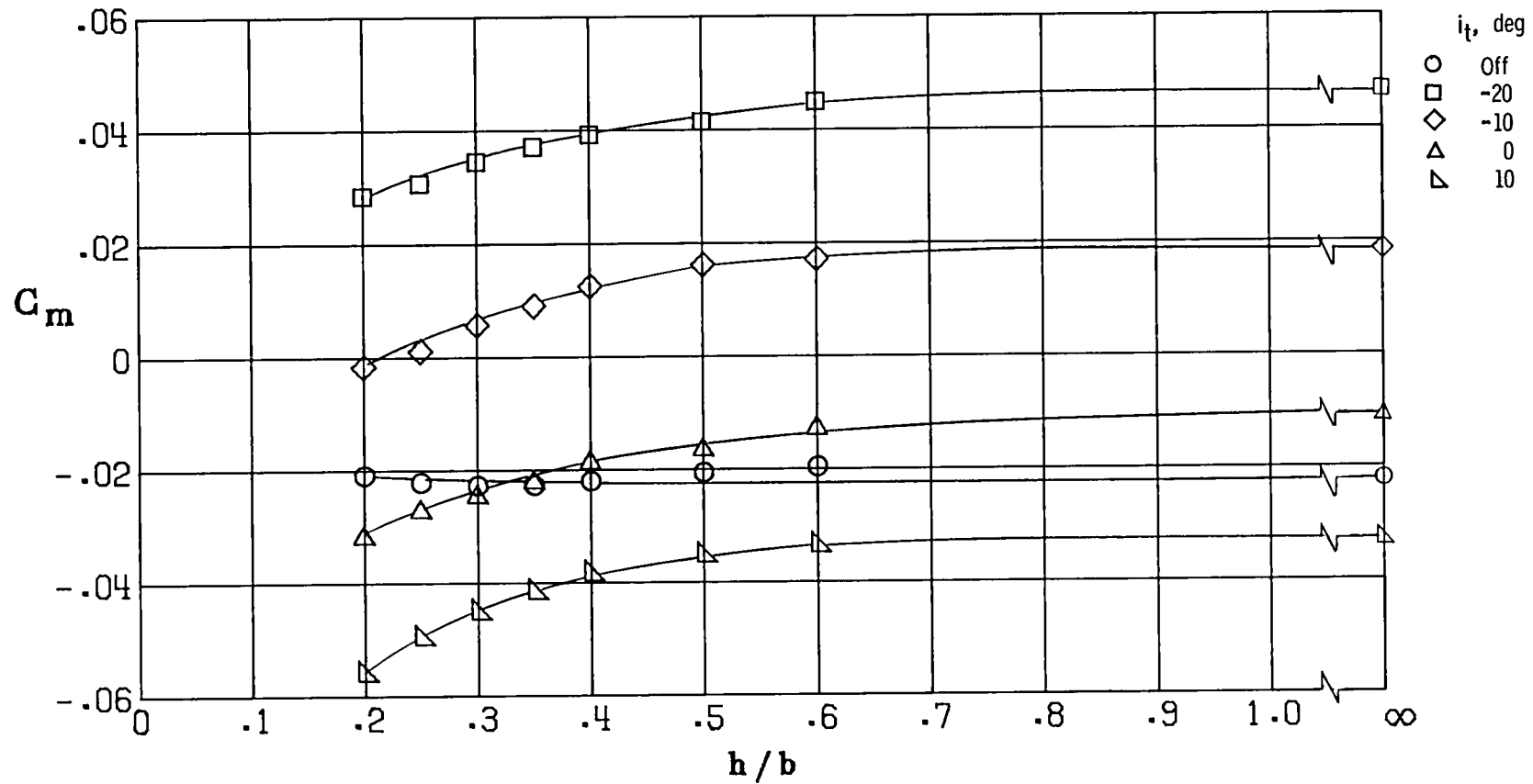
(c) $\alpha = 4^\circ$.

Figure 13.- Continued.



(d) $\alpha = 6^\circ$.

Figure 13.- Continued.

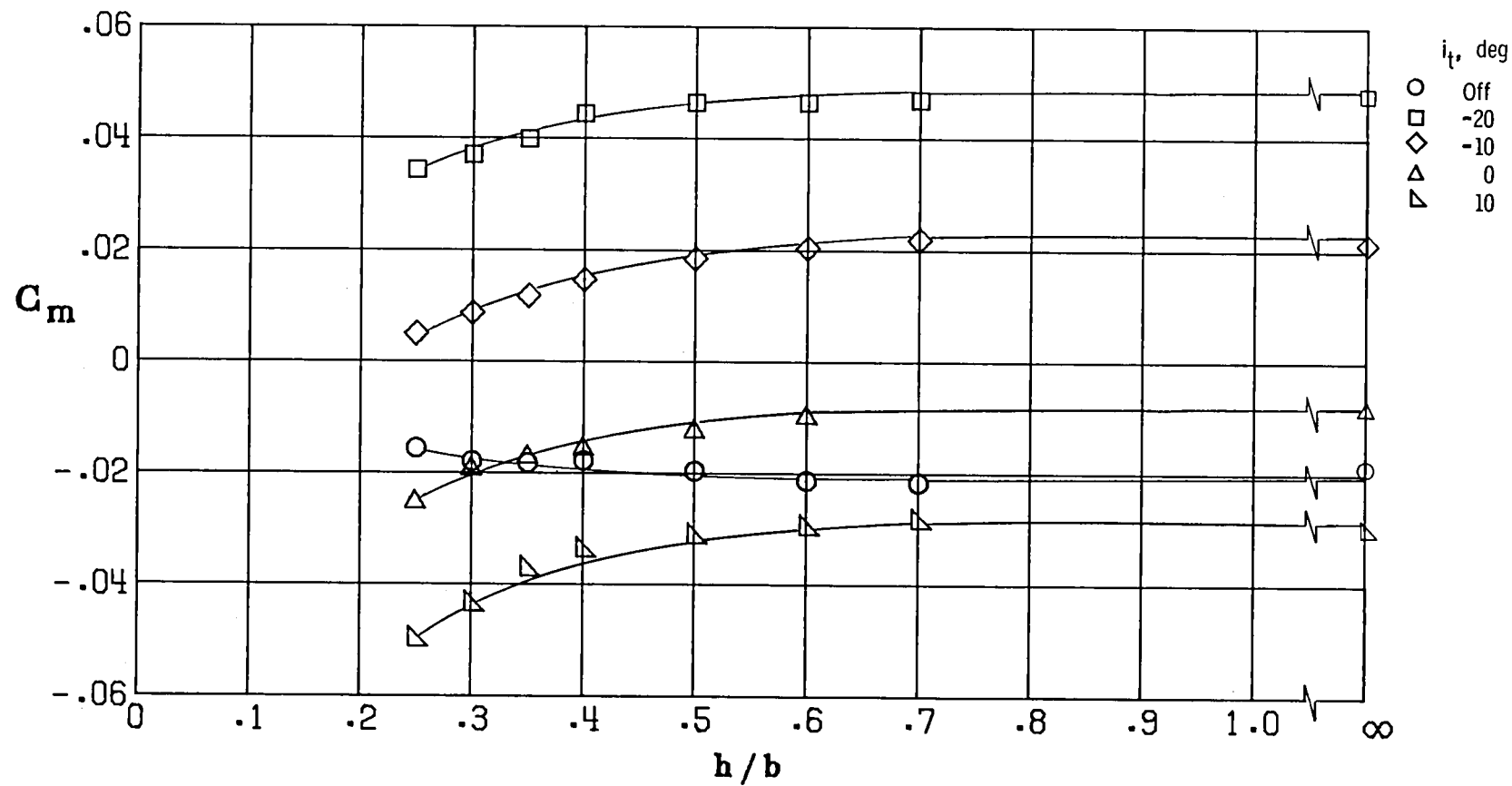
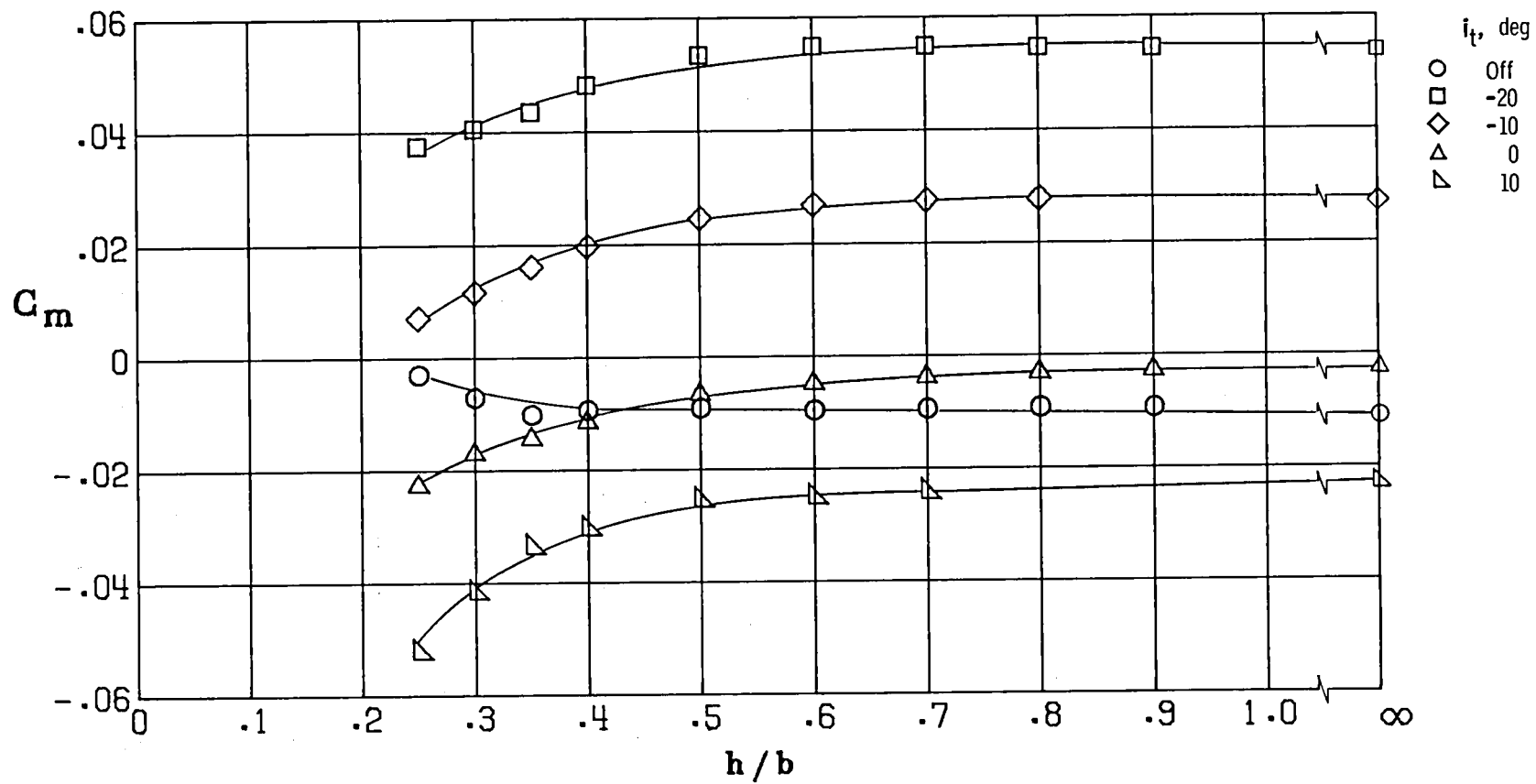
(e) $\alpha = 8^\circ$.

Figure 13.- Continued.



(f) $\alpha = 10^\circ$.

Figure 13.- Continued.

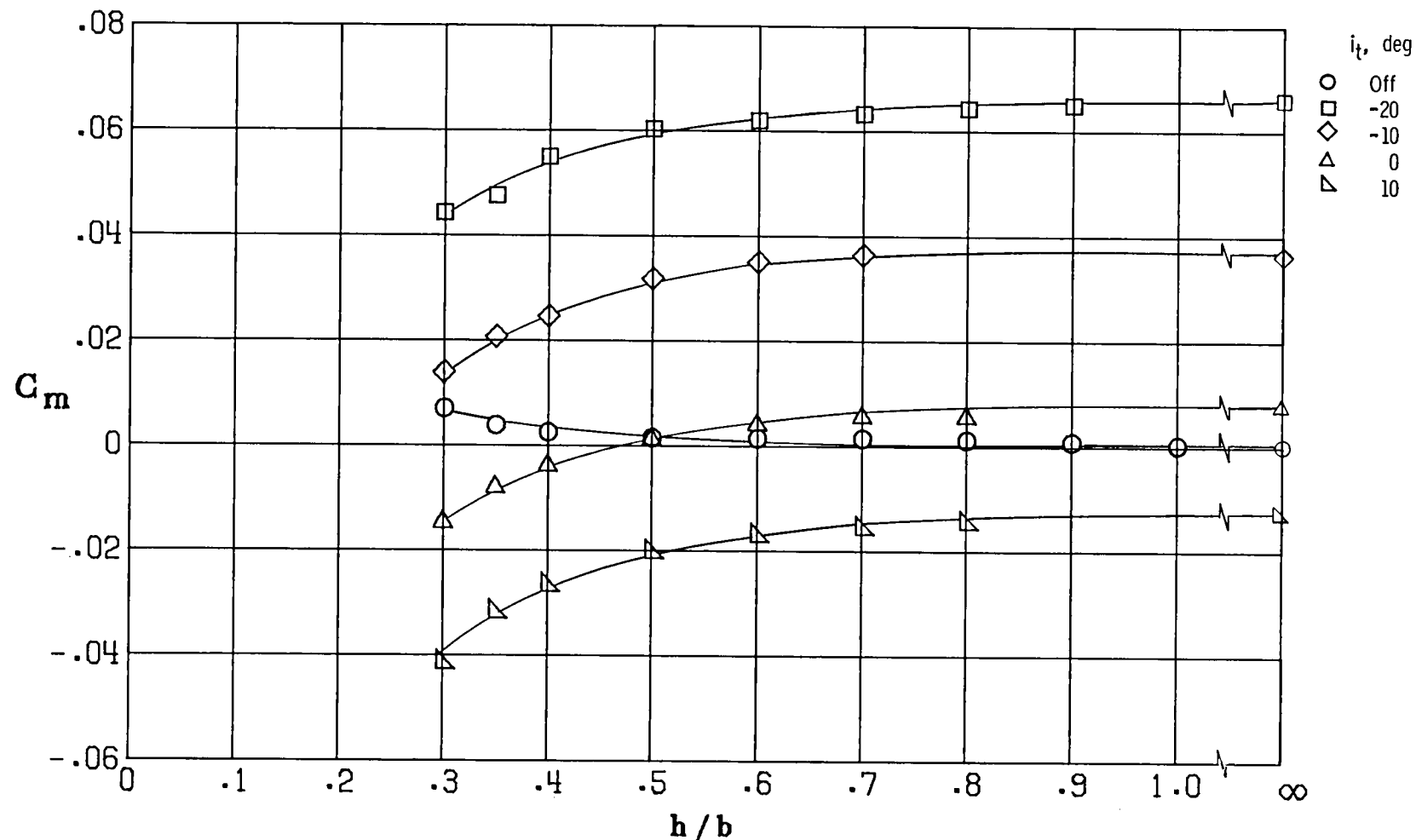
(g) $\alpha = 12^\circ$.

Figure 13.- Concluded.

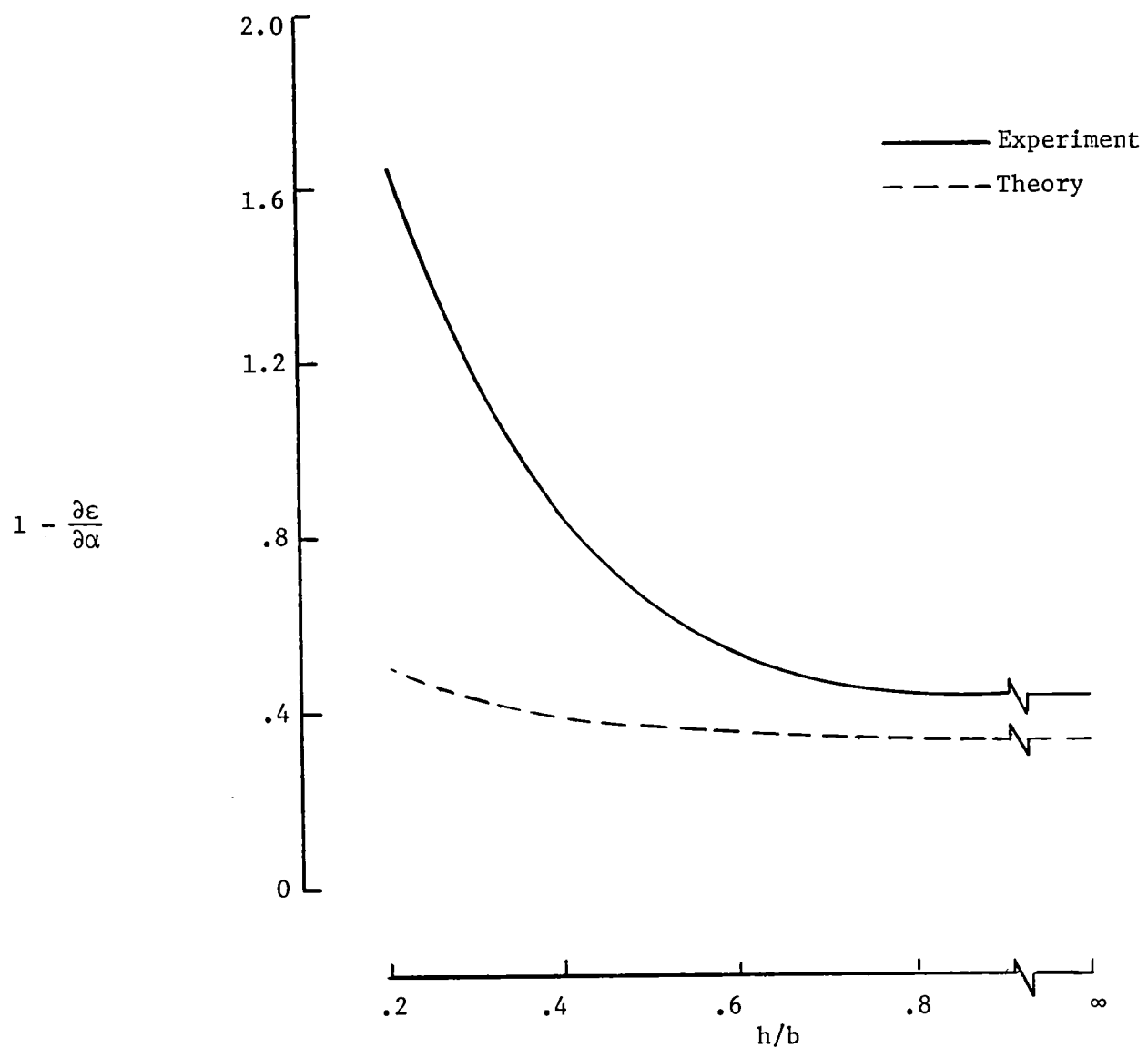


Figure 14.- Variation of tail downwash parameter with h/b . $\delta_f = 20^\circ/20^\circ/20^\circ$;
 $\delta_{le} = 30^\circ$.

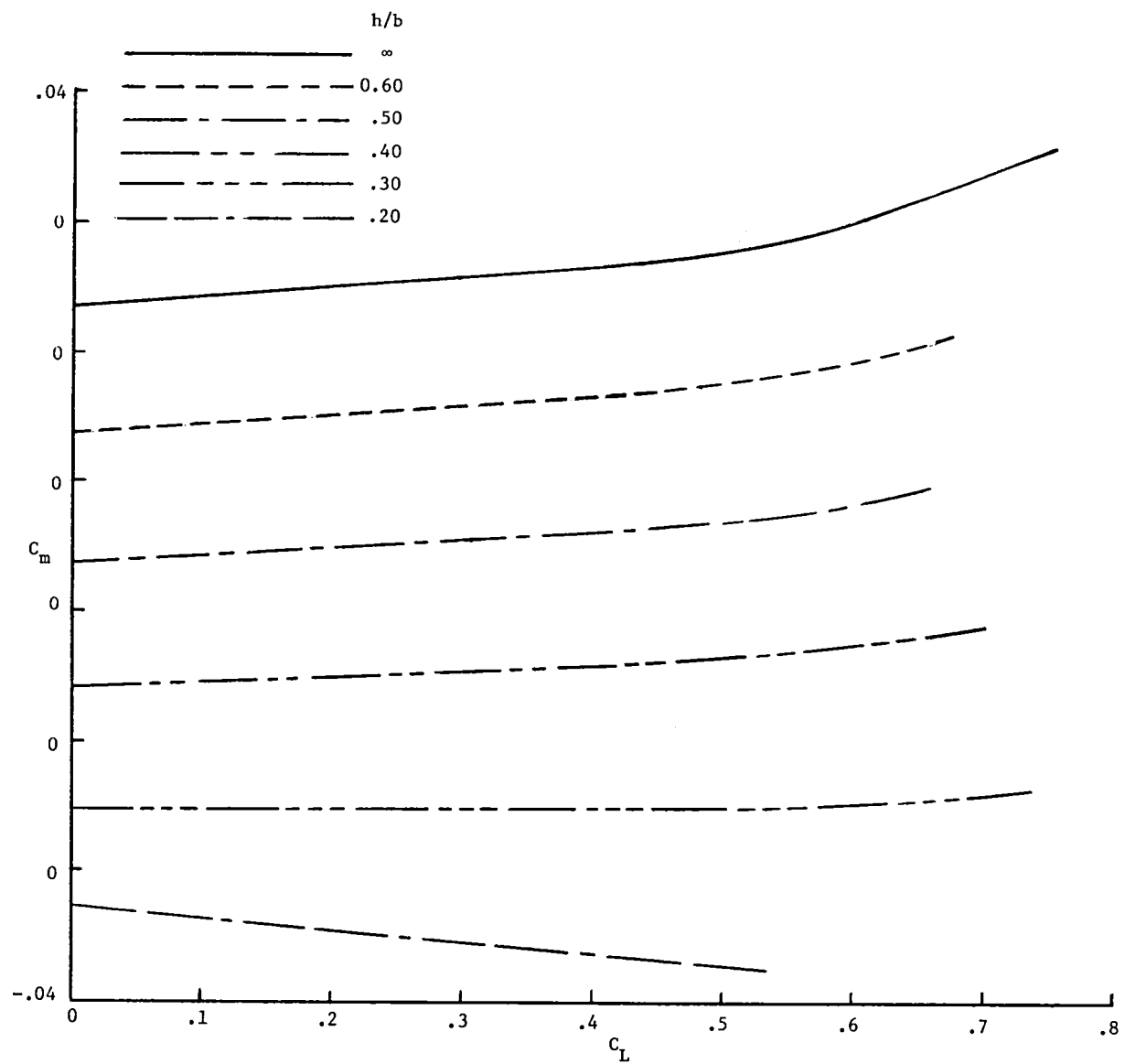


Figure 15.- Variation of C_m with C_L . WBVH; $\delta_F = 20^\circ/20^\circ/20^\circ$; $\delta_{le} = 30^\circ$; $i_t = 0^\circ$.

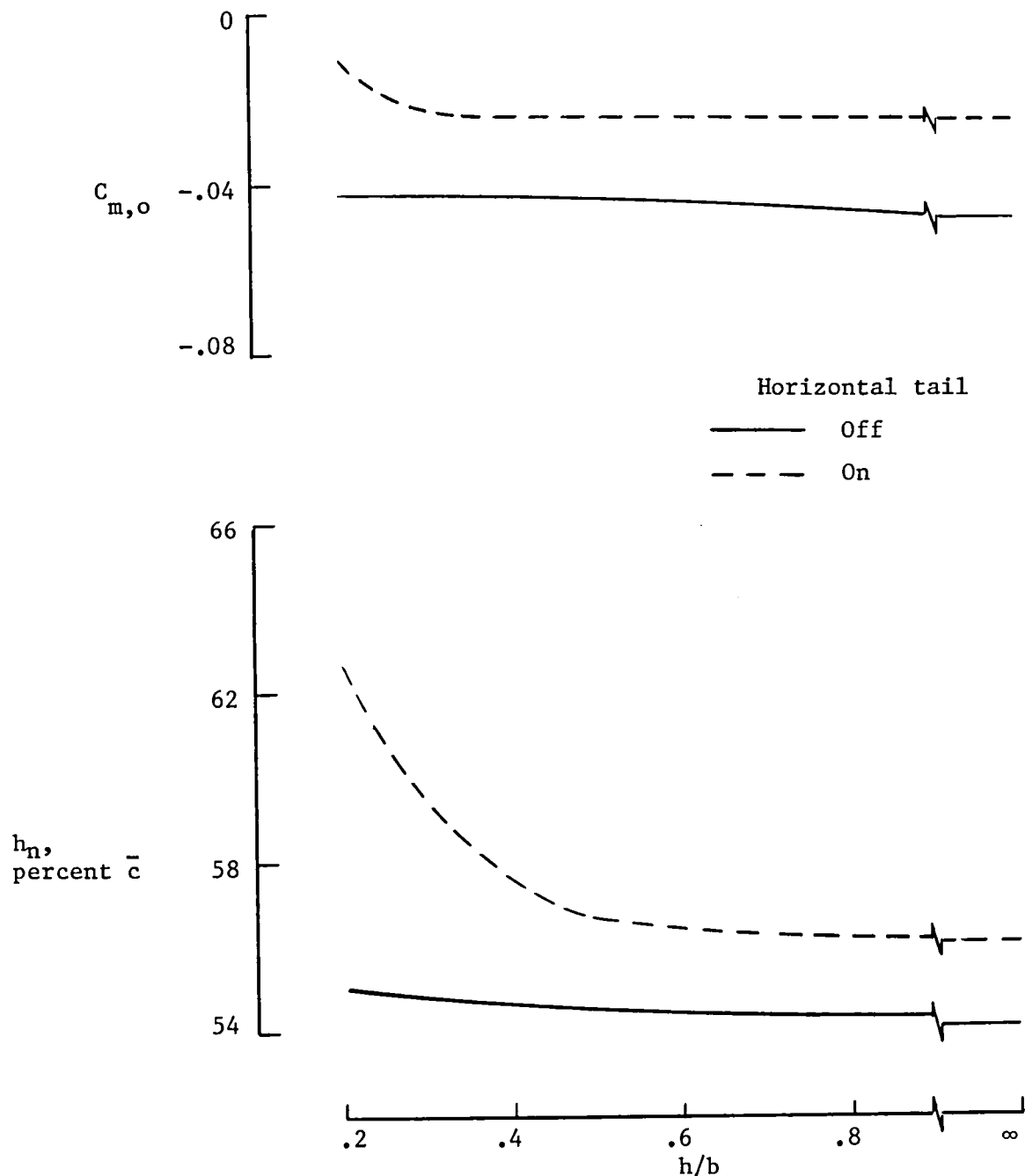


Figure 16.- Variation of $C_{m,0}$ and h_n with h/b . $\delta_f = 20^\circ/20^\circ/20^\circ$; $\delta_{le} = 30^\circ$.

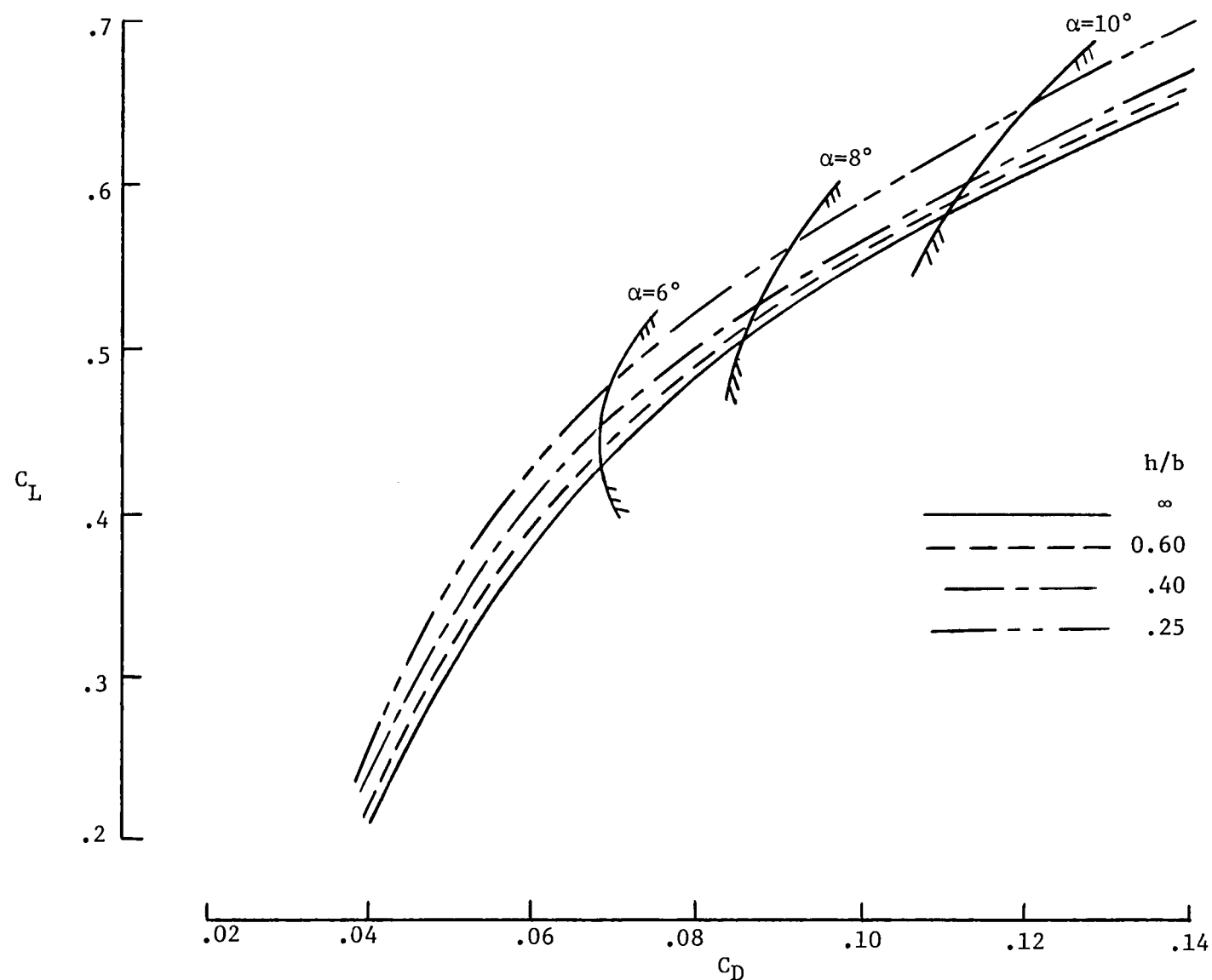


Figure 17.- Trim drag polars. Moment reference center at $0.5916\bar{c}$;
 $\delta_f = 20^\circ/20^\circ/20^\circ$; $\delta_{le} = 30^\circ$.

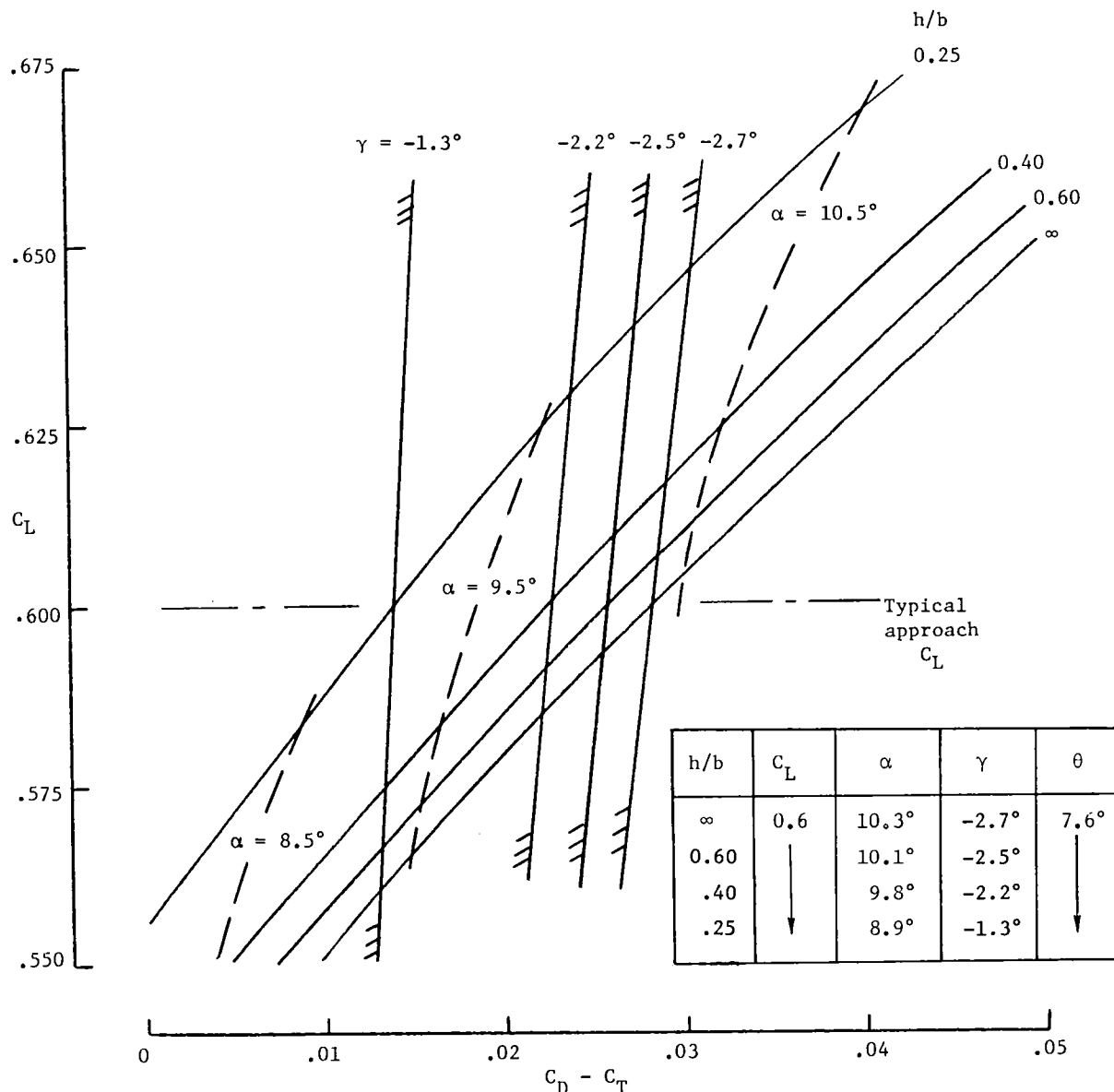
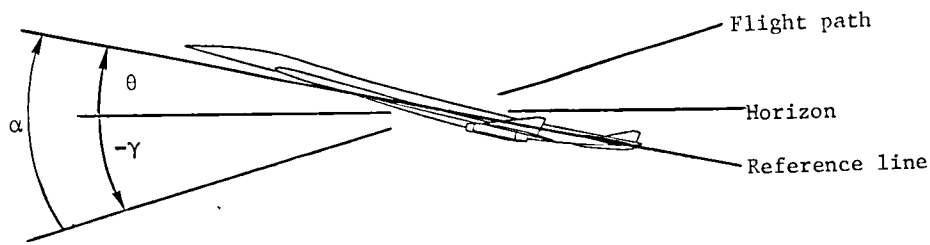


Figure 18.- Trim drag polars with thrust applied. $C_T = 0.089$;
 $\delta_f = 20^\circ/20^\circ/20^\circ$; $\delta_{le} = 30^\circ$.

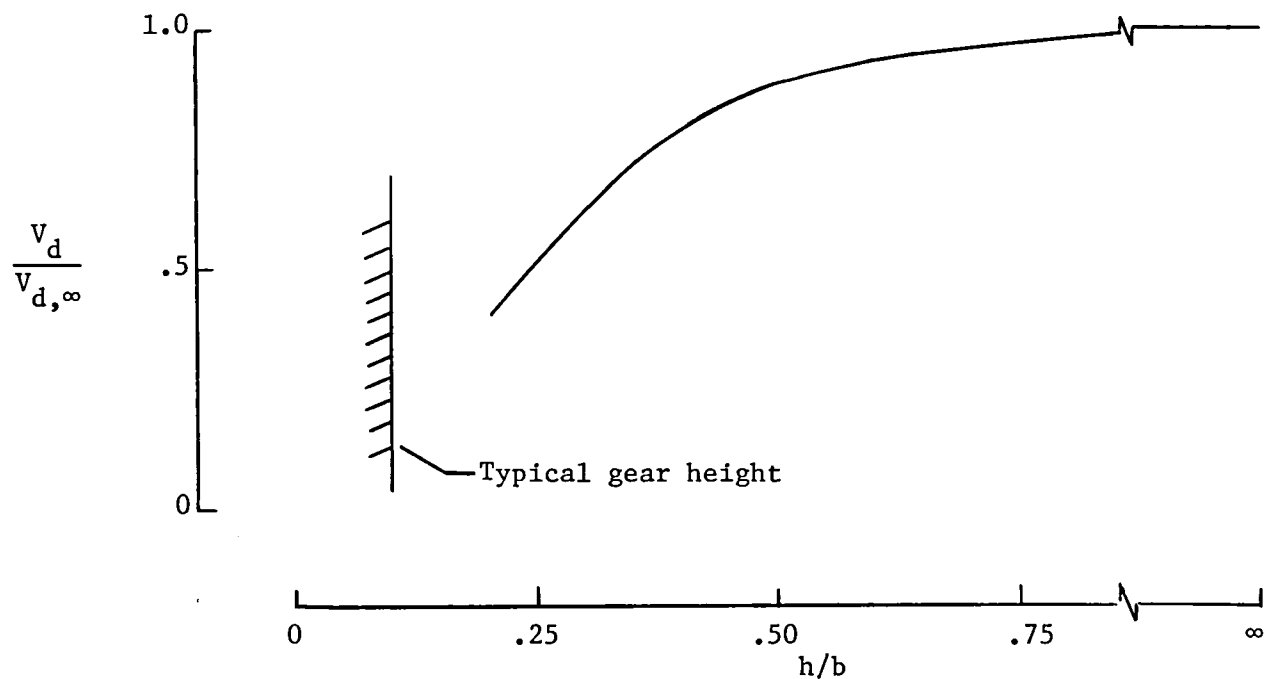


Figure 19.- Vertical sink rate versus h/b for quasi-steady-state approach maneuver.

APPENDIX A

MECHANISM OF GROUND-INDUCED EFFECTS

As is well known (see, for example, ref. 10), the aerodynamics of an airplane flying in proximity to the ground differ from that of an airplane in free air. The difference is due to the additional boundary condition of zero flow normal to the ground. This boundary condition may be satisfied by considering the ground plane as a plane of symmetry with an aircraft mirror image represented as illustrated in figure A1. (See refs. 11 and 12 for a more detailed discussion of the image system.) Both the physical wing and ground-plane image may then be replaced with a vortex-lattice arrangement. Figure A2 presents a simplistic sketch intended to illustrate the above-mentioned concept.

Application of the classical laws of vortex induction to the arrangement depicted schematically in figure A2 yields the familiar result of the configuration experiencing an upwash induced by its ground-plane image. Furthermore, by neglecting higher order terms, the magnitude of this upwash is found to be inversely proportional to the height of the configuration above the ground h . This ground-induced upwash may be considered as a ground-induced angle of attack α_G which is also inversely proportional to h . Inasmuch as the upwash, and hence α_G , is proportional to the circulation of the vortex elements, it follows that α_G is proportional to lift. Therefore, introducing nondimensional terms, α_G may be expressed as

$$\alpha_G = \frac{KC_L}{h/b} \quad (A1)$$

where K is a constant of proportionality.

Lift coefficient can be expressed as

$$C_L = C_1 + C_2\alpha \quad (A2)$$

where C_1 and C_2 are constants, and

$$\alpha = \alpha_\infty + \alpha_G \quad (A3)$$

where α_∞ is the free-stream angle of attack; it therefore follows that

$$\alpha = \alpha_\infty + \frac{KC_L}{h/b} \quad (A4)$$

APPENDIX A

Substituting equation (A4) into equation (A2) and rearranging terms yields

$$C_L = \frac{C_1}{1 - \frac{KC_2}{h/b}} + \frac{C_2 \alpha_\infty}{1 - \frac{KC_2}{h/b}} \quad (A5)$$

Comparison of equation (A5) with the conventional form

$$C_L = C_{L|_{\alpha=0}} + C_{L\alpha} \alpha_\infty \quad (A6)$$

yields

$$C_{L|_{\alpha=0}} = \frac{C_1}{1 - \frac{KC_2}{h/b}} \quad C_{L\alpha} = \frac{C_2}{1 - \frac{KC_2}{h/b}} \quad (A7)$$

The preceding simple analysis is intended to demonstrate that due to the additional upwash both the lift evaluated at $\alpha = 0^\circ$ and the lift-curve slope would be expected to increase as h/b decreases. However, at low heights and high lift coefficients, an additional backwash contribution causes a decrease in lift. This additional backwash contribution is not accounted for in the present analysis.

In addition to an increase in C_L , the ground-induced upwash also results in a reduction in induced drag. Some insight into the mechanism responsible for the reduction in induced drag can be afforded by considering the classical theorem of Kutta and Joukowski

$$\bar{F} = \rho \bar{V} \times \bar{\Gamma} \quad (A8)$$

where \bar{F} = Resultant force vector; ρ = Density; \bar{V} = Velocity vector; and $\bar{\Gamma}$ = Circulation vector.

Application of this law to the elemental vortex depicted in figure A3 shows that, in general, upwash results in a reduction of the rearward inclination of the resultant force vector. Consequently, upwash is seen to result in an increase in the lift component and a reduction in the drag component of the resultant force.

APPENDIX A

The influence of ground proximity on longitudinal stability can be determined by reconsidering the vortex arrangement depicted in figure A2. From this sketch, it can be seen that the upwash induced by the ground-plane image will vary in both the spanwise and chordwise directions. However, it would in general be expected that for a given spanwise station, the induced upwash would be greatest over the aft portion of the wing. To illustrate this point, figure A4 presents the upwash, which is induced by the ground-plane image and computed with the vortex-lattice theoretical model. The increased aft loading, which would be expected to result from the increased local angle of attack, would of course also be proportional to C_L and inversely proportional to h/b . Therefore, for a given h/b , the aerodynamic center would be located rearward relative to the location of the aerodynamic center when $h/b = \infty$. Consequently, decreasing h/b results in an increase in static longitudinal stability.

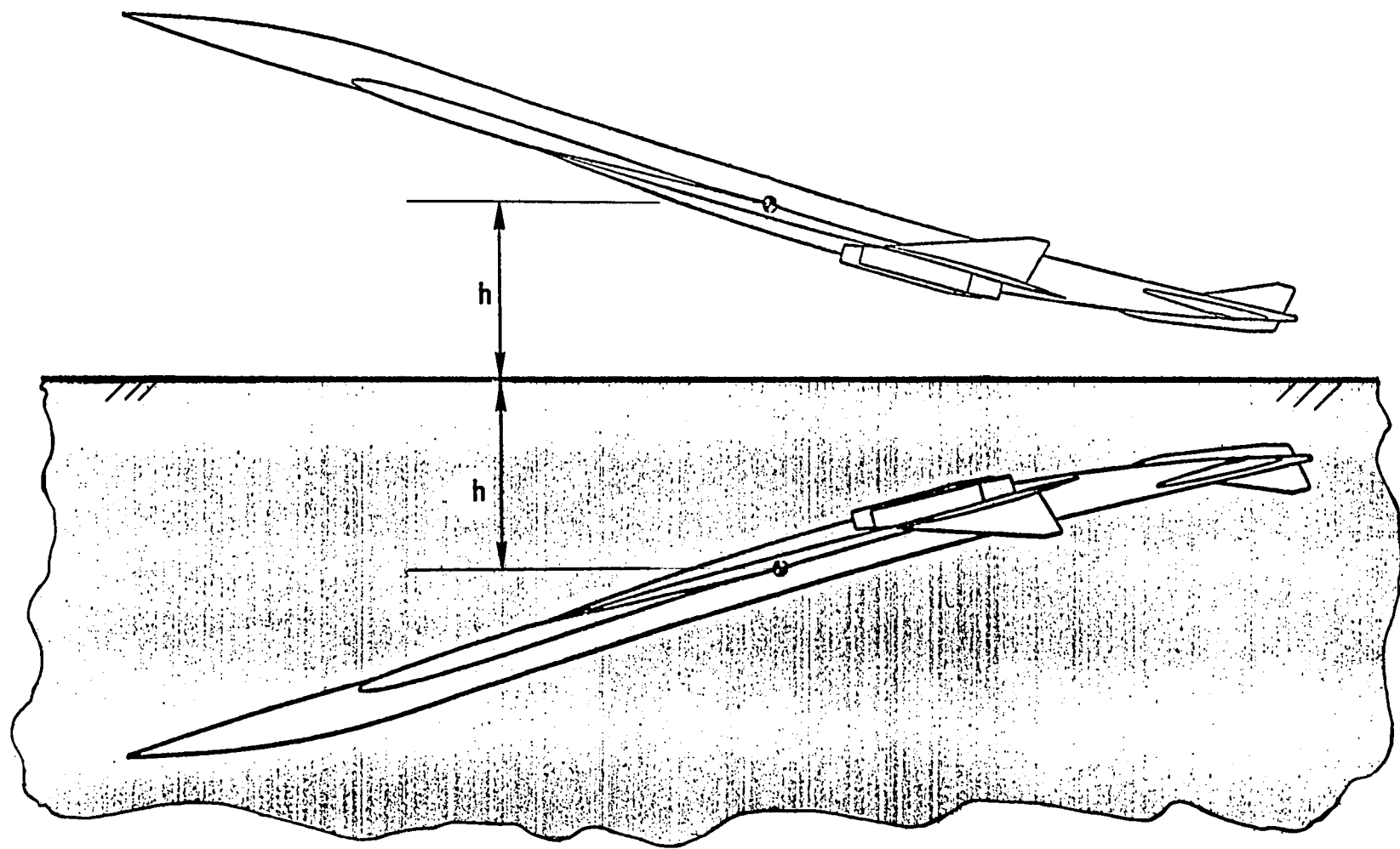


Figure A1.- Ground-plane image concept.

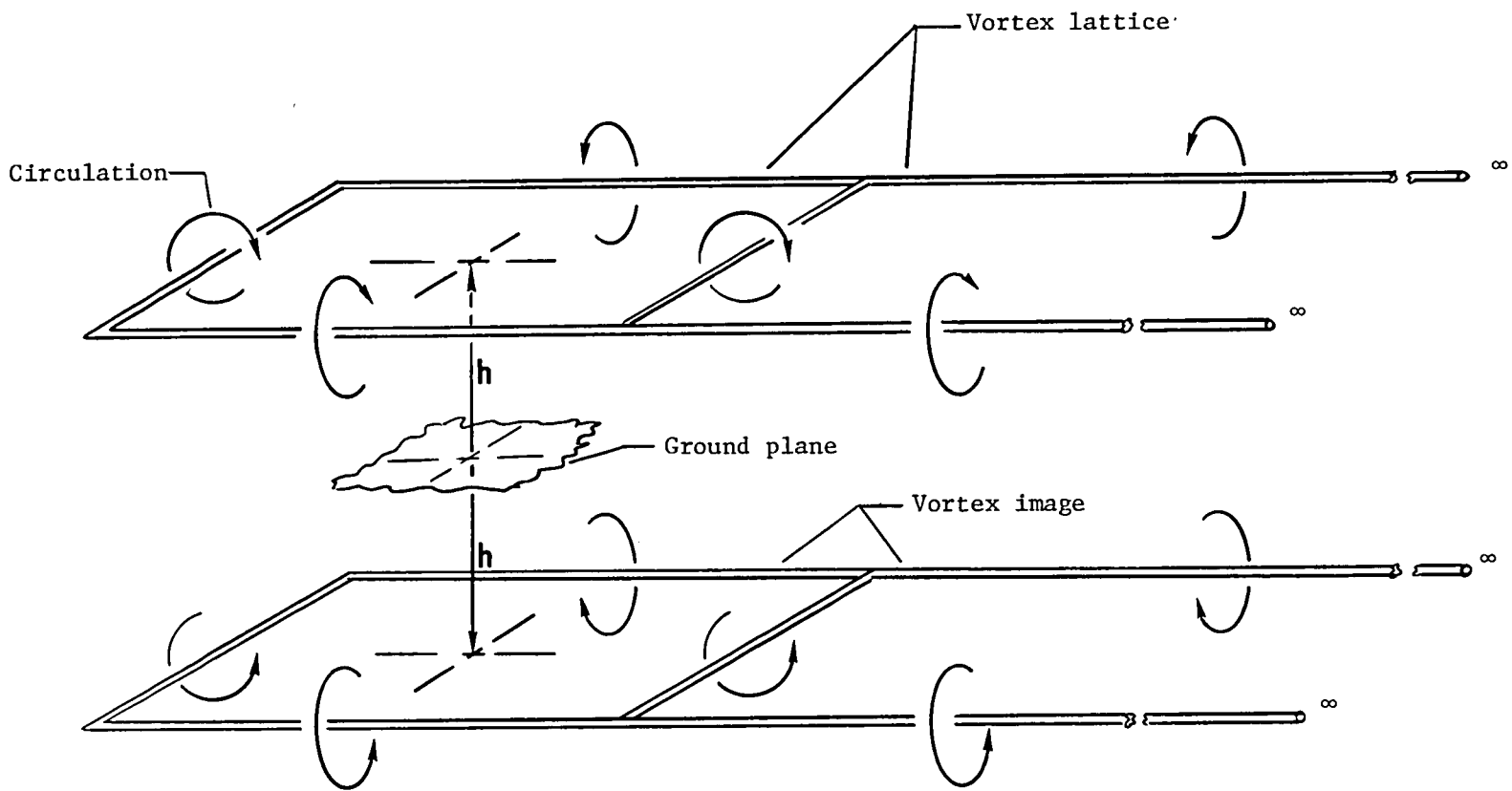
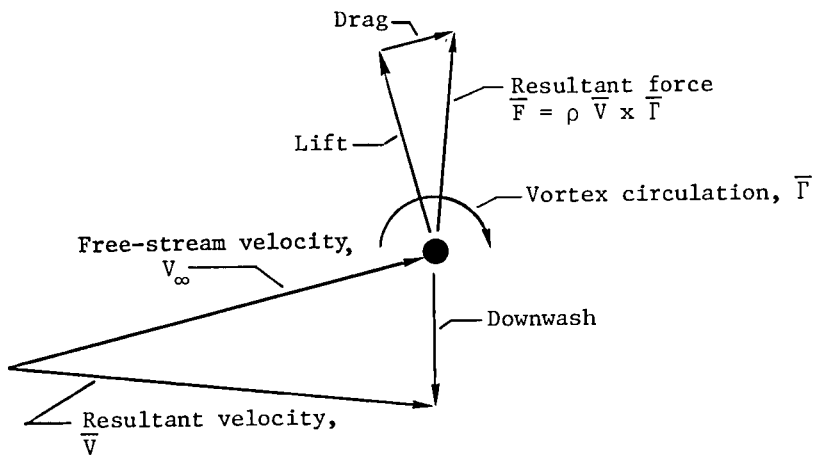
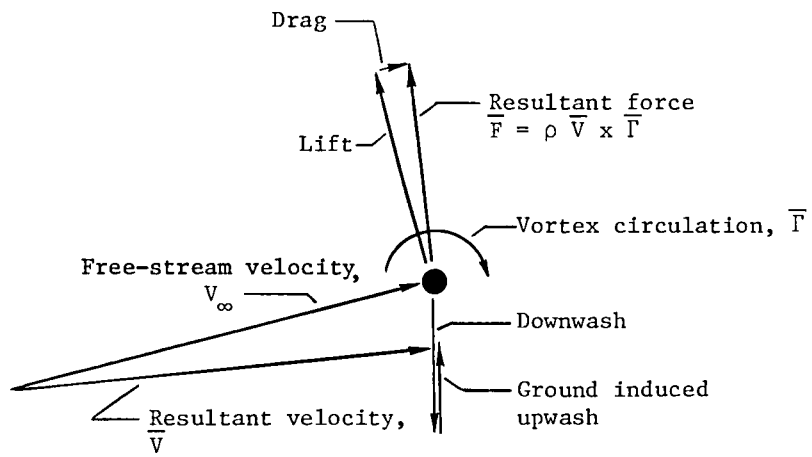


Figure A2.- Fundamental ground-induced vortex image system.



(a) Out-of-ground proximity.



(b) In-ground proximity.

Figure A3.- Effect of ground-induced upwash on lift and drag.

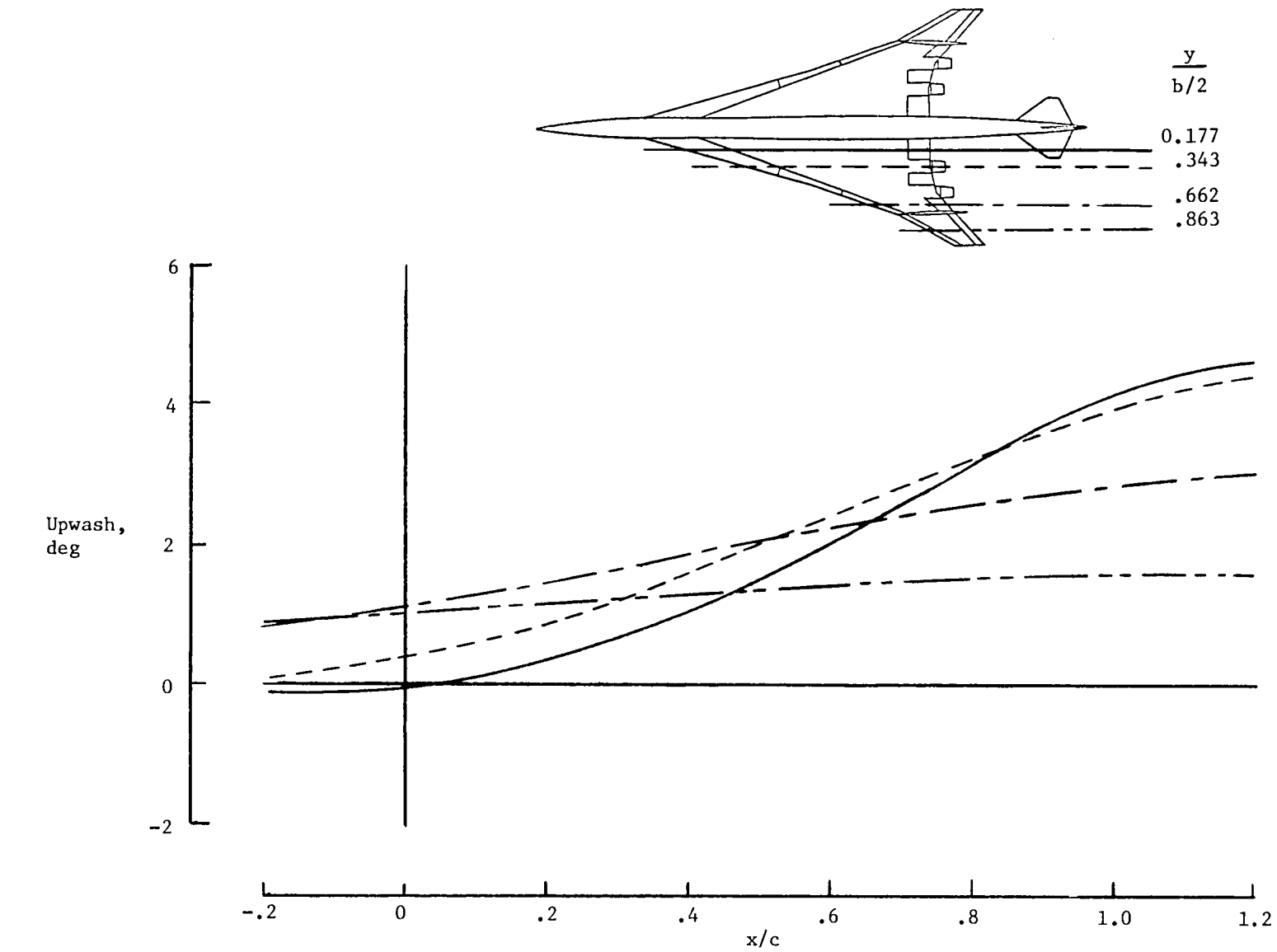


Figure A4.- Variation of upwash induced by ground-plane image. WB; $\delta_f = 20^\circ/20^\circ/20^\circ$; $\delta_{le} = 30^\circ$; $h/b = 0.2$; $C_L = 0.6$.

APPENDIX B

DATA SUPPLEMENT

A run schedule and tabulated listing of in-ground effects data are presented in tables B1 to B3. In order to provide data at constant angles of attack and ground heights, interpolated results are presented in table B3. Additionally, selected plots and tabular data from reference 2 (corresponding to the out-of-ground effect condition) are given in figures B1 and B2 and tables B4 and B5.

The symbols used in the data tabulation are defined as follows:

ALPHA	angle of attack, deg
ALPI	interpolated angle of attack, deg
CD	drag-force coefficient
CDI	interpolated drag-force coefficient
CL	lift-force coefficient
CLI	interpolated lift-force coefficient
CPM	pitching-moment coefficient
CMI	interpolated pitching-moment coefficient
H/B	height of configuration above ground plane divided by wing span

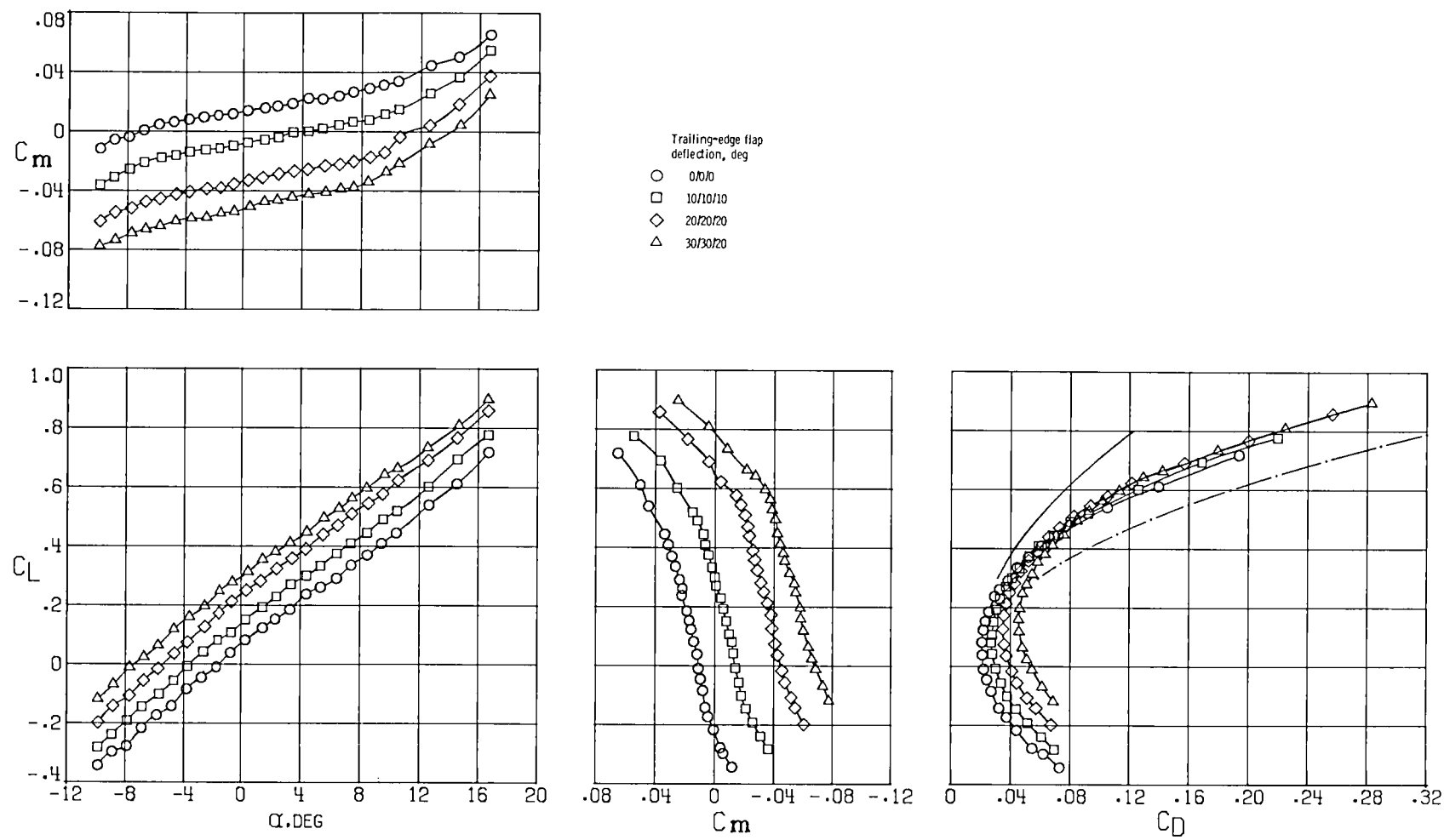


Figure B1.- Longitudinal aerodynamic characteristics for $h/b = \infty$. WB;
 $\delta_{le} = 30^\circ$. (From ref. 2.)

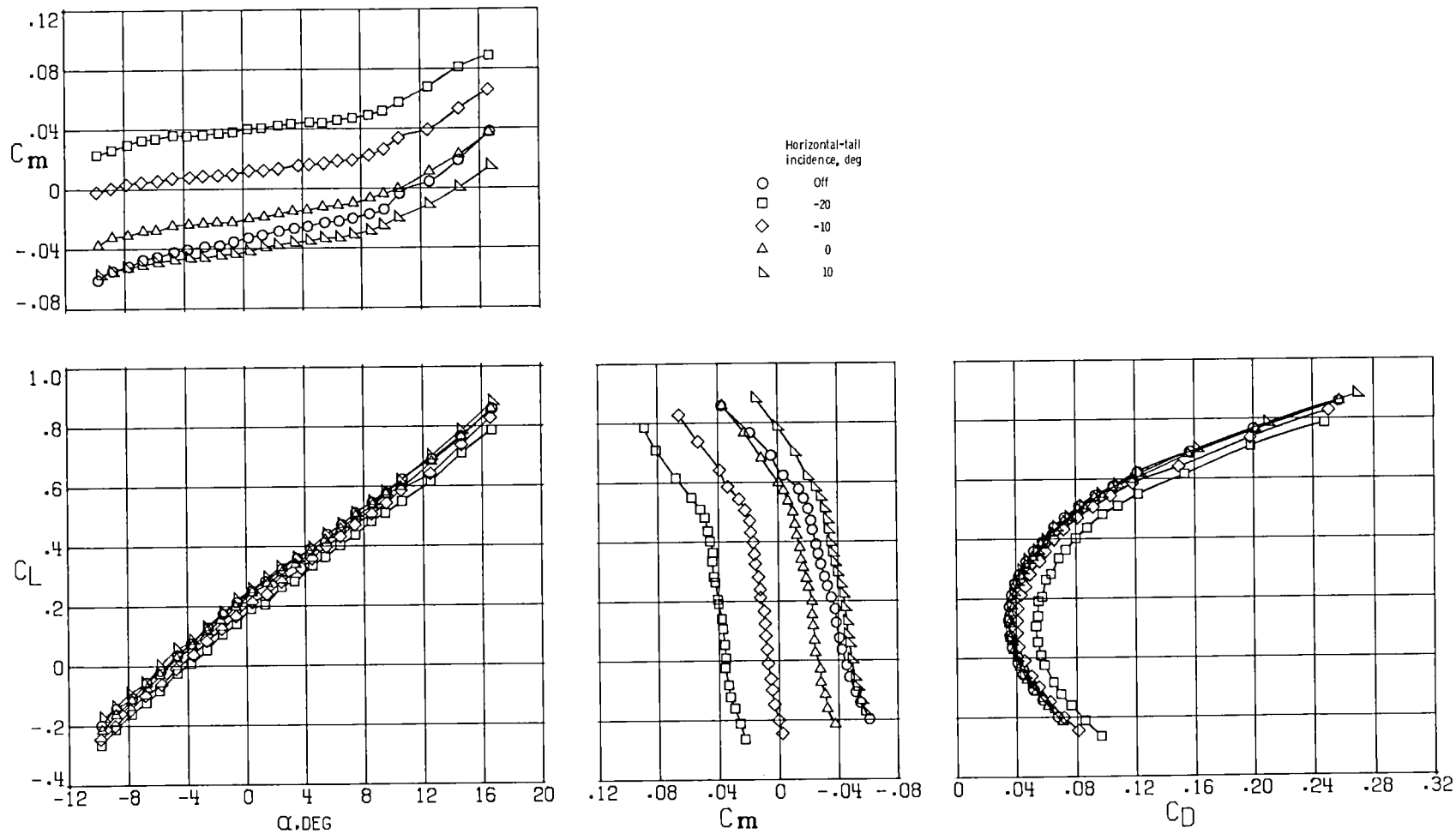


Figure B2.- Horizontal-tail effectiveness for $h/b = \infty$. $\delta_f = 20^\circ/20^\circ/20^\circ$; $\delta_{le} = 30^\circ$. (From ref. 2.)

APPENDIX B

TABLE B1.- RUN SCHEDULE FOR CONFIGURATION IN-GROUND EFFECT

Run	Interpolated run	α , deg	δ_{le} , deg	δ_f , deg			Center-line vertical tail	Horizontal-tail incidence, deg
				δ_{t_1}	δ_{t_3}	δ_{t_5}		
54	---	-2	30	0	0	0	Off	Off
55	700	0						
57	701	2						
58	702	4						
59	703	6						
60	704	8						
61	705	10						
62	706	12						
180	---	-2		10	10	10		
181	728	0						
182	729	2						
183	730	4						
184	731	6						
185	732	8						
186	733	10						
187	734	12						
110	---	-2		20	20	20		
111	707	0						
112	708	2						
113	709	4						
114	710	6						
115	711	8						
116	712	10						
117	713	12						
188	---	-2		30	30	20		
189	714	0						
190	715	2						
191	716	4						
192	717	6						
193	718	8						
194	719	10						
195	720	12						

APPENDIX B

TABLE B1 .- Concluded

Run	Interpolated run	α , deg	δ_{le} , deg	δ_f , deg			Center-line vertical tail	Horizontal-tail incidence, deg
				δ_{t_1}	δ_{t_3}	δ_{t_5}		
124	---	-2	30	20	20	20	On	0
125	742	0						
126	743	2						
127	744	4						
128	745	6						
129	746	8						
130	747	10						
131	748	12						
138	---	-2						10
139	749	0						
140	750	2						
141	751	4						
142	752	6						
143	753	8						
144	754	10						
145	755	12						
148		-2						-10
149	756	0						
150	757	2						
151	758	4						
152	759	6						
153	760	8						
154	761	10						
155	762	12						
156	---	-2						-20
157	763	0						
158	764	2						
159	765	4						
160	766	6						
161	767	8						
162	768	10						
163	769	12						

APPENDIX B

TABLE B2.- TABULATED DATA FOR CONFIGURATION IN-GROUND EFFECT

RUN 54

H/B	ALPHA	CL	CD	CPM
.118	-1.93	-.0186	.0223	.0258
.150	-1.94	-.0182	.0226	.0213
.202	-1.93	-.0134	.0225	.0184
.250	-1.93	-.0109	.0223	.0166
.288	-1.92	-.0106	.0220	.0154

RUN 55

H/B	ALPHA	CL	CD	CPM
.127	.08	.1107	.0215	.0257
.151	.06	.0926	.0211	.0214
.199	.06	.0862	.0214	.0190
.251	.07	.0840	.0214	.0178
.300	.08	.0774	.0217	.0173
.350	.09	.0754	.0216	.0166
.400	.09	.0654	.0217	.0167
.410	.09	.0651	.0217	.0163

RUN 57

H/B	ALPHA	CL	CD	CPM
.139	2.07	.2051	.0250	.0256
.151	2.06	.1991	.0247	.0249
.201	2.06	.1751	.0245	.0227
.251	2.06	.1685	.0243	.0207
.300	2.07	.1555	.0243	.0199
.350	2.08	.1490	.0246	.0201
.400	2.09	.1514	.0238	.0210
.501	2.11	.1449	.0243	.0203
.533	2.12	.1455	.0243	.0200

APPENDIX B

TABLE B2.- Continued

RUN 58

H/B	ALPHA	CL	CD	CPM
.153	4.09	.2958	.0319	.0283
.199	4.08	.2649	.0308	.0244
.250	4.09	.2442	.0304	.0237
.298	4.07	.2337	.0302	.0229
.350	4.10	.2300	.0301	.0249
.400	4.11	.2275	.0296	.0239
.500	4.12	.2176	.0301	.0241
.601	4.15	.2169	.0301	.0241
.658	4.16	.2088	.0301	.0240

RUN 59

H/B	ALPHA	CL	CD	CPM
.164	6.03	.3815	.0436	.0284
.200	6.03	.3549	.0421	.0257
.250	6.03	.3289	.0406	.0263
.300	6.04	.3136	.0391	.0263
.350	6.04	.3004	.0392	.0265
.400	6.06	.3016	.0391	.0274
.501	6.08	.2867	.0385	.0271
.601	6.09	.2864	.0383	.0269
.779	6.11	.2774	.0385	.0269

RUN 60

H/B	ALPHA	CL	CD	CPM
.202	8.06	.4473	.0605	.0264
.250	8.05	.4255	.0580	.0251
.300	8.06	.4055	.0562	.0263
.351	8.07	.3912	.0546	.0269
.399	8.07	.3801	.0537	.0271
.501	8.09	.3662	.0527	.0290
.600	8.12	.3590	.0527	.0298
.800	8.18	.3547	.0521	.0300
.905	8.21	.3518	.0522	.0296

APPENDIX B

TABLE B2.- Continued

RUN 61

H/B	ALPHA	CL	CD	CPM
.232	10.07	.5221	.0844	.0309
.251	10.07	.5103	.0830	.0301
.300	10.08	.4932	.0798	.0307
.351	10.08	.4732	.0772	.0295
.401	10.09	.4645	.0759	.0294
.500	10.12	.4441	.0740	.0303
.600	10.14	.4363	.0729	.0304
.800	10.21	.4363	.0737	.0319
1.001	10.27	.4307	.0734	.0310

RUN 62

H/B	ALPHA	CL	CD	CPM
.259	12.07	.5940	.1160	.0396
.300	12.07	.5715	.1115	.0374
.351	12.08	.5553	.1086	.0372
.399	12.09	.5495	.1072	.0380
.500	12.11	.5316	.1043	.0381
.601	12.15	.5264	.1030	.0397
.800	12.20	.5036	.0998	.0372
1.000	12.28	.5107	.1016	.0394

RUN 110

H/B	ALPHA	CL	CD	CPM
.119	-1.88	.2190	.0303	-.0350
.148	-1.88	.2034	.0316	-.0355
.200	-1.88	.1916	.0318	-.0359
.250	-1.87	.1848	.0315	-.0367
.293	-1.86	.1828	.0314	-.0358

APPENDIX B

TABLE B2.- Continued

RUN 111

H/B	ALPHA	CL	CD	CPM
.133	.08	.3139	.0336	-.0279
.159	.08	.2959	.0339	-.0306
.194	.09	.2833	.0337	-.0308
.251	.09	.2654	.0345	-.0321
.301	.09	.2561	.0355	-.0311
.351	.11	.2599	.0346	-.0302
.395	.10	.2535	.0348	-.0306
.412	.10	.2598	.0356	-.0298

RUN 112

H/B	ALPHA	CL	CD	CPM
.144	2.04	.3941	.0405	-.0216
.152	2.04	.3905	.0407	-.0239
.195	2.04	.3663	.0412	-.0253
.249	2.05	.3527	.0415	-.0248
.305	2.07	.3412	.0416	-.0267
.347	2.07	.3308	.0422	-.0261
.398	2.09	.3264	.0421	-.0255
.497	2.10	.3231	.0425	-.0247
.533	2.12	.3229	.0424	-.0249

RUN 113

H/B	ALPHA	CL	CD	CPM
.154	4.05	.4828	.0527	-.0181
.194	4.04	.4546	.0523	-.0233
.243	4.04	.4358	.0519	-.0236
.300	4.05	.4226	.0521	-.0239
.351	4.06	.4078	.0520	-.0236
.402	4.08	.4106	.0523	-.0216
.498	4.10	.3979	.0525	-.0212
.600	4.12	.3924	.0529	-.0209
.655	4.14	.3894	.0529	-.0202

APPENDIX B

TABLE B2.- Continued

RUN 114

H/B	ALPHA	CL	CD	CPM
.169	6.07	.5571	.0710	-.0148
.201	6.07	.5408	.0694	-.0209
.250	6.07	.5255	.0690	-.0220
.297	6.07	.5066	.0683	-.0226
.354	6.09	.5049	.0682	-.0209
.399	6.09	.4837	.0678	-.0219
.504	6.13	.4812	.0678	-.0204
.596	6.14	.4709	.0680	-.0196
.781	6.21	.4716	.0684	-.0191

RUN 115

H/B	ALPHA	CL	CD	CPM
.204	8.06	.6244	.0937	-.0096
.249	8.07	.6025	.0910	-.0152
.304	8.06	.5900	.0899	-.0177
.350	8.07	.5740	.0890	-.0180
.401	8.09	.5695	.0890	-.0175
.499	8.10	.5515	.0881	-.0194
.604	8.13	.5526	.0885	-.0177
.796	8.20	.5509	.0886	-.0169
.906	8.22	.5385	.0883	-.0177

RUN 116

H/B	ALPHA	CL	CD	CPM
.233	10.08	.6943	.1240	.0010
.255	10.07	.6823	.1219	-.0032
.304	10.08	.6595	.1180	-.0068
.351	10.08	.6445	.1159	-.0098
.400	10.09	.6378	.1154	-.0089
.502	10.11	.6290	.1146	-.0085
.601	10.14	.6228	.1141	-.0088
.799	10.21	.6212	.1149	-.0079
1.001	10.29	.6140	.1152	-.0090

APPENDIX B

TABLE B2.- Continued

RUN 117

H/B	ALPHA	CL	CD	CPM
.259	12.13	.7625	.1619	.0136
.304	12.12	.7351	.1558	.0077
.351	12.13	.7226	.1535	.0050
.400	12.14	.7135	.1519	.0035
.500	12.16	.7087	.1511	.0021
.593	12.18	.6950	.1489	.0024
.796	12.25	.6926	.1498	.0026
1.001	12.35	.6834	.1489	.0023

RUN 124

H/B	ALPHA	CL	CD	CPM
.119	-1.97	.1980	.0297	-.0244
.150	-1.97	.1957	.0302	-.0227
.201	-1.97	.1715	.0310	-.0224
.251	-1.96	.1624	.0312	-.0232
.286	-1.95	.1599	.0312	-.0217

RUN 125

H/B	ALPHA	CL	CD	CPM
.128	.06	.3042	.0337	-.0205
.149	.05	.2835	.0340	-.0210
.199	.05	.2683	.0342	-.0209
.251	.08	.2570	.0340	-.0187
.300	.06	.2382	.0350	-.0179
.350	.10	.2462	.0351	-.0155
.399	.08	.2345	.0349	-.0163
.408	.10	.2370	.0350	-.0161

APPENDIX B

TABLE B2.- Continued

RUN 126

H/B	ALPHA	CL	CD	CPM
.140	2.05	.3896	.0411	-.0243
.150	2.04	.3766	.0413	-.0240
.200	2.05	.3566	.0409	-.0229
.250	2.06	.3356	.0414	-.0220
.300	2.08	.3272	.0415	-.0198
.350	2.08	.3159	.0418	-.0185
.400	2.11	.3115	.0422	-.0174
.501	2.13	.3001	.0424	-.0165
.531	2.12	.3092	.0421	-.0155

RUN 127

H/B	ALPHA	CL	CD	CPM
.153	4.06	.4750	.0534	-.0272
.200	4.06	.4401	.0525	-.0279
.251	4.08	.4184	.0524	-.0239
.301	4.08	.4035	.0524	-.0207
.349	4.09	.3917	.0522	-.0186
.400	4.11	.3864	.0526	-.0165
.500	4.13	.3789	.0526	-.0149
.599	4.16	.3672	.0531	-.0137
.657	4.18	.3630	.0528	-.0130

RUN 128

H/B	ALPHA	CL	CD	CPM
.165	6.04	.5630	.0717	-.0319
.200	6.04	.5333	.0696	-.0320
.251	6.05	.5146	.0689	-.0274
.300	6.06	.4877	.0683	-.0248
.350	6.07	.4738	.0675	-.0223
.399	6.08	.4651	.0673	-.0189
.500	6.10	.4510	.0671	-.0166
.600	6.13	.4411	.0670	-.0144
.779	6.20	.4453	.0676	-.0125

APPENDIX B

TABLE B2.- Continued

RUN 129

H/B	ALPHA	CL	CD	CPM
.202	8.09	.6240	.0953	-.0299
.250	8.09	.5888	.0914	-.0253
.300	8.11	.5748	.0904	-.0192
.350	8.12	.5558	.0893	-.0170
.400	8.14	.5476	.0888	-.0155
.501	8.16	.5380	.0883	-.0121
.601	8.19	.5268	.0878	-.0107
.800	8.25	.5157	.0874	-.0085
.907	8.30	.5236	.0884	-.0082

RUN 130

H/B	ALPHA	CL	CD	CPM
.232	10.06	.6832	.1243	-.0278
.250	10.06	.6736	.1223	-.0228
.300	10.08	.6479	.1189	-.0170
.351	10.09	.6263	.1160	-.0142
.400	10.11	.6287	.1170	-.0096
.502	10.14	.6014	.1133	-.0061
.601	10.16	.5943	.1127	-.0043
.800	10.23	.5872	.1122	-.0026
.998	10.30	.5839	.1130	-.0016

RUN 131

H/B	ALPHA	CL	CD	CPM
.260	12.04	.7633	.1634	-.0246
.300	12.06	.7283	.1567	-.0146
.351	12.08	.7142	.1543	-.0076
.401	12.10	.7046	.1530	-.0017
.501	12.13	.6789	.1486	.0018
.600	12.15	.6685	.1468	.0049
.801	12.23	.6559	.1454	.0066
.999	12.31	.6562	.1465	.0081

APPENDIX B

TABLE B2.- Continued

RUN 138

H/B	ALPHA	CL	CD	CPM
.118	-1.99	.2147	.0309	-.0441
.159	-1.99	.1951	.0319	-.0429
.201	-1.98	.1886	.0317	-.0416
.251	-1.98	.1765	.0327	-.0414
.287	-1.94	.1686	.0324	-.0406

RUN 139

H/B	ALPHA	CL	CD	CPM
.126	.05	.3194	.0351	-.0412
.149	.05	.3042	.0349	-.0410
.199	.05	.2788	.0351	-.0402
.250	.06	.2628	.0360	-.0392
.301	.07	.2552	.0355	-.0380
.350	.09	.2513	.0357	-.0369
.399	.09	.2461	.0356	-.0362
.410	.09	.2487	.0355	-.0358

RUN 140

H/B	ALPHA	CL	CD	CPM
.140	2.06	.4094	.0434	-.0471
.149	2.06	.3979	.0431	-.0468
.199	2.06	.3645	.0433	-.0435
.251	2.07	.3483	.0428	-.0404
.302	2.07	.3355	.0430	-.0393
.349	2.10	.3236	.0431	-.0383
.400	2.11	.3219	.0435	-.0366
.500	2.13	.3169	.0431	-.0362
.534	2.14	.3114	.0434	-.0363

APPENDIX B

TABLE B2.- Continued

RUN 141

H/B	ALPHA	CL	CD	CPM
.154	4.04	.4948	.0568	-.0540
.200	4.05	.4551	.0552	-.0493
.251	4.07	.4404	.0543	-.0437
.300	4.07	.4205	.0537	-.0396
.350	4.09	.4091	.0534	-.0377
.401	4.11	.4081	.0539	-.0357
.500	4.11	.3862	.0540	-.0343
.600	4.15	.3893	.0546	-.0320
.657	4.15	.3777	.0545	-.0317

RUN 142

H/B	ALPHA	CL	CD	CPM
.165	6.03	.5850	.0779	-.0639
.200	6.03	.5520	.0740	-.0562
.250	6.05	.5286	.0727	-.0498
.301	6.06	.5059	.0714	-.0452
.351	6.08	.4896	.0706	-.0416
.400	6.09	.4818	.0701	-.0384
.501	6.11	.4642	.0692	-.0352
.600	6.14	.4574	.0693	-.0329
.782	6.20	.4565	.0694	-.0321

RUN 143

H/B	ALPHA	CL	CD	CPM
.201	8.05	.6448	.1018	-.0591
.250	8.06	.6078	.0968	-.0501
.300	8.08	.5894	.0943	-.0436
.350	8.10	.5765	.0929	-.0372
.400	8.11	.5669	.0925	-.0337
.500	8.15	.5530	.0910	-.0310
.600	8.18	.5353	.0899	-.0303
.799	8.25	.5351	.0905	-.0275
.909	8.29	.5289	.0904	-.0269

APPENDIX B

TABLE B2.- Continued

RUN 144

H/B	ALPHA	CL	CD	CPM
.231	10.03	.7083	.1329	-.0568
.251	10.04	.6997	.1314	-.0514
.300	10.06	.6647	.1246	-.0417
.348	10.08	.6521	.1224	-.0338
.400	10.10	.6343	.1197	-.0303
.499	10.13	.6240	.1177	-.0251
.599	10.15	.6100	.1160	-.0246
.800	10.23	.6036	.1160	-.0214
.999	10.29	.5936	.1156	-.0219

RUN 145

H/B	ALPHA	CL	CD	CPM
.259	12.04	.7803	.1725	-.0561
.299	12.05	.7464	.1643	-.0416
.349	12.07	.7302	.1602	-.0318
.400	12.09	.7095	.1564	-.0265
.500	12.13	.7000	.1542	-.0189
.599	12.16	.6835	.1511	-.0163
.800	12.23	.6690	.1493	-.0136
1.000	12.32	.6655	.1492	-.0119

RUN 146

H/B	ALPHA	CL	CD	CPM
.118	-1.93	.1767	.0378	.0109
.150	-1.93	.1459	.0387	.0096
.200	-1.93	.1383	.0393	.0108
.251	-1.92	.1281	.0401	.0121
.285	-1.91	.1277	.0396	.0130

APPENDIX B

TABLE B2.- Continued

RUN 149

H/B	ALPHA	CL	CD	CPM
.126	.06	.2721	.0400	.0138
.150	.05	.2498	.0403	.0120
.198	.05	.2302	.0410	.0129
.250	.06	.2157	.0414	.0138
.300	.07	.2117	.0415	.0143
.349	.08	.1998	.0422	.0150
.401	.09	.2005	.0423	.0166

RUN 150

H/B	ALPHA	CL	CD	CPM
.139	2.07	.3556	.0458	.0089
.150	2.07	.3479	.0458	.0073
.200	2.06	.3154	.0463	.0081
.250	2.07	.2958	.0470	.0106
.300	2.09	.2910	.0466	.0126
.349	2.09	.2808	.0471	.0141
.399	2.11	.2745	.0475	.0146
.500	2.12	.2656	.0478	.0157
.530	2.13	.2675	.0478	.0160

RUN 151

H/B	ALPHA	CL	CD	CPM
.154	4.06	.4377	.0564	.0029
.200	4.07	.4096	.0559	.0033
.251	4.08	.3857	.0559	.0077
.300	4.09	.3777	.0560	.0108
.350	4.11	.3612	.0564	.0125
.400	4.13	.3533	.0561	.0151
.500	4.15	.3378	.0569	.0173
.600	4.17	.3363	.0570	.0188
.655	4.18	.3363	.0570	.0191

APPENDIX B

TABLE B2.- Continued

RUN 152

H/B	ALPHA	CL	CD	CPM
.164	6.07	.5219	.0729	.0001
.200	6.06	.4993	.0713	-.0017
.249	6.08	.4825	.0710	.0010
.301	6.09	.4589	.0705	.0057
.350	6.10	.4461	.0702	.0090
.400	6.11	.4387	.0704	.0125
.499	6.13	.4182	.0698	.0143
.600	6.15	.4155	.0699	.0172
.779	6.21	.4072	.0705	.0192

RUN 153

H/B	ALPHA	CL	CD	CPM
.202	8.06	.5848	.0940	.0018
.250	8.05	.5617	.0913	.0051
.299	8.07	.5375	.0902	.0087
.351	8.09	.5219	.0895	.0120
.400	8.10	.5084	.0888	.0149
.501	8.13	.4994	.0889	.0188
.599	8.16	.4890	.0886	.0208
.800	8.23	.4859	.0895	.0236
.904	8.26	.4793	.0891	.0228

RUN 154

H/B	ALPHA	CL	CD	CPM
.231	10.07	.6570	.1235	.0055
.249	10.06	.6384	.1203	.0057
.299	10.08	.6165	.1180	.0116
.350	10.09	.5958	.1158	.0163
.390	10.10	.5854	.1146	.0193
.499	10.14	.5725	.1136	.0250
.599	10.16	.5561	.1118	.0253
.799	10.23	.5508	.1120	.0284
1.001	10.31	.5445	.1121	.0291

APPENDIX B

TABLE B2.- Continued

RUN 155

H/B	ALPHA	CL	CD	CPM
.260	12.07	.7212	.1576	.0102
.299	12.08	.7010	.1544	.0140
.350	12.10	.6826	.1517	.0211
.400	12.11	.6589	.1486	.0250
.500	12.15	.6428	.1467	.0325
.600	12.18	.6290	.1449	.0359
.800	12.24	.6186	.1439	.0383
1.001	12.33	.6141	.1442	.0397

RUN 156

H/B	ALPHA	CL	CD	CPM
.119	-1.91	.1538	.0511	.0403
.149	-1.92	.1390	.0508	.0387
.200	-1.96	.1142	.0518	.0375
.250	-1.95	.1075	.0526	.0377
.281	-1.94	.1004	.0530	.0368

RUN 157

H/B	ALPHA	CL	CD	CPM
.126	.05	.2390	.0520	.0435
.149	.05	.2262	.0522	.0423
.199	.05	.2099	.0524	.0416
.250	.06	.1982	.0526	.0421
.300	.06	.1834	.0528	.0405
.351	.06	.1830	.0528	.0422
.400	.07	.1752	.0533	.0418
.404	.07	.1805	.0529	.0424

APPENDIX B

TABLE B2.- Continued

RUN 158

H/B	ALPHA	CL	CD	CPM
.139	2.06	.3301	.0563	.0405
.149	2.05	.3174	.0565	.0383
.200	2.05	.2902	.0571	.0384
.250	2.06	.2790	.0571	.0388
.300	2.07	.2677	.0578	.0405
.350	2.09	.2575	.0578	.0408
.399	2.10	.2576	.0574	.0411
.501	2.12	.2420	.0581	.0415
.527	2.12	.2424	.0587	.0423

RUN 159

H/B	ALPHA	CL	CD	CPM
.153	4.08	.4131	.0652	.0359
.199	4.07	.3880	.0648	.0334
.249	4.08	.3628	.0651	.0366
.301	4.09	.3477	.0655	.0396
.350	4.09	.3331	.0654	.0406
.399	4.10	.3293	.0656	.0427
.501	4.13	.3174	.0661	.0438
.600	4.16	.3099	.0665	.0455
.652	4.17	.3080	.0664	.0453

RUN 160

H/B	ALPHA	CL	CD	CPM
.165	6.06	.4940	.0798	.0335
.201	6.05	.4735	.0781	.0284
.250	6.06	.4499	.0784	.0307
.300	6.07	.4352	.0780	.0345
.351	6.08	.4190	.0782	.0372
.399	6.08	.4099	.0782	.0392
.500	6.12	.4014	.0780	.0415
.600	6.15	.3934	.0784	.0450
.775	6.19	.3843	.0785	.0446

APPENDIX B

TABLE B2.- Continued

RUN 161

H/B	ALPHA	CL	CD	CPM
.201	8.06	.5591	.0997	.0353
.251	8.06	.5380	.0980	.0345
.300	8.07	.5103	.0967	.0372
.350	8.08	.4986	.0963	.0400
.400	8.10	.4912	.0965	.0447
.500	8.12	.4787	.0964	.0468
.599	8.15	.4656	.0957	.0477
.799	8.21	.4582	.0961	.0488
.901	8.23	.4613	.0960	.0488

RUN 162

H/B	ALPHA	CL	CD	CPM
.232	10.09	.6311	.1267	.0364
.250	10.09	.6136	.1243	.0356
.300	10.10	.5917	.1225	.0407
.351	10.12	.5730	.1213	.0438
.399	10.13	.5591	.1205	.0485
.501	10.16	.5494	.1201	.0540
.600	10.19	.5375	.1192	.0536
.800	10.25	.5292	.1189	.0555
1.000	10.33	.5204	.1188	.0555

RUN 163

H/B	ALPHA	CL	CD	CPM
.260	12.08	.7035	.1608	.0412
.300	12.09	.6748	.1569	.0445
.350	12.10	.6504	.1537	.0480
.400	12.12	.6389	.1535	.0555
.501	12.15	.6197	.1519	.0609
.599	12.17	.6048	.1498	.0625
.801	12.24	.5948	.1494	.0657
1.000	12.32	.5933	.1505	.0676

APPENDIX B

TABLE B2.- Continued

RUN 180

H/B	ALPHA	CL	CD	CPM
.120	-2.01	.0957	.0235	-.0072
.151	-2.01	.0895	.0238	-.0088
.199	-2.01	.0816	.0238	-.0093
.252	-2.00	.0772	.0240	-.0093
.286	-1.99	.0755	.0239	-.0101

RUN 181

H/B	ALPHA	CL	CD	CPM
.129	.06	.2146	.0249	-.0016
.152	.05	.1978	.0252	-.0037
.198	.05	.1792	.0251	-.0049
.251	.06	.1738	.0258	-.0054
.299	.06	.1612	.0258	-.0073
.353	.07	.1622	.0256	-.0061
.403	.08	.1579	.0258	-.0070
.411	.08	.1555	.0258	-.0069

RUN 182

H/B	ALPHA	CL	CD	CPM
.143	2.14	.3046	.0303	.0031
.162	2.13	.2874	.0305	.0008
.199	2.13	.2708	.0304	-.0008
.249	2.13	.2570	.0305	-.0020
.303	2.14	.2516	.0305	-.0013
.358	2.15	.2451	.0306	-.0017
.398	2.20	.2459	.0307	.0003
.511	2.21	.2360	.0305	-.0013
.539	2.23	.2401	.0306	.0005

APPENDIX B

TABLE B2.- Continued

RUN 183

H/B	ALPHA	CL	CD	CPM
.154	4.08	.3896	.0401	.0065
.195	4.06	.3587	.0388	.0032
.252	4.07	.3395	.0383	.0018
.299	4.07	.3264	.0386	.0026
.348	4.08	.3188	.0385	.0033
.400	4.09	.3131	.0382	.0031
.508	4.12	.3038	.0387	.0038
.603	4.14	.2963	.0388	.0030
.657	4.16	.2969	.0393	.0035

RUN 184

H/B	ALPHA	CL	CD	CPM
.170	6.03	.4675	.0546	.0065
.201	6.02	.4482	.0537	.0029
.248	6.00	.4232	.0519	.0028
.301	6.02	.4076	.0510	.0049
.355	6.01	.3968	.0507	.0039
.398	6.02	.3894	.0505	.0046
.498	6.04	.3778	.0502	.0048
.597	6.06	.3810	.0506	.0064
.779	6.11	.3589	.0500	.0056

RUN 185

H/B	ALPHA	CL	CD	CPM
.202	8.05	.5392	.0752	.0089
.250	8.04	.5139	.0720	.0066
.306	8.05	.4931	.0703	.0051
.353	8.06	.4822	.0695	.0052
.400	8.07	.4704	.0686	.0049
.501	8.09	.4601	.0679	.0068
.604	8.12	.4596	.0682	.0083
.798	8.18	.4440	.0673	.0076
.905	8.22	.4470	.0679	.0080

APPENDIX B

TABLE B2.- Continued

RUN 186

H/B	ALPHA	CL	CD	CPM
.235	10.04	.6049	.1022	.0167
.251	10.04	.5937	.1004	.0152
.302	10.04	.5637	.0952	.0117
.352	10.04	.5622	.0948	.0131
.400	10.05	.5459	.0926	.0115
.508	10.07	.5338	.0910	.0113
.598	10.09	.5273	.0905	.0117
.796	10.14	.5205	.0905	.0117
1.003	10.22	.5240	.0914	.0135

RUN 187

H/B	ALPHA	CL	CD	CPM
.262	12.09	.6754	.1365	.0284
.302	12.09	.6508	.1314	.0239
.352	12.10	.6382	.1289	.0236
.404	12.09	.6271	.1264	.0231
.502	12.11	.6052	.1230	.0221
.593	12.14	.6014	.1222	.0224
.803	12.22	.5969	.1225	.0228
1.011	12.30	.5882	.1216	.0224

RUN 188

H/B	ALPHA	CL	CD	CPM
.117	-1.99	.2919	.0391	-.0546
.149	-2.00	.2744	.0398	-.0568
.198	-2.00	.2553	.0412	-.0578
.254	-1.99	.2525	.0414	-.0563
.287	-1.99	.2443	.0428	-.0583

APPENDIX B

TABLE B2.- Continued

RUN 189

H/B	ALPHA	CL	CD	CPM
.136	.08	.3796	.0446	-.0453
.145	.08	.3709	.0448	-.0469
.195	.07	.3500	.0460	-.0494
.255	.08	.3364	.0469	-.0498
.313	.09	.3225	.0475	-.0504
.352	.10	.3219	.0481	-.0504
.396	.10	.3201	.0481	-.0500
.413	.11	.3190	.0490	-.0494

RUN 190

H/B	ALPHA	CL	CD	CPM
.147	2.02	.4534	.0529	-.0394
.158	2.01	.4455	.0539	-.0409
.194	2.01	.4348	.0542	-.0420
.250	2.01	.4116	.0556	-.0443
.302	2.03	.4026	.0561	-.0431
.351	2.03	.3945	.0569	-.0439
.399	2.04	.3818	.0573	-.0446
.501	2.08	.3820	.0573	-.0428
.532	2.09	.3822	.0575	-.0430

RUN 191

H/B	ALPHA	CL	CD	CPM
.158	4.03	.5339	.0668	-.0347
.193	4.02	.5167	.0678	-.0407
.242	4.01	.4932	.0683	-.0417
.300	4.03	.4808	.0690	-.0417
.351	4.04	.4693	.0697	-.0416
.400	4.06	.4626	.0693	-.0419
.495	4.06	.4563	.0699	-.0408
.592	4.08	.4479	.0702	-.0398
.655	4.11	.4496	.0702	-.0393

APPENDIX B

TABLE B2.- Continued

RUN 192

H/B	ALPHA	CL	CD	CPM
.171	6.06	.5970	.0853	-.0271
.199	6.05	.5827	.0848	-.0341
.247	6.05	.5673	.0860	-.0379
.297	6.06	.5580	.0867	-.0398
.352	6.07	.5499	.0870	-.0400
.403	6.09	.5466	.0870	-.0387
.502	6.11	.5385	.0873	-.0391
.591	6.12	.5308	.0877	-.0385
.782	6.19	.5237	.0882	-.0385

RUN 193

H/B	ALPHA	CL	CD	CPM
.205	7.98	.6528	.1087	-.0198
.247	7.98	.6390	.1072	-.0267
.302	7.97	.6270	.1079	-.0317
.349	7.98	.6076	.1070	-.0347
.403	8.00	.6097	.1079	-.0334
.498	8.01	.5968	.1084	-.0348
.605	8.04	.5895	.1081	-.0339
.798	8.11	.5834	.1085	-.0335
.902	8.14	.5802	.1081	-.0344

RUN 194

H/B	ALPHA	CL	CD	CPM
.233	10.00	.7065	.1378	-.0076
.253	10.00	.6928	.1358	-.0121
.299	10.00	.6869	.1358	-.0153
.354	10.01	.6750	.1344	-.0187
.402	10.01	.6583	.1326	-.0215
.501	10.03	.6546	.1329	-.0222
.600	10.07	.6519	.1330	-.0228
.816	10.14	.6493	.1337	-.0222
.988	10.20	.6346	.1331	-.0247

APPENDIX B

TABLE B2.- Concluded

RUN 195

H/B	ALPHA	CL	CD	CPM
.261	12.06	.7677	.1754	.0055
.304	12.05	.7508	.1720	-.0018
.357	12.05	.7357	.1702	-.0066
.397	12.07	.7371	.1710	-.0057
.506	12.09	.7282	.1703	-.0093
.594	12.10	.7186	.1692	-.0111
.799	12.19	.7118	.1699	-.0117
.997	12.27	.7104	.1703	-.0107

APPENDIX B

TABLE B3.- TABULATED INTERPOLATED DATA FOR CONFIGURATION IN-GROUND EFFECT

RUN 700

H/B	ALPI	CLI	CDI	CMI
.150	0.00	.0896	.0212	.0215
.200	0.00	.0833	.0214	.0189
.250	0.00	.0809	.0213	.0178

RUN 701

H/B	ALPI	CLI	CDI	CMI
.150	2.00	.1963	.0246	.0248
.200	2.00	.1725	.0244	.0227
.250	2.00	.1661	.0241	.0207
.300	2.00	.1530	.0241	.0198
.350	2.00	.1460	.0245	.0200
.400	2.00	.1427	.0245	.0203

RUN 702

H/B	ALPI	CLI	CDI	CMI
.200	4.00	.2609	.0305	.0243
.250	4.00	.2409	.0301	.0236
.300	4.00	.2306	.0299	.0228
.350	4.00	.2260	.0297	.0247
.400	4.00	.2230	.0292	.0237
.500	4.00	.2132	.0297	.0239

RUN 703

H/B	ALPI	CLI	CDI	CMI
.200	6.00	.3537	.0419	.0257
.250	6.00	.3276	.0404	.0263
.300	6.00	.3119	.0389	.0263
.350	6.00	.2987	.0390	.0264
.400	6.00	.2994	.0388	.0273
.500	6.00	.2841	.0381	.0270
.600	6.00	.2832	.0378	.0268

APPENDIX B

TABLE B3.- Continued

RUN 704

H/B	ALPI	CLI	CDI	CMI
.250	8.00	.4230	.0574	.0251
.300	8.00	.4031	.0556	.0262
.350	8.00	.3884	.0539	.0269
.400	8.00	.3770	.0530	.0270
.500	8.00	.3627	.0519	.0289
.600	8.00	.3545	.0517	.0296
.700	8.00	.3505	.0512	.0298

RUN 705

H/B	ALPI	CLI	CDI	CMI
.250	10.00	.5080	.0820	.0298
.300	10.00	.4899	.0787	.0305
.350	10.00	.4702	.0762	.0294
.400	10.00	.4609	.0748	.0292
.500	10.00	.4392	.0725	.0302
.600	10.00	.4307	.0712	.0301
.700	10.00	.4292	.0710	.0308
.800	10.00	.4279	.0715	.0317
.900	10.00	.4248	.0712	.0316

RUN 706

H/B	ALPI	CLI	CDI	CMI
.300	12.00	.5688	.1102	.0372
.350	12.00	.5520	.1071	.0368
.400	12.00	.5454	.1055	.0375
.500	12.00	.5263	.1023	.0375
.600	12.00	.5194	.1005	.0387
.700	12.00	.5088	.0986	.0380
.800	12.00	.4969	.0972	.0367
.900	12.00	.4941	.0968	.0367

APPENDIX B

TABLE B3.- Continued

RUN 707

H/B	ALPI	CLI	CDI	CMI
.150	0.00	.2971	.0337	-.0302
.200	0.00	.2775	.0335	-.0311
.250	0.00	.2619	.0342	-.0324

RUN 708

H/B	ALPI	CLI	CDI	CMI
.150	2.00	.3894	.0405	-.0236
.200	2.00	.3627	.0411	-.0252
.250	2.00	.3505	.0413	-.0250
.300	2.00	.3398	.0413	-.0268
.350	2.00	.3275	.0419	-.0261

RUN 709

H/B	ALPI	CLI	CDI	CMI
.200	4.00	.4497	.0519	-.0237
.250	4.00	.4322	.0516	-.0236
.300	4.00	.4205	.0517	-.0239
.350	4.00	.4056	.0516	-.0237
.400	4.00	.3972	.0516	-.0229
.500	4.00	.3942	.0519	-.0213

RUN 710

H/B	ALPI	CLI	CDI	CMI
.200	6.00	.5382	.0687	-.0209
.250	6.00	.5225	.0683	-.0221
.300	6.00	.5025	.0675	-.0227
.350	6.00	.4882	.0671	-.0227
.400	6.00	.4797	.0670	-.0220
.500	6.00	.4701	.0669	-.0206
.600	6.00	.4656	.0667	-.0196

APPENDIX B

TABLE B3.- Continued

RUN 711

H/B	ALPI	CLI	CDI	CMI
.250	8.00	.5995	.0900	-.0156
.300	8.00	.5885	.0892	-.0179
.350	8.00	.5709	.0881	-.0182
.400	8.00	.5661	.0879	-.0178
.500	8.00	.5472	.0869	-.0196
.600	8.00	.5303	.0859	-.0213
.700	8.00	.5223	.0854	-.0216

RUN 712

H/B	ALPI	CLI	CDI	CMI
.250	10.00	.6819	.1210	-.0030
.300	10.00	.6584	.1170	-.0071
.350	10.00	.6419	.1147	-.0102
.400	10.00	.6347	.1141	-.0094
.500	10.00	.6249	.1129	-.0091
.600	10.00	.6172	.1120	-.0096
.700	10.00	.6139	.1117	-.0094
.800	10.00	.6116	.1120	-.0092
.900	10.00	.6087	.1118	-.0093

RUN 713

H/B	ALPI	CLI	CDI	CMI
.300	12.00	.7322	.1536	.0071
.350	12.00	.7177	.1508	.0039
.400	12.00	.7083	.1491	.0026
.500	12.00	.6954	.1467	.0015
.600	12.00	.6890	.1454	.0015
.700	12.00	.6867	.1452	.0015
.800	12.00	.6836	.1454	.0013
.900	12.00	.6789	.1446	.0009
1.000	12.00	.6717	.1432	.0004

APPENDIX B

TABLE B3.- Continued

RUN 714

H/B	ALPI	CLI	CDI	CMI
.150	0.00	.3674	.0448	-.0470
.200	0.00	.3454	.0459	-.0498
.250	0.00	.3342	.0466	-.0501

RUN 715

H/B	ALPI	CLI	CDI	CMI
.150	2.00	.4515	.0529	-.0396
.200	2.00	.4316	.0544	-.0423
.250	2.00	.4113	.0556	-.0443
.300	2.00	.4017	.0559	-.0432
.350	2.00	.3937	.0567	-.0440
.400	2.00	.3802	.0571	-.0447

RUN 716

H/B	ALPI	CLI	CDI	CMI
.200	4.00	.5123	.0677	-.0413
.250	4.00	.4902	.0683	-.0417
.300	4.00	.4796	.0688	-.0417
.350	4.00	.4680	.0694	-.0416
.400	4.00	.4602	.0688	-.0419
.500	4.00	.4536	.0695	-.0408

RUN 717

H/B	ALPI	CLI	CDI	CMI
.200	6.00	.5806	.0844	-.0346
.250	6.00	.5650	.0856	-.0382
.300	6.00	.5555	.0862	-.0400
.350	6.00	.5474	.0863	-.0402
.400	6.00	.5435	.0862	-.0389
.500	6.00	.5345	.0862	-.0393
.600	6.00	.5259	.0865	-.0386

APPENDIX B

TABLE B3.- Continued

RUN 718

H/B	ALPI	CLI	CDI	CMI
.250	8.00	.6389	.1074	-.0270
.300	8.00	.6282	.1082	-.0314
.350	8.00	.6189	.1083	-.0329
.400	8.00	.6101	.1079	-.0333
.500	8.00	.5964	.1084	-.0348
.600	8.00	.5887	.1077	-.0341
.700	8.00	.5837	.1074	-.0336

RUN 719

H/B	ALPI	CLI	CDI	CMI
.300	10.00	.6868	.1358	-.0154
.350	10.00	.6759	.1344	-.0185
.400	10.00	.6648	.1331	-.0208
.500	10.00	.6538	.1325	-.0224
.600	10.00	.6497	.1320	-.0232
.700	10.00	.6482	.1318	-.0230
.800	10.00	.6454	.1320	-.0229
.900	10.00	.6385	.1314	-.0239

RUN 720

H/B	ALPI	CLI	CDI	CMI
.300	12.00	.7504	.1712	-.0017
.350	12.00	.7357	.1693	-.0065
.400	12.00	.7285	.1687	-.0087
.500	12.00	.7250	.1684	-.0098
.600	12.00	.7145	.1670	-.0119
.700	12.00	.7084	.1663	-.0128
.800	12.00	.7061	.1666	-.0127
.900	12.00	.7035	.1661	-.0126

APPENDIX B

TABLE B3.- Continued

RUN 728

H/B	ALPI	CLI	CDI	CMI
.150	0.00	.1964	.0252	-.0037
.200	0.00	.1766	.0250	-.0051
.250	0.00	.1688	.0248	-.0058

RUN 729

H/B	ALPI	CLI	CDI	CMI
.150	2.00	.2910	.0301	.0017
.200	2.00	.2646	.0299	-.0011
.250	2.00	.2513	.0300	-.0022
.300	2.00	.2464	.0301	-.0016
.350	2.00	.2403	.0301	-.0020
.400	2.00	.2344	.0301	-.0024

RUN 730

H/B	ALPI	CLI	CDI	CMI
.200	4.00	.3535	.0384	.0029
.250	4.00	.3367	.0379	.0017
.300	4.00	.3232	.0382	.0025
.350	4.00	.3155	.0381	.0032
.400	4.00	.3095	.0377	.0029
.500	4.00	.3002	.0380	.0036

RUN 731

H/B	ALPI	CLI	CDI	CMI
.200	6.00	.4479	.0536	.0030
.250	6.00	.4225	.0519	.0028
.300	6.00	.4069	.0508	.0049
.350	6.00	.3975	.0506	.0040
.400	6.00	.3883	.0504	.0046
.500	6.00	.3763	.0500	.0047
.600	6.00	.3672	.0497	.0046

TABLE B3.- Continued

RUN 732

H/B	ALPI	CLI	CDI	CMI
.250	8.00	.5123	.0716	.0065
.300	8.00	.4928	.0699	.0050
.350	8.00	.4803	.0689	.0051
.400	8.00	.4677	.0679	.0048
.500	8.00	.4566	.0670	.0066
.600	8.00	.4499	.0664	.0081
.700	8.00	.4428	.0659	.0082

RUN 733

H/B	ALPI	CLI	CDI	CMI
.250	10.00	.5916	.0996	.0149
.300	10.00	.5630	.0948	.0116
.350	10.00	.5496	.0927	.0109
.400	10.00	.5440	.0919	.0113
.500	10.00	.5320	.0901	.0111
.600	10.00	.5238	.0892	.0115
.700	10.00	.5185	.0888	.0117

RUN 734

H/B	ALPI	CLI	CDI	CMI
.300	12.00	.6477	.1298	.0234
.350	12.00	.6341	.1270	.0228
.400	12.00	.6241	.1249	.0225
.500	12.00	.6072	.1215	.0217
.600	12.00	.5957	.1197	.0214
.700	12.00	.5875	.1184	.0212

APPENDIX B

TABLE B3.- Continued

RUN 742

H/B	ALPI	CLI	CDI	CMI
.150	0.00	.2807	.0339	-.0211
.200	0.00	.2658	.0341	-.0209
.250	0.00	.2537	.0338	-.0188

RUN 743

H/B	ALPI	CLI	CDI	CMI
.150	2.00	.3811	.0408	-.0240
.200	2.00	.3544	.0407	-.0228
.250	2.00	.3330	.0411	-.0219
.300	2.00	.3242	.0412	-.0197
.350	2.00	.3129	.0415	-.0184
.400	2.00	.3076	.0417	-.0174

RUN 744

H/B	ALPI	CLI	CDI	CMI
.200	4.00	.4374	.0521	-.0278
.250	4.00	.4153	.0519	-.0238
.300	4.00	.4005	.0519	-.0206
.350	4.00	.3879	.0516	-.0185
.400	4.00	.3821	.0519	-.0165
.500	4.00	.3739	.0518	-.0149

RUN 745

H/B	ALPI	CLI	CDI	CMI
.200	6.00	.5313	.0692	-.0319
.250	6.00	.5128	.0684	-.0274
.300	6.00	.4851	.0678	-.0247
.350	6.00	.4709	.0669	-.0223
.400	6.00	.4616	.0666	-.0188
.500	6.00	.4469	.0662	-.0167
.600	6.00	.4474	.0664	-.0129

APPENDIX B

TABLE B3.- Continued

RUN 746

H/B	ALPI	CLI	CDI	CMI
.250	8.00	.5853	.0902	-.0254
.300	8.00	.5700	.0890	-.0194
.350	8.00	.5513	.0878	-.0172
.400	8.00	.5422	.0872	-.0157
.500	8.00	.5318	.0865	-.0125
.600	8.00	.5240	.0859	-.0100

RUN 747

H/B	ALPI	CLI	CDI	CMI
.250	10.00	.6704	.1211	-.0228
.300	10.00	.6450	.1176	-.0171
.350	10.00	.6231	.1146	-.0144
.400	10.00	.6090	.1127	-.0116
.500	10.00	.5968	.1113	-.0066
.600	10.00	.5890	.1105	-.0048
.700	10.00	.5837	.1100	-.0038
.800	10.00	.5799	.1094	-.0032
.900	10.00	.5769	.1092	-.0028

RUN 748

H/B	ALPI	CLI	CDI	CMI
.300	12.00	.7258	.1555	-.0147
.350	12.00	.7105	.1526	-.0080
.400	12.00	.6984	.1504	-.0039
.500	12.00	.6736	.1460	.0012
.600	12.00	.6626	.1440	.0040
.700	12.00	.6552	.1429	.0056
.800	12.00	.6481	.1416	.0056

APPENDIX B

TABLE B3.- Continued

RUN 749

H/B	ALPI	CLI	CDI	CMI
.150	0.00	.3013	.0348	-.0410
.200	0.00	.2763	.0350	-.0402
.250	0.00	.2602	.0358	-.0392

RUN 750

H/B	ALPI	CLI	CDI	CMI
.150	2.00	.3965	.0431	-.0463
.200	2.00	.3613	.0429	-.0433
.250	2.00	.3453	.0424	-.0404
.300	2.00	.3331	.0427	-.0393
.350	2.00	.3195	.0426	-.0383
.400	2.00	.3177	.0430	-.0365

RUN 751

H/B	ALPI	CLI	CDI	CMI
.200	4.00	.4527	.0548	-.0491
.250	4.00	.4376	.0538	-.0436
.300	4.00	.4173	.0532	-.0395
.350	4.00	.4053	.0528	-.0376
.400	4.00	.3967	.0528	-.0364
.500	4.00	.3822	.0533	-.0344

RUN 752

H/B	ALPI	CLI	CDI	CMI
.200	6.00	.5503	.0736	-.0560
.250	6.00	.5267	.0723	-.0497
.300	6.00	.5037	.0708	-.0452
.350	6.00	.4866	.0699	-.0417
.400	6.00	.4783	.0693	-.0385
.500	6.00	.4598	.0682	-.0353
.600	6.00	.4474	.0676	-.0336

APPENDIX B

TABLE B3.- Continued

RUN 753

H/B	ALPI	CLI	CDI	CMI
.250	8.00	.6051	.0959	-.0500
.300	8.00	.5862	.0933	-.0437
.350	8.00	.5724	.0916	-.0373
.400	8.00	.5625	.0912	-.0339
.500	8.00	.5471	.0892	-.0313
.600	8.00	.5358	.0877	-.0298
.700	8.00	.5290	.0872	-.0286

RUN 754

H/B	ALPI	CLI	CDI	CMI
.250	10.00	.6912	.1292	-.0522
.300	10.00	.6624	.1236	-.0417
.350	10.00	.6483	.1209	-.0337
.400	10.00	.6308	.1181	-.0304
.500	10.00	.6196	.1157	-.0255
.600	10.00	.6047	.1137	-.0251
.700	10.00	.5956	.1125	-.0242

RUN 755

H/B	ALPI	CLI	CDI	CMI
.300	12.00	.7439	.1630	-.0415
.350	12.00	.7270	.1587	-.0317
.400	12.00	.7058	.1545	-.0267
.500	12.00	.6837	.1497	-.0202
.600	12.00	.6775	.1480	-.0171
.700	12.00	.6694	.1464	-.0156
.800	12.00	.6616	.1455	-.0145

APPENDIX B

TABLE B3.- Continued

RUN 756

H/B	ALPI	CLI	CDI	CMI
.150	0.00	.2470	.0402	.0120
.200	0.00	.2273	.0409	.0130
.250	0.00	.2132	.0412	.0138

RUN 757

H/B	ALPI	CLI	CDI	CMI
.150	2.00	.3447	.0456	.0075
.200	2.00	.3124	.0461	.0082
.250	2.00	.2928	.0467	.0107
.300	2.00	.2871	.0463	.0126
.350	2.00	.2770	.0468	.0142
.400	2.00	.2704	.0472	.0146

RUN 758

H/B	ALPI	CLI	CDI	CMI
.200	4.00	.4063	.0554	.0035
.250	4.00	.3824	.0554	.0078
.300	4.00	.3740	.0555	.0109
.350	4.00	.3568	.0558	.0126
.400	4.00	.3482	.0554	.0151
.500	4.00	.3321	.0561	.0173

RUN 759

H/B	ALPI	CLI	CDI	CMI
.200	6.00	.4968	.0707	-.0016
.250	6.00	.4787	.0703	.0011
.300	6.00	.4558	.0697	.0057
.350	6.00	.4421	.0694	.0091
.400	6.00	.4344	.0695	.0125
.500	6.00	.4205	.0693	.0162
.600	6.00	.4094	.0687	.0172

APPENDIX B

TABLE B3.- Continued

RUN 760

H/B	ALPI	CLI	CDI	CMI
.250	8.00	.5596	.0907	.0050
.300	8.00	.5343	.0894	.0087
.350	8.00	.5188	.0886	.0118
.400	8.00	.5049	.0878	.0147
.500	8.00	.4945	.0874	.0185
.600	8.00	.4829	.0869	.0204
.700	8.00	.4765	.0868	.0219

RUN 761

H/B	ALPI	CLI	CDI	CMI
.250	10.00	.6416	.1205	.0071
.300	10.00	.6132	.1168	.0116
.350	10.00	.5923	.1144	.0161
.400	10.00	.5794	.1128	.0197
.500	10.00	.5674	.1116	.0246
.600	10.00	.5584	.1107	.0269
.700	10.00	.5499	.1098	.0276
.800	10.00	.5433	.1094	.0278

RUN 762

H/B	ALPI	CLI	CDI	CMI
.300	12.00	.6970	.1527	.0140
.350	12.00	.6780	.1497	.0208
.400	12.00	.6547	.1464	.0247
.500	12.00	.6377	.1440	.0319
.600	12.00	.6237	.1418	.0351
.700	12.00	.6138	.1402	.0365

APPENDIX B

TABLE B3.- Continued

RUN 763

H/B	ALPI	CLI	CDI	CMI
.150	0.00	.2239	.0522	.0422
.200	0.00	.2074	.0523	.0416
.250	0.00	.1958	.0525	.0420

RUN 764

H/B	ALPI	CLI	CDI	CMI
.150	2.00	.3207	.0562	.0400
.200	2.00	.2947	.0564	.0385
.250	2.00	.2766	.0570	.0388
.300	2.00	.2650	.0576	.0405
.350	2.00	.2543	.0575	.0408
.400	2.00	.2458	.0574	.0409

RUN 765

H/B	ALPI	CLI	CDI	CMI
.200	4.00	.3843	.0644	.0336
.250	4.00	.3590	.0647	.0368
.300	4.00	.3442	.0651	.0397
.350	4.00	.3295	.0649	.0407
.400	4.00	.3251	.0651	.0428
.500	4.00	.3125	.0655	.0438

RUN 766

H/B	ALPI	CLI	CDI	CMI
.200	6.00	.4718	.0777	.0286
.250	6.00	.4475	.0780	.0307
.300	6.00	.4324	.0774	.0346
.350	6.00	.4161	.0777	.0372
.400	6.00	.4064	.0776	.0392
.500	6.00	.3967	.0772	.0414
.600	6.00	.3876	.0774	.0449

APPENDIX B

TABLE B3.- Concluded

RUN 767

H/B	ALPI	CLI	CDI	CMI
.250	8.00	.5358	.0973	.0344
.300	8.00	.5078	.0959	.0371
.350	8.00	.4956	.0954	.0398
.400	8.00	.4874	.0955	.0445
.500	8.00	.4742	.0951	.0464
.600	8.00	.4641	.0946	.0464
.700	8.00	.4572	.0943	.0470

RUN 768

H/B	ALPI	CLI	CDI	CMI
.250	10.00	.6156	.1239	.0375
.300	10.00	.5874	.1210	.0406
.350	10.00	.5687	.1196	.0435
.400	10.00	.5541	.1186	.0482
.500	10.00	.5438	.1179	.0534
.600	10.00	.5372	.1173	.0550
.700	10.00	.5290	.1165	.0550
.800	10.00	.5209	.1161	.0546
.900	10.00	.5152	.1156	.0545

RUN 769

H/B	ALPI	CLI	CDI	CMI
.300	12.00	.6711	.1552	.0444
.350	12.00	.6465	.1519	.0477
.400	12.00	.6339	.1513	.0550
.500	12.00	.6146	.1492	.0604
.600	12.00	.5998	.1469	.0620
.700	12.00	.5915	.1457	.0634
.800	12.00	.5868	.1457	.0644
.900	12.00	.5837	.1455	.0652

APPENDIX B

TABLE B4.- RUN SCHEDULE FOR CONFIGURATION OUT-OF-GROUND EFFECT

[From ref. 2]

Run	δ_{le} , deg	δ_F , deg			Center-line vertical tail	Horizontal-tail incidence, deg
		δ_{t1}	δ_{t3}	δ_{t5}		
105	30	0	0	0	Off	Off
119		10	10	10		
122		20	20	20		
120		30	30	20		
123		20	20	20	On	0
124						10
125						-10
126	↓	↓	↓	↓	↓	-20

APPENDIX B

TABLE B5.- TABULATED FOR CONFIGURATION OUT-OF-GROUND EFFECT

[From ref. 2]

RUN 105

ALPHA	CL	CD	CPM
-9.85	-.3532	.0750	-.0134
-8.98	-.3175	.0652	-.0086
-7.89	-.2731	.0549	-.0046
-6.85	-.2141	.0447	.0010
-5.89	-.1693	.0380	.0028
-4.85	-.1298	.0324	.0047
-3.88	-.0998	.0286	.0065
-2.82	-.0410	.0249	.0088
-1.80	-.0062	.0223	.0102
-.69	.0447	.0213	.0116
.31	.0802	.0217	.0139
1.31	.1339	.0219	.0155
2.31	.1619	.0236	.0178
3.31	.1972	.0265	.0197
4.34	.2360	.0296	.0230
5.41	.2728	.0334	.0244
6.43	.3072	.0387	.0269
7.40	.3380	.0450	.0283
8.42	.3766	.0523	.0305
9.44	.4299	.0632	.0328
10.47	.4623	.0752	.0338
12.59	.5466	.1072	.0422
14.63	.6251	.1445	.0521
16.70	.7238	.1951	.0671

RUN 119

ALPHA	CL	CD	CPM
-9.87	-.2817	.0691	-.0362
-8.93	-.2389	.0605	-.0309
-7.90	-.1912	.0514	-.0256
-6.89	-.1440	.0436	-.0209
-5.72	-.1010	.0375	-.0178
-4.73	-.0569	.0333	-.0161
-3.78	-.0071	.0298	-.0137
-2.71	.0424	.0275	-.0122
-1.68	.0811	.0268	-.0113
-.68	.1070	.0272	-.0096
.30	.1512	.0283	-.0074
1.42	.1935	.0301	-.0054
2.38	.2294	.0326	-.0038
3.38	.2712	.0365	-.0006
4.40	.3001	.0406	.0002
5.35	.3334	.0459	.0021
6.42	.3753	.0524	.0044
7.37	.4098	.0585	.0068
8.46	.4457	.0686	.0079
9.55	.4911	.0800	.0119
10.52	.5196	.0919	.0151
12.61	.6017	.1258	.0259
14.57	.6941	.1687	.0369
16.69	.7764	.2195	.0548

APPENDIX B

TABLE B5.- Continued

RUN 120

ALPHA	CL	CD	CPM
-9.86	-.1184	.0686	-.0776
-8.79	-.0691	.0612	-.0736
-7.69	-.0116	.0545	-.0688
-6.74	.0232	.0509	-.0662
-5.77	.0632	.0481	-.0639
-4.69	.1186	.0459	-.0605
-3.62	.1599	.0453	-.0587
-2.61	.1964	.0462	-.0581
-1.53	.2486	.0480	-.0551
-.59	.2786	.0507	-.0540
.49	.3136	.0544	-.0507
1.46	.3547	.0580	-.0473
2.36	.3801	.0629	-.0462
3.34	.4113	.0682	-.0442
4.47	.4480	.0756	-.0422
5.61	.4957	.0844	-.0408
6.60	.5270	.0926	-.0386
7.47	.5621	.1020	-.0374
8.46	.5966	.1132	-.0338
9.67	.6426	.1295	-.0272
10.56	.6634	.1424	-.0214
12.59	.7331	.1800	-.0083
14.70	.8084	.2249	.0044
16.69	.8961	.2828	.0252

RUN 122

ALPHA	CL	CD	CPM
-9.84	-.1982	.0671	-.0607
-8.83	-.1422	.0569	-.0547
-7.74	-.1069	.0510	-.0518
-6.77	-.0560	.0443	-.0475
-5.81	-.0162	.0408	-.0455
-4.69	.0362	.0370	-.0423
-3.77	.0752	.0354	-.0407
-2.62	.1273	.0346	-.0387
-1.61	.1734	.0352	-.0381
-.65	.2126	.0368	-.0354
.35	.2511	.0391	-.0329
1.29	.2824	.0425	-.0310
2.41	.3242	.0468	-.0285
3.45	.3589	.0517	-.0267
4.36	.3904	.0576	-.0254
5.53	.4395	.0651	-.0229
6.50	.4708	.0726	-.0219
7.44	.5103	.0822	-.0201
8.55	.5452	.0932	-.0172
9.53	.5766	.1051	-.0140
10.59	.6231	.1214	-.0036
12.58	.6909	.1570	.0044
14.56	.7664	.2001	.0187
16.68	.8582	.2569	.0377

APPENDIX B

TABLE B5.- Continued

RUN 123

ALPHA	CL	CD	CPM
-9.77	-.2156	.0704	-.0377
-8.83	-.1640	.0607	-.0324
-7.76	-.1160	.0528	-.0311
-6.71	-.0750	.0469	-.0282
-5.85	-.0303	.0425	-.0279
-4.73	.0248	.0384	-.0247
-3.67	.0660	.0361	-.0240
-2.67	.1150	.0354	-.0232
-1.76	.1521	.0355	-.0226
-.72	.1975	.0370	-.0224
.42	.2452	.0394	-.0202
1.45	.2745	.0432	-.0189
2.43	.3113	.0466	-.0168
3.37	.3382	.0511	-.0154
4.35	.3789	.0566	-.0146
5.42	.4193	.0634	-.0126
6.47	.4563	.0722	-.0115
7.51	.4984	.0815	-.0101
8.62	.5356	.0929	-.0067
9.51	.5703	.1042	-.0039
10.50	.5964	.1172	-.0006
12.60	.6809	.1560	.0108
14.62	.7641	.2019	.0223
16.64	.8579	.2575	.0368

RUN 124

ALPHA	CL	CD	CPM
-9.67	-.1738	.0638	-.0576
-8.84	-.1357	.0567	-.0553
-7.87	-.0910	.0498	-.0527
-6.86	-.0571	.0451	-.0510
-5.81	.0009	.0400	-.0491
-4.68	.0563	.0364	-.0475
-3.63	.0852	.0357	-.0464
-2.70	.1300	.0349	-.0460
-1.56	.1773	.0363	-.0446
-.58	.2223	.0383	-.0436
.42	.2565	.0408	-.0419
1.45	.2950	.0439	-.0394
2.32	.3297	.0481	-.0378
3.44	.3606	.0541	-.0363
4.49	.3960	.0598	-.0352
5.49	.4384	.0671	-.0336
6.52	.4727	.0757	-.0331
7.47	.5098	.0850	-.0311
8.59	.5480	.0969	-.0285
9.46	.5806	.1081	-.0250
10.48	.6185	.1232	-.0199
12.55	.7002	.1620	-.0112
14.61	.7853	.2100	.0003
16.73	.8812	.2691	.0147

APPENDIX B

TABLE B5.- Concluded

RUN 125

ALPHA	CL	CD	CPM
-9.91	-.2446	.0806	-.0019
-8.91	-.2009	.0713	.0005
-7.88	-.1478	.0617	.0032
-6.86	-.0989	.0545	.0047
-5.75	-.0619	.0497	.0054
-4.77	-.0099	.0451	.0071
-3.63	.0373	.0415	.0078
-2.71	.0828	.0404	.0085
-1.70	.1237	.0405	.0090
-.72	.1661	.0410	.0095
.40	.2119	.0433	.0120
1.39	.2395	.0460	.0122
2.37	.2812	.0489	.0133
3.75	.3251	.0554	.0154
4.48	.3574	.0592	.0161
5.48	.3976	.0654	.0167
6.42	.4314	.0721	.0184
7.41	.4701	.0810	.0190
8.53	.5062	.0916	.0222
9.52	.5427	.1032	.0262
10.51	.5853	.1182	.0335
12.47	.6408	.1497	.0391
14.61	.7372	.1978	.0533
16.58	.8272	.2500	.0657

RUN 126

ALPHA	CL	CD	CPM
-9.86	-.2643	.0960	.0231
-8.84	-.2120	.0852	.0263
-7.78	-.1601	.0761	.0298
-6.79	-.1225	.0695	.0328
-5.89	-.0821	.0645	.0337
-4.69	-.0244	.0582	.0358
-3.77	.0085	.0559	.0355
-2.70	.0537	.0540	.0362
-1.64	.1066	.0528	.0373
-.67	.1408	.0541	.0381
.34	.1911	.0545	.0402
1.27	.2059	.0569	.0407
2.39	.2632	.0595	.0423
3.28	.2821	.0631	.0432
4.54	.3341	.0686	.0442
5.39	.3625	.0734	.0438
6.41	.4015	.0799	.0457
7.45	.4367	.0875	.0471
8.51	.4811	.0980	.0491
9.46	.5099	.1080	.0519
10.58	.5487	.1220	.0577
12.52	.6154	.1536	.0680
14.64	.7092	.1981	.0810
16.68	.7853	.2472	.0887

REFERENCES

1. Robins, A. Warner; Morris, Odell A.; and Harris, Roy V., Jr.: Recent Research Results in the Aerodynamics of Supersonic Vehicles. *J. Aircr.*, vol. 3, no. 6, Nov.-Dec. 1966, pp. 573-577.
2. Coe, Paul L., Jr.; and Weston, Robert P.: Effects of Wing Leading-Edge Deflection on Low-Speed Aerodynamic Characteristics of a Low-Aspect-Ratio Highly Swept Arrow-Wing Configuration. *NASA TP-1434*, 1979.
3. Coe, Paul L., Jr.; McLemore, H. Clyde; and Shivers, James P.: Effects of Upper-Surface Blowing and Thrust Vectoring on Low-Speed Aerodynamic Characteristics of a Large-Scale Supersonic Transport Model. *NASA TN D-8296*, 1976.
4. Tulinius, J.: Unified Subsonic, Transonic, and Supersonic NAR Vortex Lattice, TFD-72-523, Los Angeles Div., North American Rockwell, Apr. 27, 1972.
5. Hampton Technical Center, LTV Aerospace Corp.: Advanced Supersonic Technology Concept Study Reference Characteristics. *NASA CR-132374*, 1973.
6. Turner, Thomas R.: Endless-Belt Technique for Ground Simulation. Conference on V/STOL and STOL Aircraft, NASA SP-116, 1966, pp. 435-446.
7. Recant, Isidore G.: Wind-Tunnel Investigation of Ground Effect on Wings With Flaps. *NACA TN 705*, 1939.
8. Pope, Alan; and Harper, John J.: Low-Speed Wind Tunnel Testing. John Wiley & Sons, Inc., c.1966.
9. Braslow, Albert L.; and Knox, Eugene C.: Simplified Method for Determination of Critical Height of Distributed Roughness Particles for Boundary-Layer Transition at Mach Numbers From 0 to 5. *NACA TN 4363*, 1958.
10. Kemp, William B., Jr.; Lockwood, Vernard E.; and Phillips, W. Pelham: Ground Effects Related to Landing of Airplanes With Low-Aspect-Ratio Wings. *NASA TN D-3583*, 1966.
11. DeYoung, John: Symmetric Loading of a Wing in a Wide Slipstream. Rep. No. ADR 01-04-66.1, Grumman Aircraft Eng. Corp., Oct. 1966.
12. Fox, Charles H., Jr.: Prediction of Lift and Drag for Slender Sharp-Edge Delta Wings in Ground Proximity. *NASA TN D-4891*, 1969.

1. Report No. NASA TP-1508	2. Government Accession No.	3. Recipient's Catalog No.	
4. Title and Subtitle THEORETICAL AND EXPERIMENTAL INVESTIGATION OF GROUND-INDUCED EFFECTS FOR A LOW-ASPECT-RATIO HIGHLY SWEPT ARROW-WING CONFIGURATION		5. Report Date September 1979	
7. Author(s) Paul L. Coe, Jr., and James L. Thomas		6. Performing Organization Code	
9. Performing Organization Name and Address NASA Langley Research Center Hampton, VA 23665		8. Performing Organization Report No. L-13088	
12. Sponsoring Agency Name and Address National Aeronautics and Space Administration Washington, DC 20546		10. Work Unit No. 517-53-43-02	
		11. Contract or Grant No.	
		13. Type of Report and Period Covered Technical Paper	
		14. Sponsoring Agency Code	
15. Supplementary Notes			
16. Abstract <p>An investigation has been conducted in the Langley V/STOL tunnel to determine the influence of ground proximity on the aerodynamic characteristics of a low-aspect-ratio highly swept arrow-wing configuration. The experimental results showed that as the height above the ground decreases, the configuration experiences substantial increases in lift and reductions in induced drag. Although a significant percentage of these ground-induced performance improvements are lost due to trim requirements, the net performance improvement remains quite favorable. The tests also showed that decreasing ground height results in a substantial increase in the horizontal-tail contribution to longitudinal stability.</p> <p>Comparison of the experimental results with results predicted by a planar vortex-lattice theoretical model shows that the theoretical model provides a good estimate of the ground-induced effect on lift, drag, and longitudinal stability for the wing-body combination. However, the theoretical model does not adequately predict either the zero lift pitching moment or the horizontal-tail downwash characteristics.</p>			
17. Key Words (Suggested by Author(s)) Ground effects Arrow wing		18. Distribution Statement Unclassified - Unlimited	
Subject Category 08			
19. Security Classif. (of this report) Unclassified	20. Security Classif. (of this page) Unclassified	21. No. of Pages 100	22. Price* \$6.00

* For sale by the National Technical Information Service, Springfield, Virginia 22161

NASA-Langley, 1979



National Aeronautics and
Space Administration

Washington, D.C.
20546

Official Business
Penalty for Private Use, \$300

THIRD-CLASS BULK RATE

Postage and Fees Paid
National Aeronautics and
Space Administration
NASA-451



NASA

POSTMASTER: If Undeliverable (Section 158
Postal Manual) Do Not Return
